GE Energy

Final Report

Analysis of Wind Generation Impact on ERCOT Ancillary Services Requirements

Prepared for:

Electric Reliability Council of Texas

March 28, 2008

FOREWORD

This document was prepared by General Electric International, Inc. under contract to Electric Reliability Council of Texas, Inc.

Project Manager:

Reigh A. Walling

GE Energy
One River Road
Building 2, Room 618
Schenectady, New York 12345

GE Project Team:

Venkat Banunarayanan
Amanvir Chahal
Lavelle Freeman
Jerry Martinez
Nicholas Miller
Devin Van Zandt
Mark Walling
Reigh Walling

LEGAL NOTICE

TABLE OF CONTENTS

1. INTRODUCTION

GE Energy has performed an extensive study of the ancillary service requirements for the Electric Reliability Council of Texas (ERCOT) system to accommodate large-scale expansion of wind generation capacity. This report documents the approach used to perform this study, the results obtained, and the final study recommendations.

1.1. Background

Texas is the leader among the United States in adding wind power to the state's power generation portfolio. Texas leads the country with the most installed wind capacity, and the greatest annual capacity additions. In contrast to many parts of the United States where transmission inadequacy presently constrains wind energy development, Texas has overcome the transmission barrier by the bold and progressive step of establishing Competitive Renewable Energy Zones (CREZs). The Public Utility Commission of Texas (PUCT), in consultation with ERCOT, has designated CREZs in areas suitable for renewable energy development, and is developing a plan to construct the necessary transmission capacity to deliver the energy from the renewable resources to the customers in the state.

Wind generation has technical characteristics which inherently differ from those of conventional generation facilities. Conventional generation can be controlled, or "dispatched", to a precise output level. The primary energy source for wind generation, however, is inherently variable and incompletely predictable. Thus, electrical output of wind generation plants cannot be dispatched[1].

Because electric energy cannot be easily or economically stored on a large-scale basis, the amount of power generation must be exactly matched, on a near-instantaneous basis, to the amount of customer load demand. There is considerable art and science applied to the operations of a power system to maintain the balance of load and generation. Because the ERCOT system is not synchronously interconnected with any other power system, a mismatch between instantaneous load and generation inherently results in variation of the system frequency. Load demand varies on a daily cyclic basis, and has a considerable degree of random variation around the daily trend. Load levels also cannot be precisely predicted in advance. Addition of wind generation resources increases the amount of variability and unpredictability that must be addressed in system operations.

[1] Wind generation can be "turned down", or curtailed, from its potential output, but cannot be increased beyond the power level provided by the existing wind velocity. Curtailment "spills" non-recoverable energy., thus curtailment on a continuous basis to render a wind plant equally dispatchable as a conventional plant is not practical. Where appropriate wind plant controls are installed, wind plant turndown can potentially be used to provide regulation service in certain circumstances.

A category of services, called "ancillary services", are procured by the ERCOT power market to facilitate the operation and balancing of the system. ERCOT currently uses several ancillary services to control system frequency and protect system reliability from imbalances between generation and load. In the past, this imbalance might occur due to the variability of load, inaccuracies in the prediction of load levels or resource utilization, or the unplanned loss of resources.

The ERCOT market structure will be transitioned in 2009 from the current zonal structure to a nodal structure. The ancillary services in the ERCOT nodal market design are:

- *Regulation Service* – is used to maintain the instantaneous balance between load and generation resources.
- *Responsive Reserve Service* – is generation resources held in reserve to address loss of generation resources and unexpected large changes in generation requirements.
- *Non-Spinning Reserve Service* – are generation resources that can come on line with short (presently thirty minute) notice to compensate for load forecast errors.
- *Replacement Reserves* – are used to commit additional capacity based on forecasted load, either for load balance or congestion.

The integration of increasing amounts of wind generation capacity into the ERCOT system inevitably leads to changing requirements for ancillary services procurement.

ERCOT has commissioned this study of ancillary services requirements to provide the information needed to guide ERCOT and the PUCT in evaluating the reliability implications of wind generation penetration, and to develop the procedures and protocols for ancillary services procurement needed to strike the proper balance between system reliability and economic operation of the system.

1.2. Project Scope and Objectives

The specific objectives of this study are to:

1. Quantitatively assess the impact of various wind development scenarios on the levels of ancillary services required.
2. Evaluate the methodology used by ERCOT to determine the amount of ancillary services required, and recommend improvements to that methodology where appropriate.
3. Estimate the impact of wind generation on the costs to procure ancillary services.
4. Identify changes to current procedures or new procedures required for operations with impending severe weather conditions.

This study is based on sequential time-series modeling of the wind and load behaviors, as well as the processes used to forecast both wind and load. Extensive statistical analyses are used to characterize the wind and load variability. Detailed modeling is performed of ancillary service deployments to determine both the amount of ancillary service required to be procured as a function of wind penetration, and to assess the suitability of procurement procedures.

The study focuses on five wind penetration scenarios that have been defined by ERCOT, ranging from zero to 15,000 MW of wind capacity. Although this 15,000 MW level of wind generation will take several years to evolve, and the present wind capacity is on the order of 5,000 MW, these wind scenarios are applied to a system model representing 2008 load levels and generation composition for consistency. The 15,000 MW of wind generation applied to the 2008 loading results in a 23% penetration on a nameplate wind generation capacity to peak load basis. This is equivalent in terms of wind penetration to 18,456 MW of wind generation applied to the forecast 2017 system load. The penetration is approximately 17% on an energy basis.

Applying the different wind scenarios to one system model implicitly assumes that the conventional (dispatchable) generation portfolio mix remains constant as wind penetration increases. This is not necessarily what will happen. However, forecasting how the conventional generation mix evolves in response to increasing wind generation, changing environmental requirements, shifts in capital markets, and generation technology improvements is extremely complex and highly speculative. Therefore, such prognostication is not included in the scope of this study.

This study, by design, also intentionally ignores present-day transmission constraints. Public policy in Texas is to develop the transmission system to support renewable generation additions. Thus, it would be inconsistent to incorporate constraints in the study which should not be present when the wind generation is developed, if this policy is carried out.

1.3. Study Participants

The prime contractor for this study is the Energy Applications and Systems Engineering group of GE Energy. This group is the power system consulting arm of GE, and has been involved in the cutting edge of power engineering technology for nearly a century. Recent activities of this group have included a number of important and pioneering studies of wind integration, including studies of the New York, California, and Ontario systems.

This study combines both power systems and meteorological aspects. AWS Truewind was retained by GE Energy as a subcontractor for this study, providing wind generation data, wind forecast data, and important insights on severe weather conditions. AWS

Truewind has performed previous studies of wind generation resources for ERCOT, and has been retained by ERCOT to provide wind forecasting services on an operational basis. The GE–AWS Truewind team has worked together on prior highly successful projects, and the benefits of that prior experience have been applied to this study.

1.4. Organization of Report

Section 2 describes the approach used in this study, with specific information on the generation of the contemporaneous load and wind generation data used as the basis for this study.

Section 3 provides an extensive analysis of the variability of the net load[2], with correlations of this variability with time of day, season, and load level.

Section 4 analyzes the impact of wind generation forecast errors on the resulting net load forecast error. Forecast errors are correlated with time of day, season.

Section 5 describes how the presence of wind generation affects the commitment and dispatch of the conventional generation fleet, showing impacts on energy production by various generation types, emissions, spot prices, and output ramping capabilities.

Section 6 provides the results of an extensive analysis of regulation service requirements, including the impacts on regulation procurements as wind penetration increases, evaluation of regulation procurement methodology, ability of the conventional generation to provide the needed regulation, and the impacts on costs of regulation service.

Section 7 discusses extreme weather conditions. Extensive meteorological analysis is provided of the critical issues associated with extreme weather, as it pertains to rapid wind generation output changes.

Section 8 discusses responsive and non-spin reserve services

Section 9 completes the main body of the report with conclusions and recommendations.

Appendix A provides the Table of Figures for this report.

Additional appendices provide supplemental and detailed information supporting the report. Of particular note is *Appendix H* which is AWS Truewind's report on the wind generation output characteristics during extreme weather conditions.

---

[2] Net load is defined as the load demand minus the wind generation output at that time. An extensive discussion of net load, and why this perspective of analysis is critical, is provided in Section 2. See Appendix A for definitions of other terms used in this report.

2. STUDY APPROACH

The overall study approach is outlined in this section. The types of analysis, study scenarios, data, and model development are all described below.

2.1. The Critical Importance of Net Load

Wind generation output and system electrical demand (load) have a number of common elements, as both are:

- Cyclic on an annual (seasonal) basis, and a diurnal (daily) basis
- Subject to random short-term variations around the multi-hour trends.
- Not directly controllable (i.e., non-dispatchable)
- Subject to deviations from predicted day-ahead behavior
- Mutually dependent on prevailing weather conditions.

From this, it can be seen that wind generation has more in common with load, on an operational basis, than it does with conventional, dispatchable generation resources. The major difference is one of sign; wind generation effectively acts like a negative load.

The impacts of wind generation on ancillary service requirements cannot be evaluated by examining wind generation output characteristics, such as variability and predictability, independently from the simultaneous behavior of the load. Factors causing inaccuracy in wind forecasting may also affect load forecasting (e.g., arrival time of a cold front).

Thus, analysis of wind variation independent of load variation is inadequate and inappropriate to determine impacts of wind on ancillary services requirements and procurement methodologies. The inherent variability and imperfect predictability of wind generation adds to the variability and prediction errors of system load. The variabilities cannot simply be combined as if they are independently random, as they are both affected by the common factor of the weather. Nor can they be added algebraically because the correlation is only partial and the coefficient can be either positive or negative, or vary in sign with time or location of the wind resource.

Operationally, the dispatchable generation output must conform to the characteristics of the *net load*, defined as the aggregate customer load demand minus the aggregate wind generation output. The fundamental approach of this study is to analyze the **net load** variability and the resulting impacts on ancillary services requirements brought on by increasing penetrations of wind generation.

2.2. Wind Generation Scenarios

ERCOT defined five different wind generation scenarios to be used as the basis for this study, with four levels of wind capacity ranging from zero to 15,000 MW. There are two 10,000 MW scenarios, with the second substituting capacity in South Texas near the Gulf of Mexico (CREZ 24) in lieu of similar capacity in the Panhandle in CREZ 4. In addition to the total wind generation capacity for each scenario, ERCOT also defined the capacity assignments for each CREZ shown in Table 2-1. Figure 2-1 provides the geographic location of the various CREZs.

Table 2-1 - Wind Capacity Allocation by CREZ

	Wind Development Scenario			
CREZ Zone	**5000 MW**	**10,000 MW (1)**	**10,000 MW (2)**	**15,000 MW**
none	120	120	120	120
2	60	1,560	1,560	2,340
4	0	1,500	0	0
5	355	1,355	1,355	1,355
6	400.5	400.5	400.5	1,278.3
7	65	65	65	97.5
9	814	1,314	1,314	1,971
10	2,464.5	2,964.5	2,964.5	4,446.8
12	400	400	400	600
14	160	160	160	240
15	60	60	60	90
19	101	101	101	211.5
24	0	0	1,500	2,250

Minute-by-minute ERCOT load data from 2005 and 2006, combined with synchronized wind generation expectations for the same time period, were used to build time series models for the scenarios. The load data were scaled such that the 2006 loads are at the forecast 2008 level, and the same scale factor is also applied to the 2005 data. The scaling and preparation of load data is described later in Section 2.2.2. Most of the wind generation resources in the scenarios have not yet been installed. Therefore, it was necessary to construct minute-by-minute wind generation output data from available meteorological data for 2005 and 2006. The derivation of wind generation data is described in Section 2.2.1.

Similarly, historical day-ahead load forecasts were obtained from ERCOT for each day of the 2005 – 2006 period. Day-ahead wind forecasts were synthesized by AWS Truewind using techniques that have been applied to previous wind integration studies.

This process developed a detailed minute-by-minute, synchronized model of ERCOT system load and wind generation. To the extent possible, this approach takes into account the mutual factors affecting both wind output and load demand, and factors affecting forecast errors.

The primary purpose for analyzing two years of data is because ERCOT's present methodology to determine regulation requirements is based on historical deployments of regulation for the same period in the prior year. Also, comparison of the statistical differences between the two years provides indication of year-to-year differences.

Although the 2006 data are scaled to the 2008 level, this report does not use "2008" for this year, and "2007" for the scaled 2005 data. Such a designation could be misleading as readers may note specific dates for events in the data which do not correlate to actual events in the 2007 and 2008 years. Therefore, the 2006 data scaled to 2008 are referred to as "Study Year", and the scaled 2005 data are called "Prior Year" in this report.

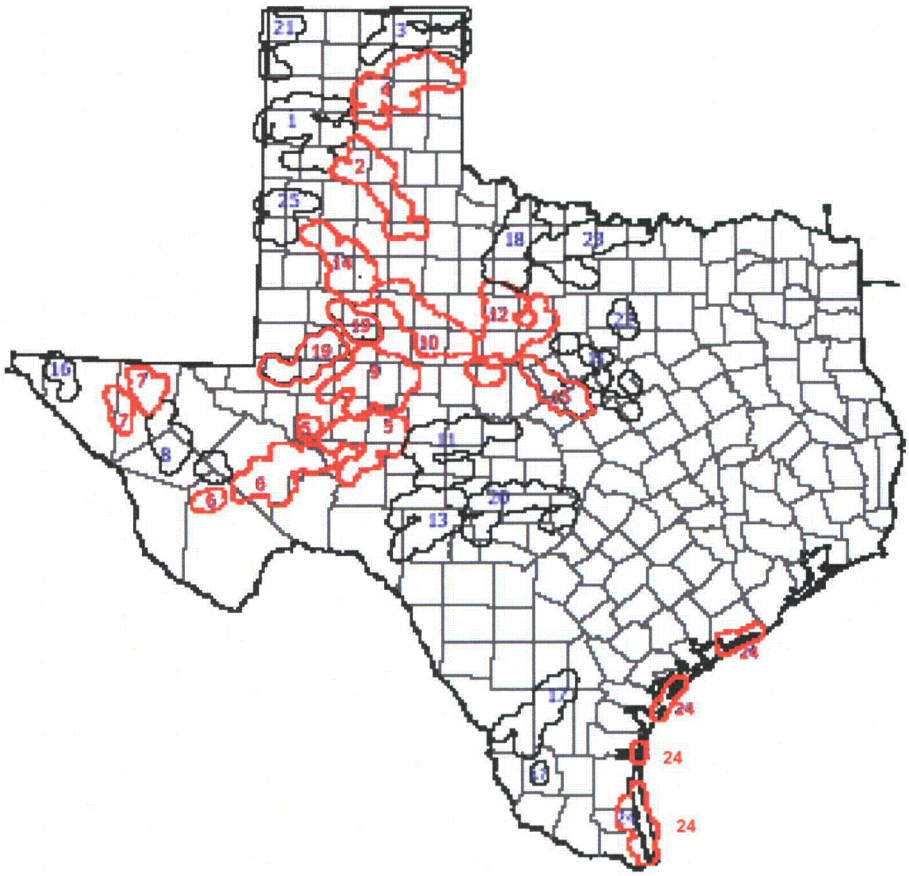

Figure 2-1 - CREZ map, zones included in the study are shown in red.

2.2.1. Wind Generation Power Output Data

The generation of wind data for this study was performed by AWS Truewind, LLC, (AWST) as a subcontractor to GE Energy. AWST's deliverables were:

- Wind generation, by individual plant, on a minute-by-minute basis.
- Day-ahead hourly wind generation output forecasts, by individual plant.

AWST also performed an evaluation of severe weather conditions, and the resulting potential for rapid changes in wind power output. This task is described separately in Section 7.1.

The generation of the wind generation data is summarized in this report section. A full report of AWST's work to develop wind generation data is attached as Appendix B.

Meso-Scale Weather Model

AWST had previously been engaged directly by ERCOT to develop wind generation data for 716 identified potential wind plant sites in 25 CREZs. For the present study, AWST used the same modeling approach to determine wind generation and forecast data for 2005 (Prior Year) and 2006 (Study Year) so that the wind data is for a contiguous time period synchronized with system load data provided by ERCOT.

AWST's starting point for developing the wind generation data was a highly-detailed meso-scale numerical weather model representing weather behavior on an hourly basis. This model was initialized and adjusted to conform to historic weather recordings, including tall-tower wind recordings, for the two-year period. The model was used to generate hourly wind velocities and directions for each of the identified sites.

Plant Generation Data

The wind velocity and direction were then converted to hourly electrical power levels for each plant using typical wind turbine-generator performance curves. Adjustments were made for a number of factors, including directionally-dependent wake interference, and various other non-directional losses and unit unavailability.

One-Minute Generation Data

The weather model yielded hourly wind plant output. Minute-by-minute variations in power output were synthesized using a process based on recordings of actual Texas wind plant output data with one-minute resolution. This synthesis process has been widely used for many wind integration studies.

Wind Forecasts

Wind forecasts for one day ahead and four hours ahead were synthesized by AWST using a Markov chain approach, using typical wind forecasting error patterns reflecting the current state of the wind forecasting art. An unbiased, or 50% confidence level, forecast was generated. The reasons for using a statistical, rather than a meteorological approach to developing the forecast data is explained in AWST's report. This process, too, has been widely used on other major wind integration studies in which AWST has participated.

Because a short-term load forecast is not applied to ERCOT's planned nodal operations, when the anticipatory "tuning factor"[1] is zero, the four hour forecast data developed by AWST were not used in this study.

CREZ Wind Output Data

Wind generation and forecast data were provided by AWST on a per-plant basis. Some of these are existing plants. In developing the wind generation output for each CREZ, existing plants were considered first. Then, potential plants, identified by AWST in the prior work for ERCOT, were added in the order of decreasing annual capacity value, until the total wind plant capacity in a CREZ equaled the capacity values defined in Table 2-1.

2.2.2. System Load Data

System load data for 2005 and 2006 were provided by ERCOT. The load for each minute in both years was scaled by a factor of 1.037 to reflect load growth from 2005-2006 to 2007-2008. The same factor was also applied to scale day-ahead load forecasts.

2.3. Types of Analysis

Three primary analytical methods were used to meet the objectives of this study; statistical analysis, production simulation analysis, and historical meteorological analysis.

Statistical analysis was applied to variability of load and net load, forecast errors, and regulation deployments. Correlations with time of day, season or month of year, and system load level were identified. The adequacy of present ancillary services procurement methodologies was statistically characterized.

---

[1] This tuning factor is discussed later in this section and in Section 6.

Production simulation analysis with GE-MAPS™ was used to evaluate hour-by-hour system operation for each scenario for 3 years with different assumptions regarding the use of wind generation forecasting in the day-ahead unit commitment. The results quantified numerous impacts on grid operation including:

- Amount of maneuverable generation on-line during a given hour, including its available ramp-up and ramp-down capability to deal with grid.
- Changes in dispatch of conventional generation resources due to the addition of wind generation
- Changes in emissions for oxides of sulfur (SO_x), oxides of nitrogen (NO_x) and carbon dioxide (CO_2) due to wind generation
- Changes in costs and revenues associated with grid operation, and changes in net cost of energy

The impacts of severe weather on system reliability, through potential large-scale loss of wind generation output, were assessed using multiple approaches. These approaches included statistical analysis of the modeled data, as well as historical analysis of critical wind generation output change events observed in the ERCOT system during recent years. For the identified events, AWS Truewind has examined the available data on wind output generation, and has researched the weather behavior of the same period to identify root causes for the generation output changes. With this meteorological analysis of historic wind-change events, predictions have been made regarding the severity and mean recurrence of severe wind-change events in the future.

2.4. Study Assumptions and Limitations

The following are major assumptions made in the performance of this study:

- Because actual historical wind measurements are not available for all the sites included in the scenarios, wind generation output is calculated using meso-scale weather modeling and typical wind turbine performance characteristics. Wind forecasts (50% confidence level) were also synthesized by a statistical process. Wind generation output and forecast data derivation are as described in Section 2.2.1 and Appendix B.
- The scope of this study was to analyze two years of data. Data gathered over a longer term may yield different results, particularly with regard to extreme conditions; i.e., statistical outliers.
- Transmission constraints are not considered in this study. The intent of the CREZ development is to make the transmission system additions needed to facilitate wind and other renewable forms of generation. The limitations of today's ERCOT transmission system is not a valid consideration for future scenarios of high wind penetration. Although building a completely constraint-free transmission system is not economically efficient, future transmission

constraints on a yet-to-be designed system cannot be determined at this time, and thus were excluded from the scope of this study.

- The composition of the non-wind generation portfolio in ERCOT is assumed to remain constant. This means that the percentages of generation, by type (i.e., nuclear, single-cycle GT, coal, etc.) is invariant. During the time required for up to 15,000 MW of wind to be developed in ERCOT, other generation additions will be also required to meet load growth. Some generation unit retirements may occur as well. The generation portfolio may very well shift in response to fuel costs, changing technologies, changed environmental and regulatory policies, and to the presence of wind generation as well. As shown later in this report, the presence of wind capacity tends to displace energy production from mid-merit units such as combined cycle gas turbines. The market may respond with a different mix of units than are presently on the ERCOT system. Forecasting this long-cycle impact of wind generation on generation unit development is beyond this study's scope.
- Wind conditions for the analyzed years (2005 and 2006 data) are assumed to be indicative of the long-term characteristics. Meteorologists indicate that the year-to-year variations in typical wind patterns are not large. However, there is uncertainty regarding the extrapolation of extreme wind events from the limited observation period.
- There will be "tuning factors" used in the ERCOT nodal market to predictively adjust economic dispatch for expected load change within a five-minute dispatch period, based on the short-term load forecast. The tuning factors have not yet been determined by ERCOT. This study proceeded with modeling regulation assuming that the tuning factor is always zero. Thus, predictive adjustment of dispatch was not represented.
- In the present ERCOT zonal market, units providing regulation service are required to have sufficient ramping capability to achieve the offered regulation range in ten minutes

3. NET LOAD VARIABILITY CHARACTERIZATION

For the purposes of this study, net load is defined as the instantaneous system load, minus the generation output of non-dispatchable wind generation (Load-Wind). Net load is the amount of generation required from dispatchable units. This section focuses on the variability of net-load rather than wind generation in isolation because experience has shown that some of the variation in load and wind output cancel each other in a combined series. In other words, given synchronized load and wind generation time series, the net variability of load-wind over a time period is less than the sum of the variability of the individual series over the same time period.

For illustration, Figure 3-1 charts the profile of load, wind generation, and net load for one hour on April 23rd of the study year, (from one-minute data). Load and net load are plotted on the left axis and wind generation output on the right axis. Table 3-1 quantifies the variation of the raw data over the entire hour, and the variation of minute-to-minute changes using the standard deviation (σ) statistic.

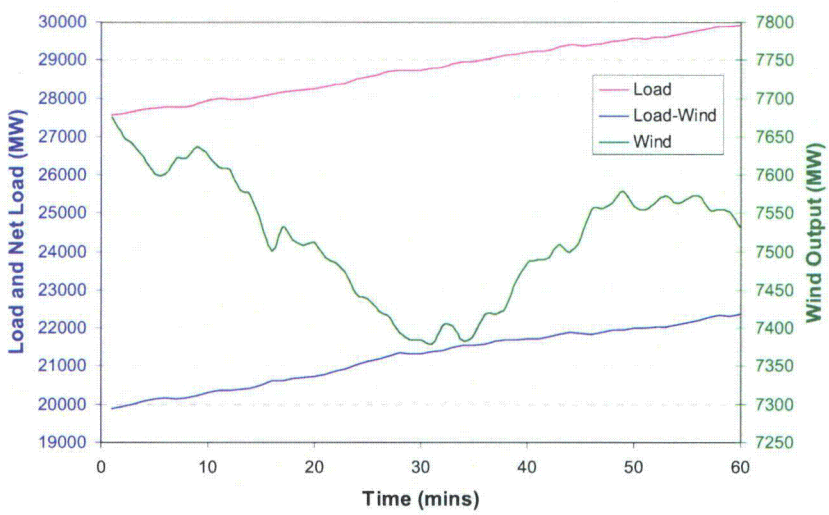

Figure 3-1 - Load, Wind and Net Load time series plots for April 23, 7-8 AM

Table 3-1 - Standard Deviation (σ) of Load, Wind and Net Load Series

	Load	Wind	Load-Wind
Raw Data σ (MW)	723.9	80.5	**750.4**
Min-to-Min Changes σ (MW)	28.8	16.9	**35.6**

In both cases, the net load standard deviation is *less than the sum* of the individual load and wind sigmas. Therefore, the best way to understand the incremental variability due to wind, is to measure the difference in variability between net load and load.

3.1. Wind and Load Relationships

The temporal relationship between wind output and load is the key driver for resulting net load variability. Depending on how the wind is behaving when load is rising or falling, the net variability could be better or worse than load alone. In some cases, wind may exaggerate or curtail net load peaks and valleys, increase or decrease ramp rates (period-period-changes), shift time-of-peak, and generally aggravate or mitigate operationally challenging periods. All these are important factors when considering the impact of wind on ancillary services, especially regulation, (discussed further in Section 6).

Figure 3-2 plots individual time series for load and 15,000 MW of wind generation during April of the study year. Note that wind output is plotted against the right scale with its dynamic range amplified by two for illustration. The plots illustrate that over the course of the month, load and wind output vary considerably from day to day and throughout the day, but a distinct diurnal cycle in the load can be observed. The wind output does not exhibit similarly strong periodic behavior, but *there is an observable tendency for wind output to be anti-correlated with the load*, i.e. load peaks tend to coincide with wind generation valleys. This is even more clearly illustrated in Figure 3-3 below which plots the average daily profiles[1] of load and 15,000 MW of wind generation for four seasonally representative months: January, April, July and October (see Appendix C.1 for other plots). Note that load is plotted against the left scale and wind generation against the right, amplified by five.

The average daily profiles reveal four general trends with regard to the relationship between load and wind output:

- Wind generation is generally out-of-phase with load during an average day across all seasons. The inverse-phase relationship appears to be stronger in the summer than other seasons, probably due to the heavy use of electric cooling during mid-day periods when wind tends to be less prevalent.
- Wind generation tends to drop sharply in the morning when load is rising quickly, generally between 6 and 9 AM. This tends to be heightened in the spring and summer where the load rise is steeper and more sustained, and the wind down-ramp is greater.
- Wind generation generally increases sharply in the evening when load is dropping. Across all seasons, load tends to rapidly decline between 9 PM and Midnight, during which time, wind output tends to be ramping up quickly.

[1] The average daily profile is created by taking the mean of observations occurring at the same time-of-day across all days of the month, to create a day-long series which reveals broad daily trends in the data over the month -- day-to-day variations and extreme observations are naturally subsumed by averaging

- During winter months, the late afternoon 5-7 PM load rise tends to coincide (roughly) with a general increase in wind production, but it is more variable.

These observations have implications for net-load variability (and operational requirements) at different times of the day and during the various seasons of the year, as discussed later in this section.

Figure 3-4 shows the April load and wind generation series (previously plotted in Figure 3-2) on the same scale, along with the net load resulting from the load-wind combination. To further illustrate the net load variability, a typical day from the same month, April 23rd, is plotted in Figure 3-5. The plots show that the net load shape is similar to the load shape but with some added nuances due to the influence of wind. Wind output produces an offset in the net load that varies in terms of its magnitude and phase. Naturally, the greatest offset is in the early morning when wind output is highest, and the smallest occurs at peak time. A slight shift in the time of peak for net load also occurs, as the minimum wind output does not coincide with the peak load for this day. Across the month, the overall superposition of load and wind output results in periods where the daily range (peak-to-trough measurement) of net load exceeds that of load alone. The result is that the net load ramp rates increase due to wind generation.

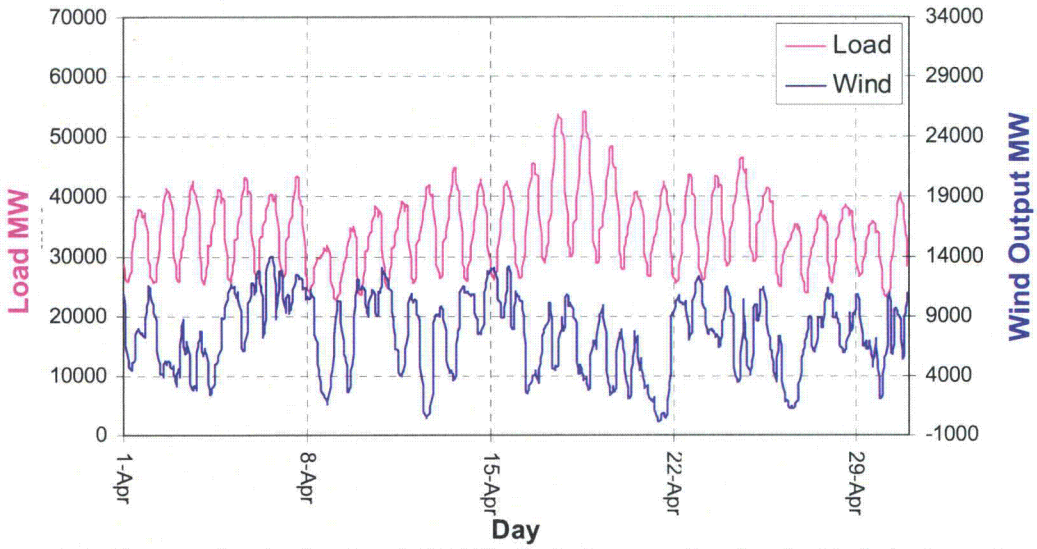

Figure 3-2 - Time series for load and 15 GW of wind generation for April of study year.

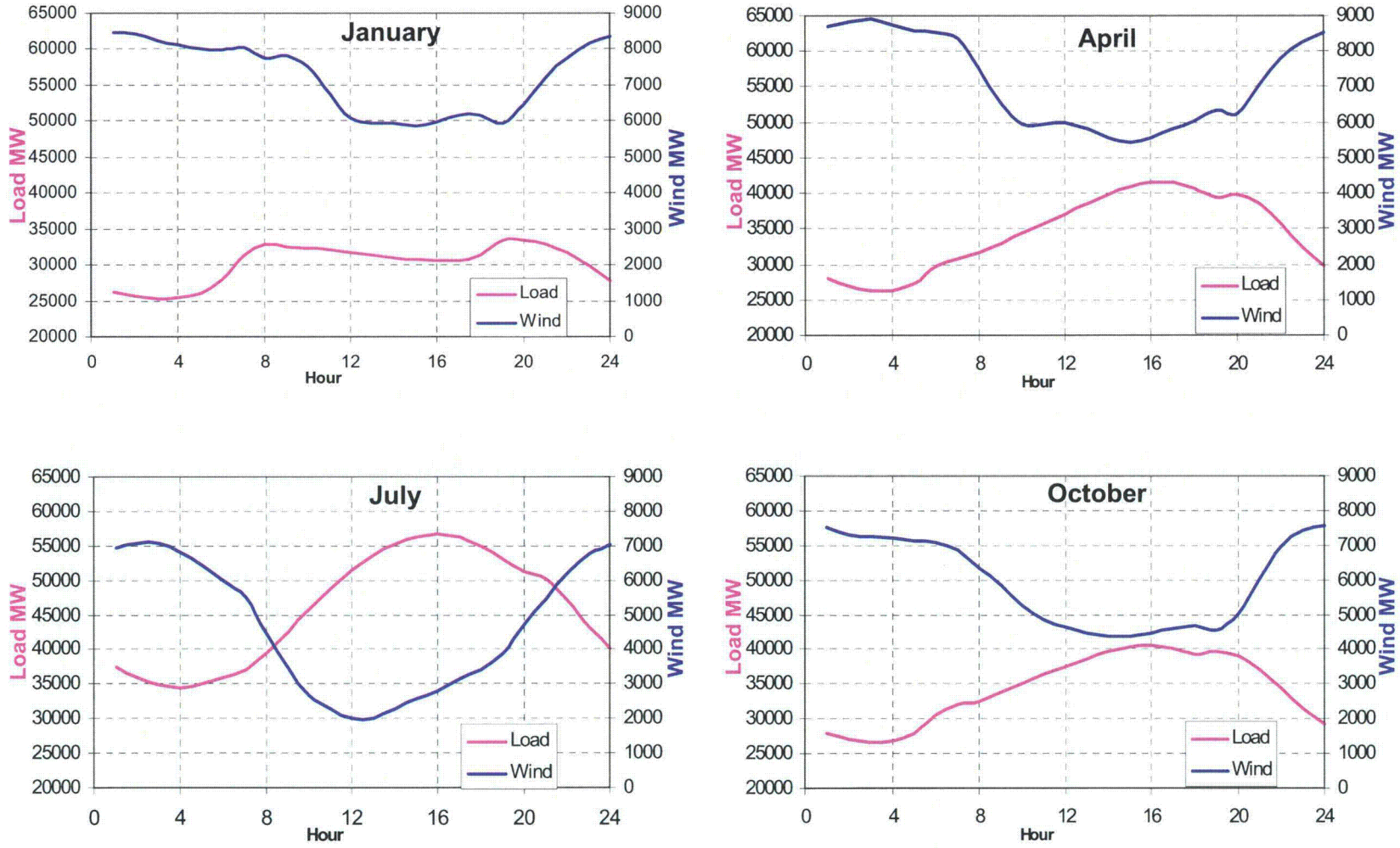

Figure 3-3 - Average daily profiles for load and 15 GW of wind generation for four seasonally representative months

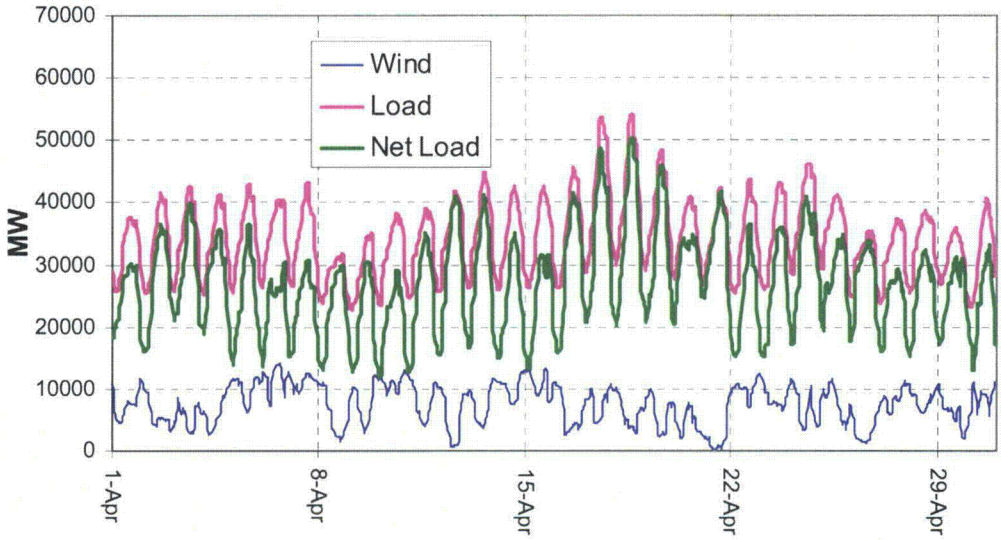

Figure 3-4 - Load, 15 GW of wind generation, and net load for April of study year

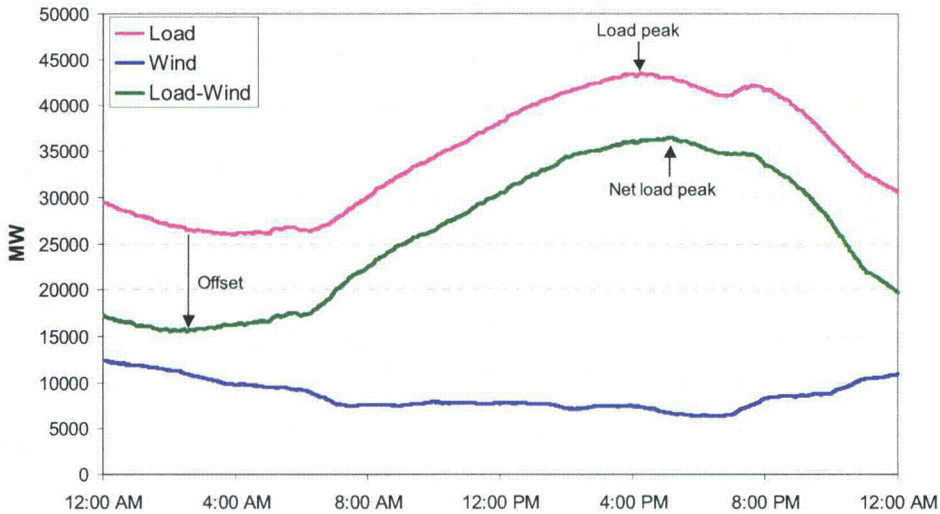

Figure 3-5 - Load, 15 GW of wind generation, and net load for April 23rd of study year

Similarly, higher wind generation penetration would produce larger net load ramp rates. Figure 3-6 plots the net load for the various wind output scenarios for one January week.

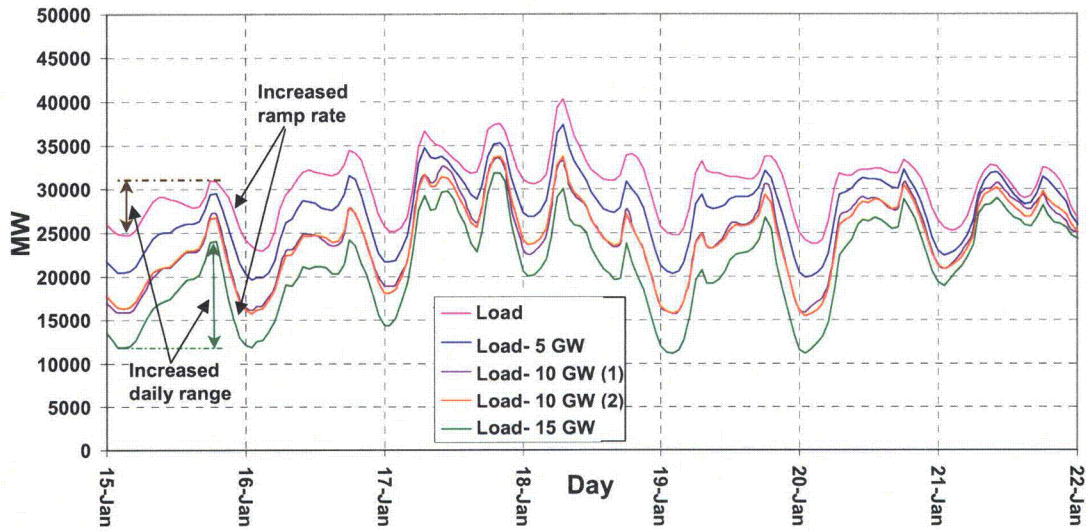

Figure 3-6 - Net load plots for various wind scenarios for a January week of the study year

As expected, the curve shape is relatively similar for all wind generation scenarios, but the daily peak-to-valley changes (range) increases with wind generation, and the period-to-period changes or ramp rates become increasingly larger. This is illustrated by the arrows on Figure 3-6, which highlight the differences in daily range and hourly ramp rate between load alone (no wind generation) and net load with 15,000 MW of wind generation.

Figure 3-7 shows the net load times series for one week in April. During this week, wind generation has less impact on the ramp rates than during the January week in Figure 3-6. However, this plot highlights a very important concept – the importance of load and wind time synchronization when studying net load.

On April 15th, there is a noticeable perturbation in the load which is even more pronounced in net load. Profiles for load, 15 GW of wind, and the net load on April 15th are shown on the bottom-left inset chart. At the time when the load dips, the wind generation increases. This perturbation in both wind and load *at the same time*, likely from common source such as a cold front, causes an even larger drop in net load. These types of phenomena are precisely why load and wind data should be time-synchronized.

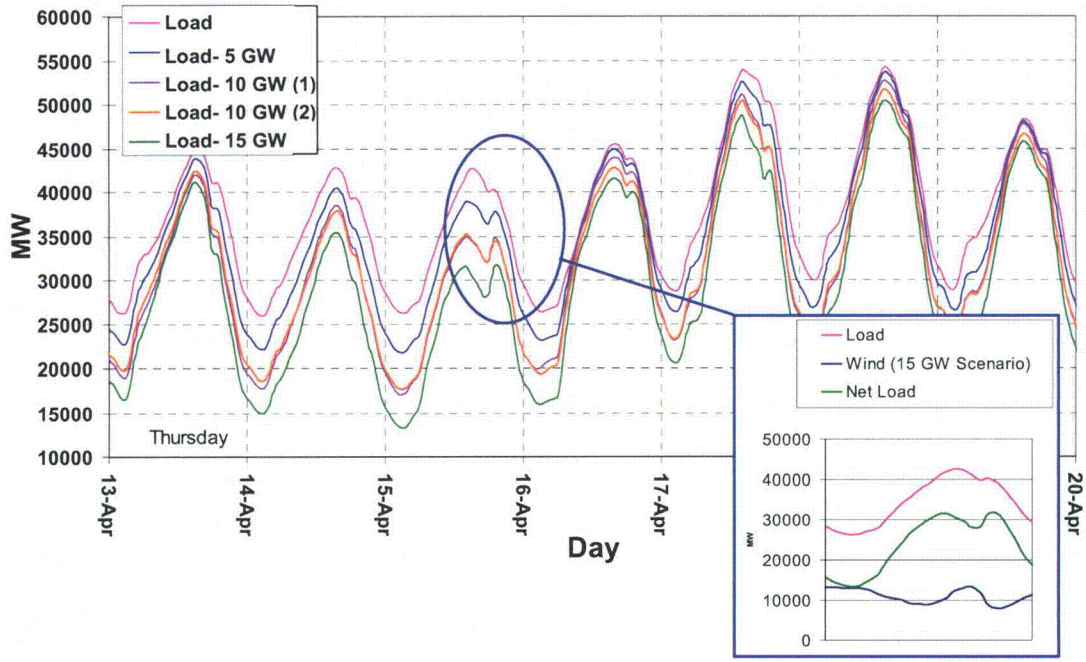

Figure 3-7 - Net load comparisons for an April week of the study year

The following subsections examine net load variability in different timeframes and discusses seasonal and daily trends. In all cases, the key driver is the load and wind coincidence. But seasonal and daily variation in load and wind generation due to lifestyle and meteorological influences, are manifest differently in the net load when it is examined at various levels of resolution, and in different timeframes.

3.2. Variability Over Different Timeframes

The variability of net load in different timeframes impacts various aspects of bulk power system operation. Implications for regulation requirements, ramp and range considerations, operating reserves and unit commitment issues can be drawn from an analysis of net load variability in the 1-, 5-, 15-, 30-, and 60-minute timeframes, depending on the ancillary service definitions and market rules. This section will focus on the statistical analysis of load and net load variability in the various timeframes and reserve a fuller discussion of operation requirements and ancillary services for later Sections.

In this section several terms are used to characterize the load and net load variability. They include:

- Delta (Δ) – The difference between successive data points in a series, or period-to-period ramp rate
- Sigma (σ) – The standard deviation of a dataset or a measure of how dispersed observations are, relative to the mean

Since deltas can be positive or negative depending on the slope of the series at a point in time, the average of the deltas is somewhat meaningless. In fact, for a series of a day or longer, the mean of the deltas is zero or near zero. The standard deviation of the deltas, however, is a good indication of how much the series changes from period-to-period, therefore *sigma of the deltas is used as a measure of variability in this study*. If the deltas are normally distributed (a rational assumption based on experience) then sigma relates to the proportion of deltas within a certain distance of the mean μ, (as illustrated to the right).

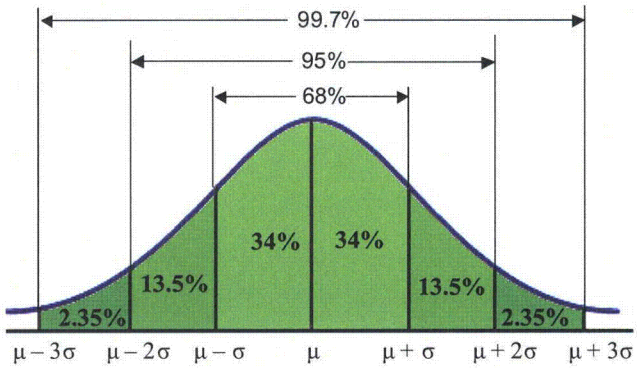

3.2.1. One-Minute Variability

Computing one-minute deltas is the statistical technique known as differencing, or first-differencing to be exact. Differencing, $(x_t - x_{t-1})$, essentially removes the long term trend in the mean, effectively converting a non-stationary time series into a stationary one. A "differenced" series (of deltas) is the first derivative of the original series.

This process is illustrated in Figure 3-8, which shows a three-hour segment of the load on April 23rd of the study year, and the series produced by computing and plotting one-minute deltas. Note that the original series is plotted against the left axis and the deltas are plotted against the right axis, magnified for display.

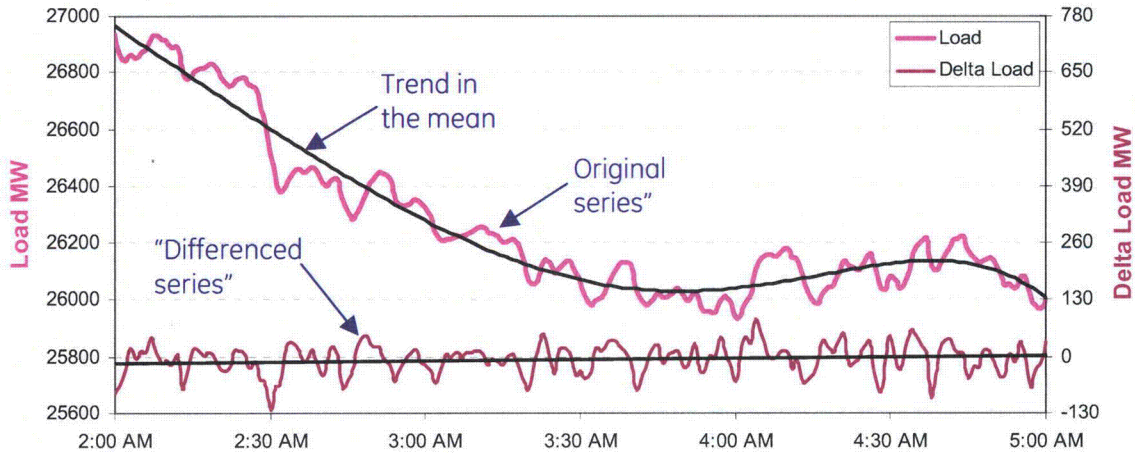

Figure 3-8 - Segment of a load series and the deltas produced by first "differencing"

Experience has shown that in this timeframe, variability of load and net load is driven mostly by "random" jitter in load and wind generation. In between dispatch cycles, these changes must be accommodated by a market-driven ancillary service. The degree to which wind generation increases the variability of net load in the one-minute timeframe (and by proxy ancillary service requirements) is quantified by computing the standard deviation of the deltas. Table 3-2 below summarizes the variability of load and net load in the one-minute timeframe for the entire study year.

Table 3-2 - Summary of One-Minute Net Load Variability for the Study Year

Case	Sigma (σ) of Net Load Deltas (MW/min)	Max. Negative Net Load Delta (MW/min)	Max. Positive Net Load Delta (MW/min)	No. Deltas > 2.5 (load) σ (–/+) (%)	σ % Increase with Wind
Base Case: Load w/ no Wind Generation	43.2	-513.7	491.6	4696 / 3805 (0.89 / 0.72)	--
Load w/ 5000 MW Wind Generation	45.6	-526.6	507.2	6181 / 4807 (1.17 / 0.91)	**5.4%**
Load w/ 10,000 MW Wind Generation (1)	47.7	-534.0	529.3	7635 / 6041 (1.45 / 1.15)	**10.5%**
Load w/ 10,000 MW Wind Generation (2)	47.3	-536.7	520.4	7350 / 5757 (1.40 / 1.10)	**9.4%**
Load w/ 15,000 MW Wind Generation	49.7	-552.6	538.3	9277 / 7408 (1.77 / 1.41)	**14.9%**

The results confirm that, overall, the one-minute net load variability *increases linearly* with wind penetration, going from just over 5% with 5 GW of wind generation to about 15% with 15 GW. In this short timespan, the random component of the wind is an incremental component superimposed upon the random load variations.

In addition, the results reveal that the number of "large" one-minute perturbations increases with additional wind generation. This is clearly seen in Figure 3-9 which shows the distribution of one-minute deltas for load-alone, and load with 5000 and 15,000 MW of wind generation for the study year. This was produced by sorting the 525,599 deltas into 15-MW-wide bins and plotting them on a histogram.

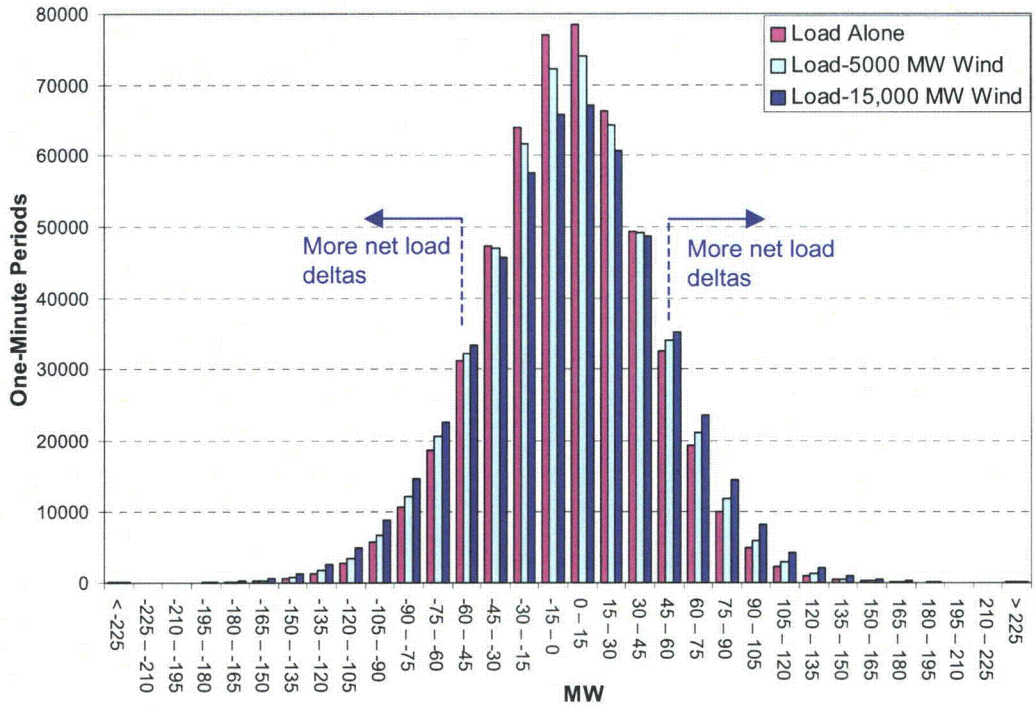

Figure 3-9 - Distribution of 1-minute deltas for load and net load with 5 and 15 GW of wind

On the frequency plot, the arrows indicate that there are more periods when net load deltas (blue bars) are larger than 45 MW/min, than periods when load deltas (magenta bars) are greater than this value. In fact, if 2.5 times sigma-of-the-load-deltas is a threshold for a large change[1], then the number of "large" one-minute down-ramps in Table 3-2 increases by 98% over load-alone, with the addition of 15 GW of wind generation. Similarly, the number of "large" one-minute up-ramps increases by 95%.

Not only does the number of large deltas increase, but the magnitude of extreme deltas also increase with wind generation. This would show up in Figure 3-9 as blue bars on extreme tails of the histogram, if the resolution were sufficiently increased. From Table 3-2, there is an approximately 40 MW/min increase in the largest down-ramp going from the no-wind case to the 15-GW wind generation case; and similarly, a 47 MW/min increase in the largest up-ramp. The same observations generally apply to the previous year's data. See Appendix C.2 for additional data and plots.

To summarize, in the one-minute timeframe, incremental wind output increases not only the overall net load variability but also the amount and size of large and extreme deltas.

[1] In a normal distribution of deltas, 98.8% of the area under the normal curve is within 2.5σ of the mean.

3.2.2. Five-Minute Variability

Five-minute time series for load and net load are produced by integrating the one minute data series. For every five minute block (or every five one-minute observations) a five-minute data point is produced by averaging the five one-minute samples. This produces one-year load and net load series with 105,120 observations each. Five-minute deltas for load and net load can then be computed in the same manner as with one-minute deltas.

Understanding variability in five-minute timeframe is important because in the nodal market units will be dispatched every five minutes. The additional operational burden imposed by wind in this timeframe will certainly translate into more ramp and range requirements for units on dispatch.

As the resolution decreases (i.e. in larger timeframes), the impact of the long term ramps in load and wind generation becomes more evident, and the impact of "random" jitter becomes less important.

Table 3-3 summarizes the variability of load and net load in the five-minute timeframe. Figure 3-10 plots the distribution of five-minute deltas for the entire study year.

Table 3-3 - Summary of Five-Minute Net Load Variability for the Study Year

Case	Sigma (σ) of Net Load Deltas (MW/5-min)	Max. Negative Net Load Delta (MW/5-min)	Max. Positive Net Load Delta (MW/5-min)	No. Deltas > 2.5 (load) σ (–/+) (%)	σ % Increase with Wind
Base Case: Load w/ no Wind Generation	167.4	-881.2	958.8	621 / 787 (0.59 / 0.75)	--
Load w/ 5000 MW Wind Generation	177.3	-916.6	988.9	1007 / 977 (0.96 / 0.93)	**5.9%**
Load w/ 10,000 MW Wind Generation (1)	188.0	-951.1	992.1	1482 / 1368 (1.41 / 1.30)	**12.3%**
Load w/ 10,000 MW Wind Generation (2)	185.2	-938.3	1002.4	1353 / 1273 (1.29 / 1.21)	**10.6%**
Load w/ 15,000 MW Wind Generation	197.1	-948.2	1022.2	1970 / 1856 (1.87 / 1.77)	**17.8%**

In this timeframe, the same general trends observed in the one-minute data with regard to sigma and large deltas can be observed. Incremental wind generation increases the overall net load variability (as measured by sigma of the deltas), as well as the number and magnitude of large period-to-period changes. However, a closer comparison of the one-minute and five-minute timeframes lead to several observations:

1. The standard deviations, sigma (σ), of the deltas are (as expected) larger in the five-minute timeframe, but *not* five times as large as the one-minute sigma.

2. For each wind generation scenario, the increase in net load variability over the load-alone case, in the five-minute timeframe, is larger than the corresponding scenario in the one-minute timeframe, i.e. *there is an additional component to five-minute variability.*
3. The *relative* (%) increase in the number of net load outliers over load-alone is greater in the five-minute timeframe, even though the *relative* increase in the size of the largest delta is comparable.
4. The distribution of the five-minute net load deltas is decidedly less bell-shaped (more triangular) than the distribution of one-minute net load deltas. This implies the presence or influence of a non-random source of variation.

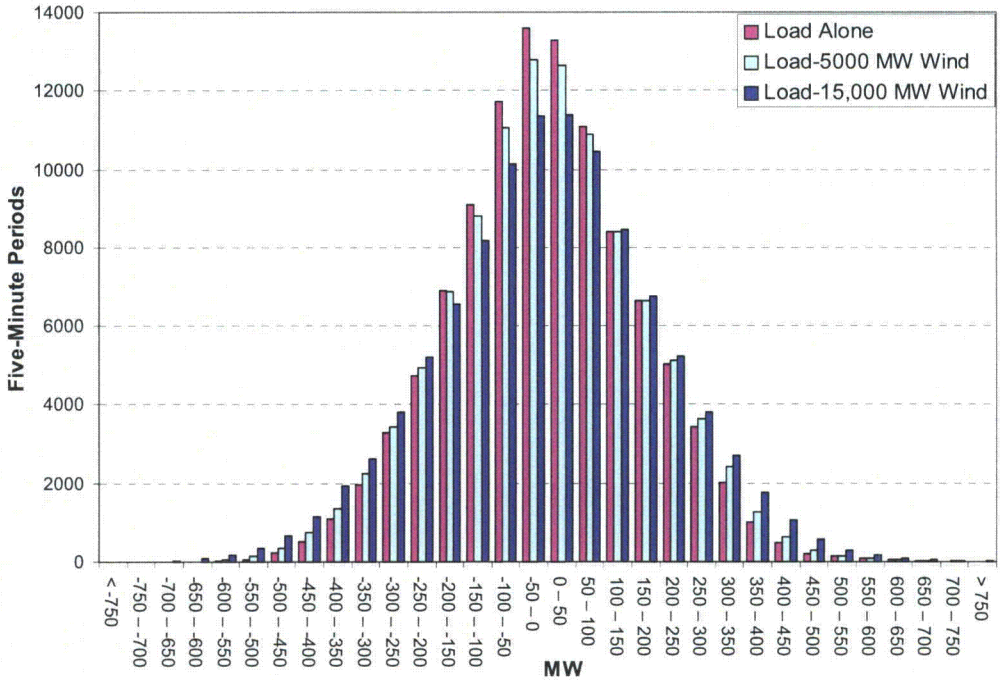

Figure 3-10 - Distribution of 5-minute deltas for load and net load with 5 and 15 GW of wind generation capacity.

These observations become even more pronounced in longer timeframes as the influence of short-term random variations begin to be dominated by the long-term ramp. This can be seen in the results for the fifteen minute and half-hour timeframes which are included in Appendix C.2.

3.2.3. Effect of Short Term Variations and Long Term of Ramping

Based on observations of net load variability over various timeframes from one minute to one hour (and longer) two general observations are:

- Variations over timespans greater than five minutes are primarily due to load cycle or long-term ramping, which dominate random noise variations
- Random "noise" variation is more influential during shorter timespans

Consider the Figure 3-11 below which shows a portion of the summer load pickup period, July 10, 6-7 AM on of the study year. The solid magenta and blue traces are load and net load series, plotted against the left scale, and the dotted magenta and blue traces and load and net load one-minute deltas, plotted against the right scale. Figure 3-12 shows the load and net load deviations from a straight line, i.e. load and net load with ramp component removed.

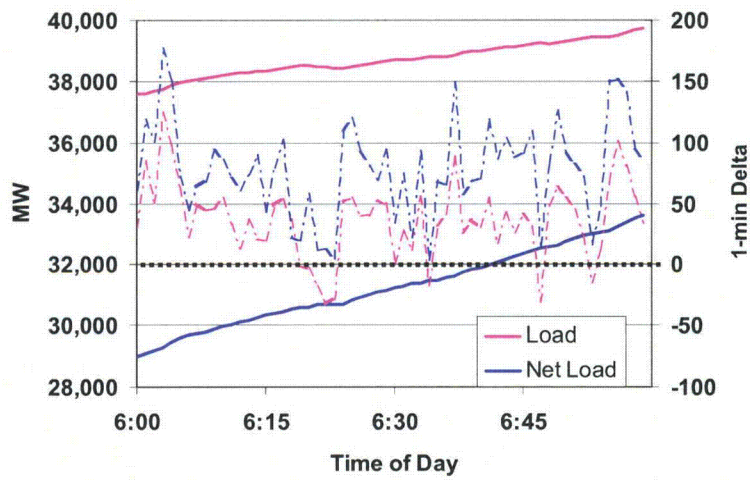

Figure 3-11 - Load and net load traces with 1-min deltas for July 10, 6-7 AM

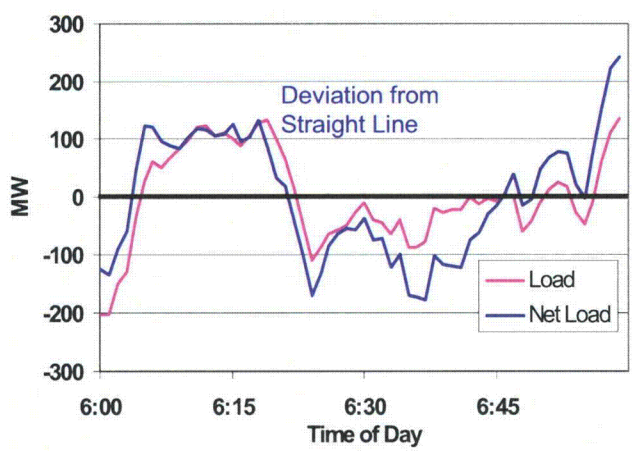

Figure 3-12 - Load and net load deviations from a straight line for summer morning period

Over the hour, load and net load vary randomly from minute to minute even while ramping steadily. The one-minute deltas in Figure 3-11 represent the minute-to-minute variation, which is essentially random noise variation with a small adder due to the portion of the long-term (hour) ramp that occurs in the minute. The effect of the ramp component is to bias the net load deltas and create incremental differences from the load deltas. Figure 3-12 illustrates without the long-term ramp component, load and net load variation exhibit similar characteristics, driven by stochastic load and wind variation.

During a light load period such as the early spring morning shown in Figure 3-13, load and net load may be fairly flat (little or no ramp). Consequently, the load and net load one-minute deltas (dotted magenta and blue traces) are more similar because the impact of the ramp component is reduced. Figure 3-14 shows the deltas without the ramp.

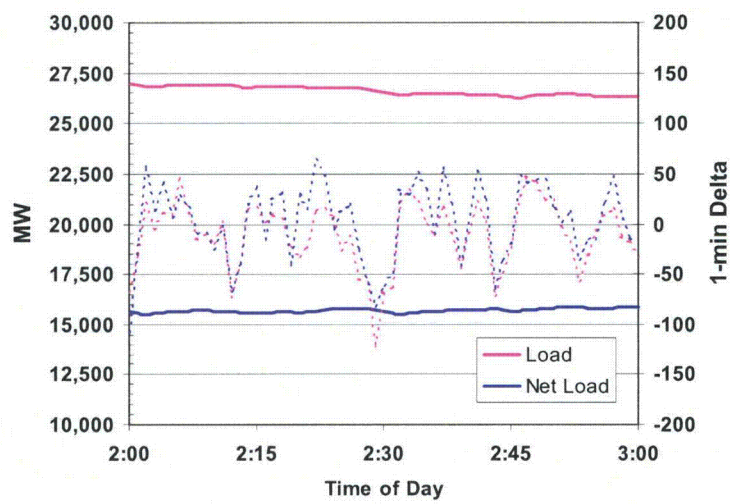

Figure 3-13 - Load and net load traces with 1-min deltas for April 23, 2-3 AM

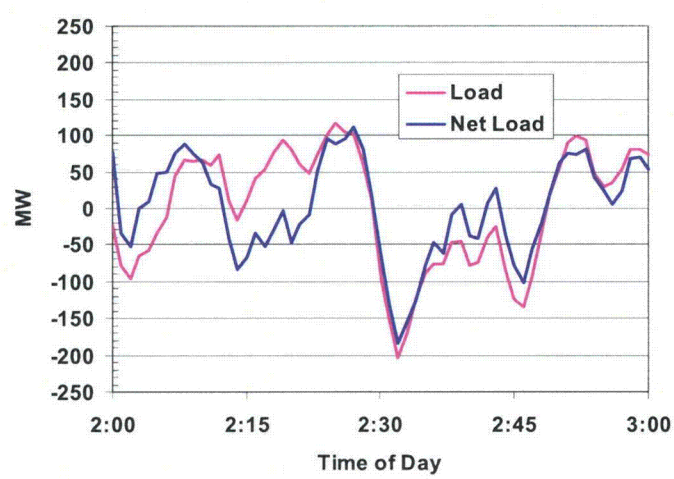

Figure 3-14 - Load and net load deviations from a straight line for light load period

As the timeframe becomes longer, the ramp component has a greater effect on the deltas because the portion of the ramp that occurs in a longer timeframe is greater. For the five-minute timeframe, the long-term ramp adder is five times as large as in the one-minute timeframe, but there is still a significant contribution from stochastic noise variation. However, by for fifteen minute timespans and greater, the deltas are dominated by the long-term ramp component (as summarized in Appendix C.2). The next section discusses variability in the one-hour timeframe, which is almost completely driven by the load and wind generation ramp rate.

3.2.4. Hourly Variability

The one-hour timeframe gives a good indication of the long term ramping requirements due to additional wind generation. At this resolution, the random perturbations of load and net load are less significant and long-term ramping dominates the net load variability. Table 3-4 summarizes one-hour load and net load variability for the study year. The results in Table 3-4 are consistent with observations in other timeframes; namely as wind penetration increases, the net load variability (as measured by sigma of the one-hour deltas) increases linearly. However, in this case, wind generation adds to variability primarily because it creates larger daily net load swings.

Table 3-4 - Summary of One-Hour Net Load Variability for the Study Year

Case	Sigma (σ) of Net Load Deltas (MW/hr)	Max. Negative Net Load Delta (MW/hr)	Max. Positive Net Load Delta (MW/hr)	No. Deltas > 2.5 (load) σ (–/+) (%)	σ % Increase with Wind
Base Case: Load w/ no Wind Generation	1758	-4838	5203	43 / 26 (0.49 / 0.30)	--
Load w/ 5000 MW Wind Generation	1867	-5813	5461	94 / 42 (1.07 / 0.48)	6.2%
Load w/ 10,000 MW Wind Generation (1)	1989	-6124	5797	127 / 85 (1.45 / 0.97)	13.1%
Load w/ 10,000 MW Wind Generation (2)	1954	-6175	5681	119 / 69 (1.36 / 0.79)	11.2%
Load w/ 15,000 MW Wind Generation	2086	-6726	6240	170 / 134 (0.94 / 1.53)	18.7%

Figure 3-15 shows the distribution of one-hour deltas for load-alone, and load with 5 GW and 15 GW of wind generation. This was produced by sorting the 8759 deltas into 400-MW-wide bins and plotting them on a histogram. The impact of the non-random ramp component can be seen in the frequency plot. As the timeframe becomes longer, the frequency plot of deltas becomes increasingly more triangular, than bell-shaped.

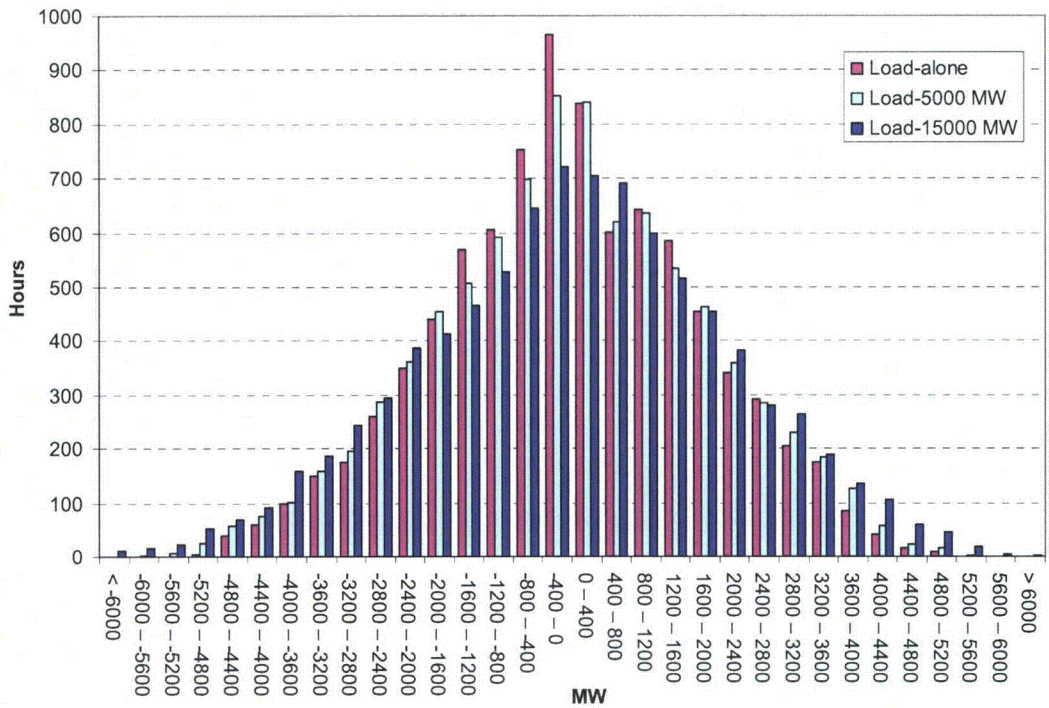

Figure 3-15 - Distribution of 1-hour load and net load deltas with 5 GW and15 GW of wind

The number and size of the extreme deltas also increases with additional wind generation. In accordance with the trend over timespans, the increase in the number of "large" deltas as wind penetration increases is greater in this time frame than previous timeframes. The next section examines this and other trends in variability over timeframes.

3.2.5. Trends in Variability over Timeframes

We have seen that in the one-minute timeframe, load and net load variability are driven primarily by random perturbations. As the timeframe becomes longer, the influence of the long-term ramp in load and wind generation has greater influence on period-to-period variability. Figure 3-16 plots the standard deviation of deltas for the wind generation scenarios over the one-minute, five-minute, fifteen-minute and one-hour timeframes. Figure 3-17 plots the normalized sigma for each timeframe in MW/min [2]. In both plots, the data points for each timeframe are fitted with a linear trend line to show the variation as wind penetration increases.

Both plots show that in each timeframe, the variability (sigma) increases linearly with wind penetration (as detailed in earlier data tables). The slope (from no wind generation to 15 GW) is relatively shallow, and *appears* to be more or less constant over all

[2] Sigma is normalized by dividing by the timespan to give sigma in MW/min (e.g. $\sigma_5/5$)

timespans in Figure 3-16. The normalized plot more clearly illustrates the increase and its linearity.

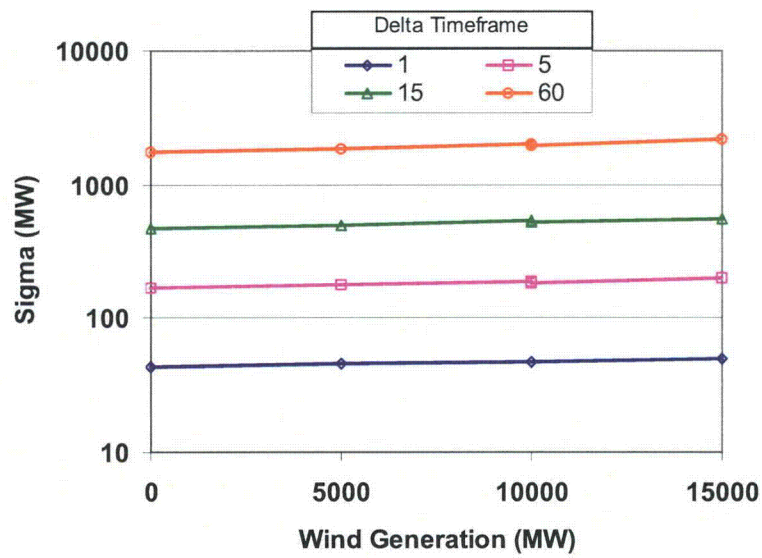

Figure 3-16 - Variability as a function of wind penetration

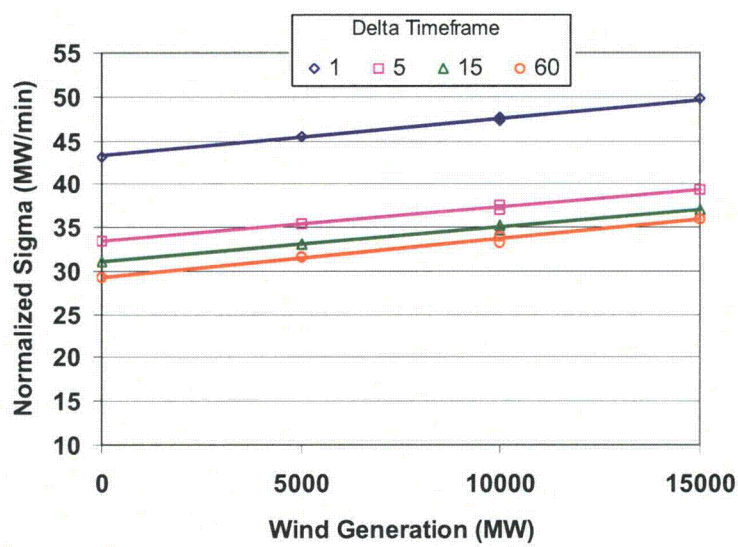

Figure 3-17 - Normalized variability as a function of wind penetration

Figure 3-18 shows a plot of normalized sigma *versus timespan* on a log scale. In this plot there is a distinct change in the slope of the normalized sigma trace as the timespan increases. The change occurs somewhere between the 5 and 15 minute timeframes. This is consistent with the observation that there is a baseline of variability that is a function of the longer-term load cycle, and an incremental amount of variation due to random noise appears at the shortest timeframes (1 and 5 minute).

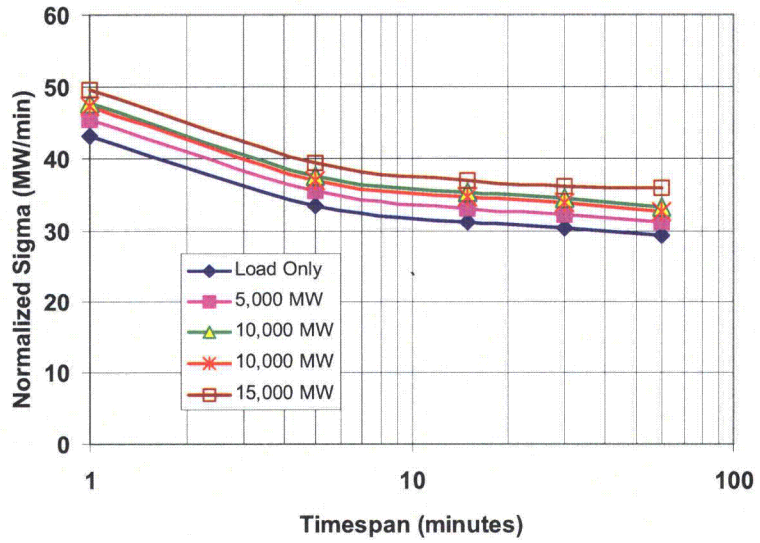

Figure 3-18 - Normalized variability as a function of timespan

Figure 3-19 shows the incremental variability (relative to load alone) due to wind generation in each timeframe. As the timespan becomes longer, the incremental variability increases, but begins to taper off, and appears saturate at longer timeframes.

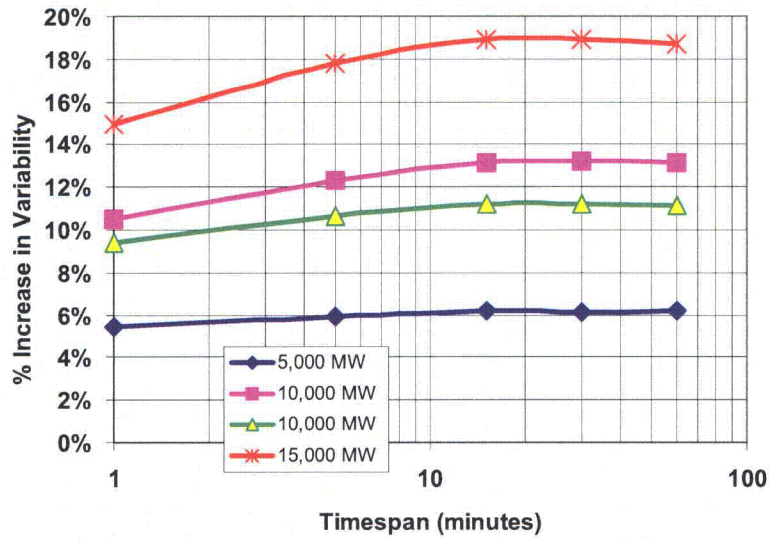

Figure 3-19 - Increase in variability due to wind as a function of time span

The key take-aways from the analysis of variability over the various timeframes are: (1) incremental wind generation causes a linear increase in period-to-period variability over all timespans, (2) in longer timespans variability is primarily driven by load cycling, but in shorter timespans there is an incremental component due to stochastic variation, and (3) the impact of wind generation on variability is more significant in longer timespans because wind generation creates larger swings in daily net load.

3.3. Seasonal Trends in Variability

Over the course of a typical year, load and net load vary with the seasons, as they are both largely driven by common weather-related factors. Therefore, some seasonal trends in period-to-period variability are expected. Figure 3-20 shows the daily average load and net load with 15 GW of wind generation over the study year, and the maximum positive and negative net load one-hour deltas for each day of the year. The upper solid magenta and blue traces are load and net load respectively. The two lower solid green traces are maximum positive and maximum negative one-hour net load deltas. The two lower dotted orange traces are maximum positive and maximum negative one-hour load deltas.

As expected, load and net load are greatest in the summer months and lowest in the spring and fall. The peak load day is August 17th and the minimum load day is March 27th. Across the year, incremental wind generation generally biases the net load, and increases the variability. The negative net load deltas or hourly down-ramps (lower green trace) generally tend to be larger in the late spring, summer, and early fall, while the up-ramps (upper green trace) are generally larger in late fall and winter. However, when the load deltas (dotted orange traces) are compared with net load deltas, it is clear that the *incremental* net load hour-to-hour change is greatest in the late spring and summer.

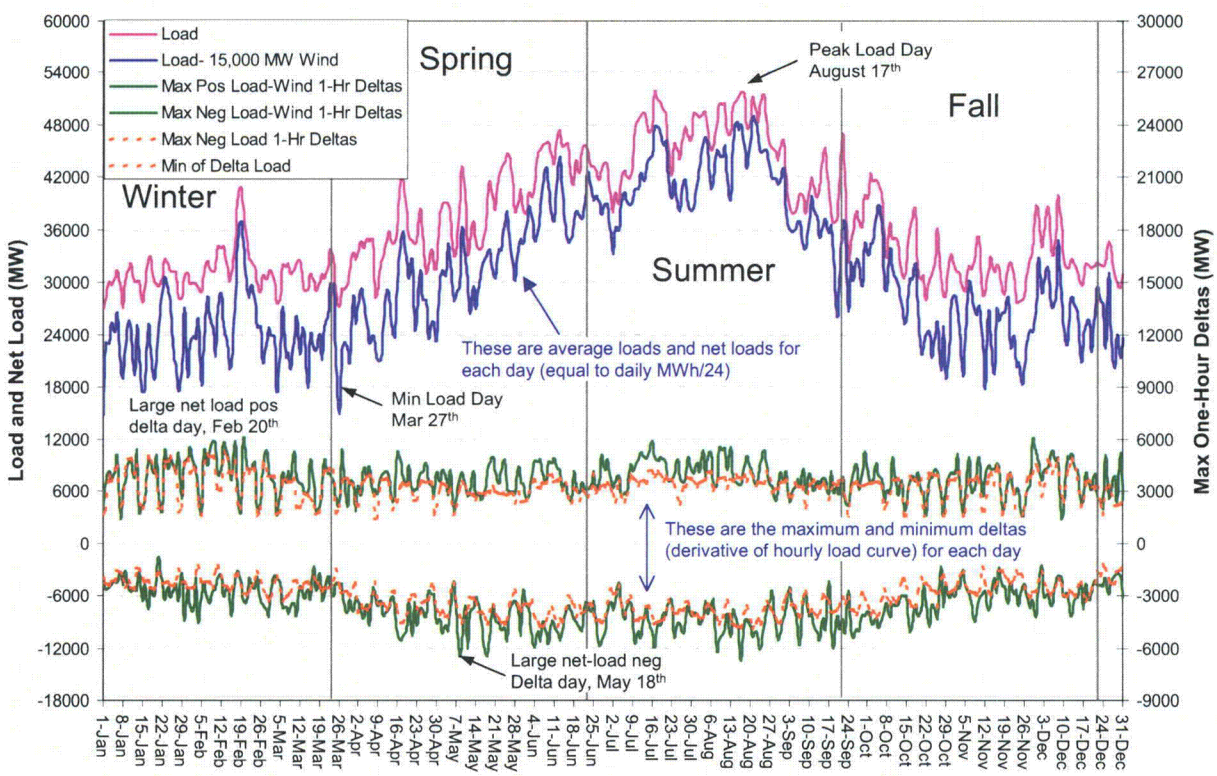

Figure 3-20 - Profiles of daily average load and net load, and maximum daily 1-hour deltas

The impact of wind generation throughout the year can be more clearly seen from an examination of a few "interesting" days from Figure 3-20. For example, load and net load variability on the peak load day (August 17th) and minimum load day (March 27th) are plotted in Figure 3-21 and Figure 3-22 for the 15-GW wind generation scenario.

Wind output has relatively little impact on the peak day, reducing the peak by about 3000 MW and shifting it by approximately 1 hour. On the minimum load day, wind generation pushes the minimum load point to a "very low" value and the ramp rate during load rise is increased. Key questions are what units are committed during this period, and do they have the required ramping capability? This issue is further explored in Section 6.

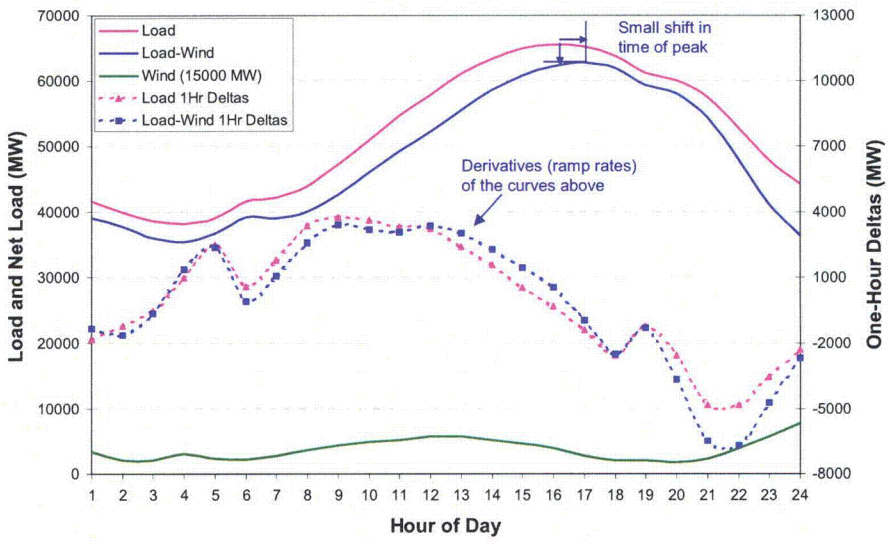

Figure 3-21 - Variability on peak load day

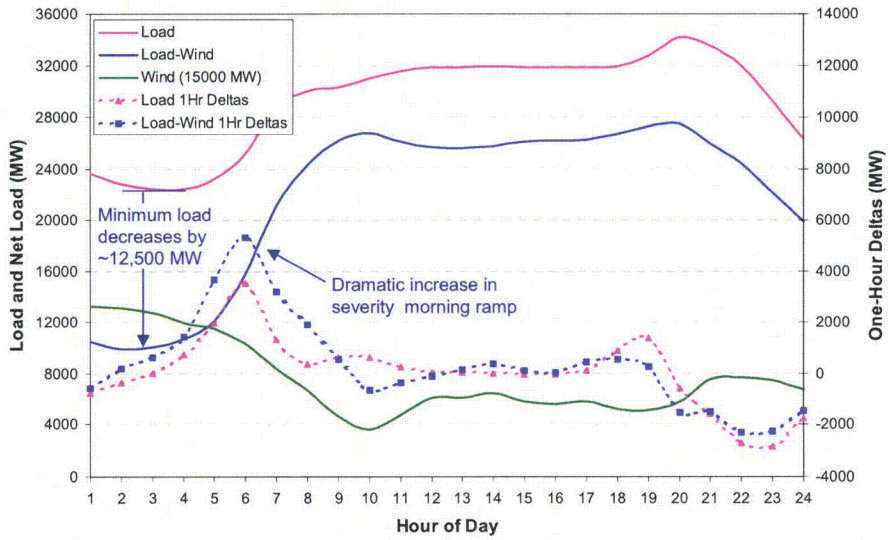

Figure 3-22 - Variability on minimum load day

Another interesting day is May 8th during which the largest net load one-hour down-ramp occurs. Figure 3-23 shows that wind generation drops precipitously in evening just before the evening load roll-off, causing a later than expected peak in net load, with resulting increases in hourly ramp rates.

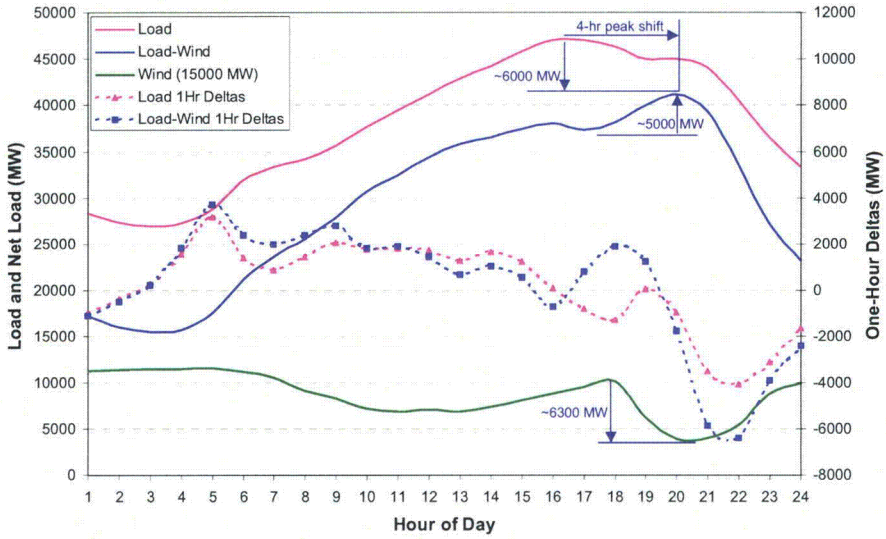

Figure 3-23 - Variability on the day with the largest net load 1-hour negative net load delta

July 12th is the day during which net load undergoes the largest hourly up-ramp and down ramp event in the same day. Figure 3-24 shows that severe anti-correlation of diurnal load and wind output curves causes large, sustained morning and evening ramps.

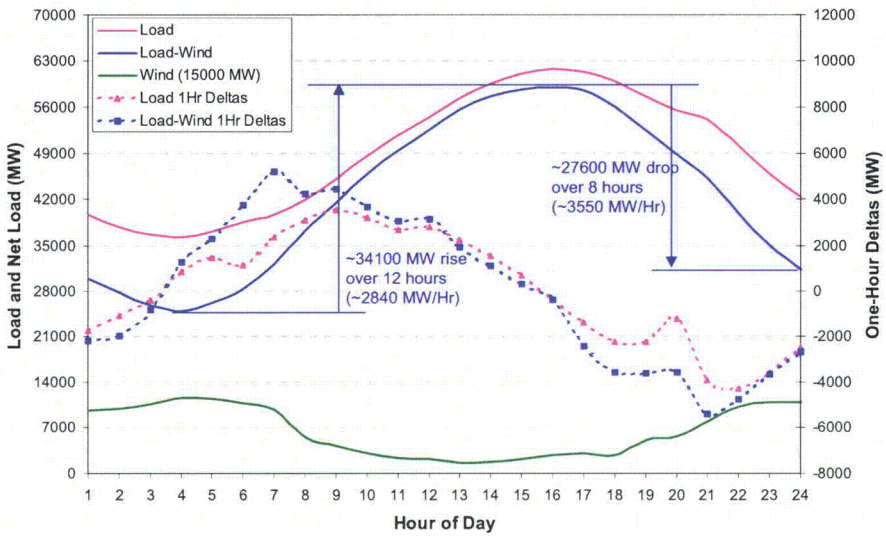

Figure 3-24 - Variability on the day with the largest net load 1-hour up-ramp and down-ramp

Another way to examine seasonal differences in load and net load variability is to look at typical winter, spring, summer, and fall days for broad trends. The plots in Figure 3-25 (next page) show load and net load variability during "typical" seasonal days for the 15-GW wind generation scenario. The representative seasonal days, January 27th, April 23rd, July 10th and October 25th were selected based on the fact that they did not significantly deviate from seasonal or expected averages.

On the plots, the solid magenta, green and blue traces are load, wind generation and net load respectively plotted against the right scale. The dotted magenta and blue traces are load deltas and net load deltas plotted against the left. Note that the scales for the typical summer day plot are different from the other three plots for display purposes.

Since these typical plots are merely snapshots of the seasonal variability, one should be careful when drawing broad inferences. However, from a macro perspective, the plots conform with previous observations: hour-to-hour changes (deltas) are generally larger in the summer, and there tends to be larger differences between load deltas and net load deltas for the non-winter days.

The bottom line from an analysis of the seasonal trends in variability is that wind generation tends to have a greater overall impact on variability in the summer, late spring and early fall, but variations in winter and early spring may be more operationally significant due to low net load levels.

Additional operational challenges may be created during periods where wind generation aggravates balance of generation ramp and range requirements. Some of these periods that may impact ancillary service requirements are discussed in the next two sections.

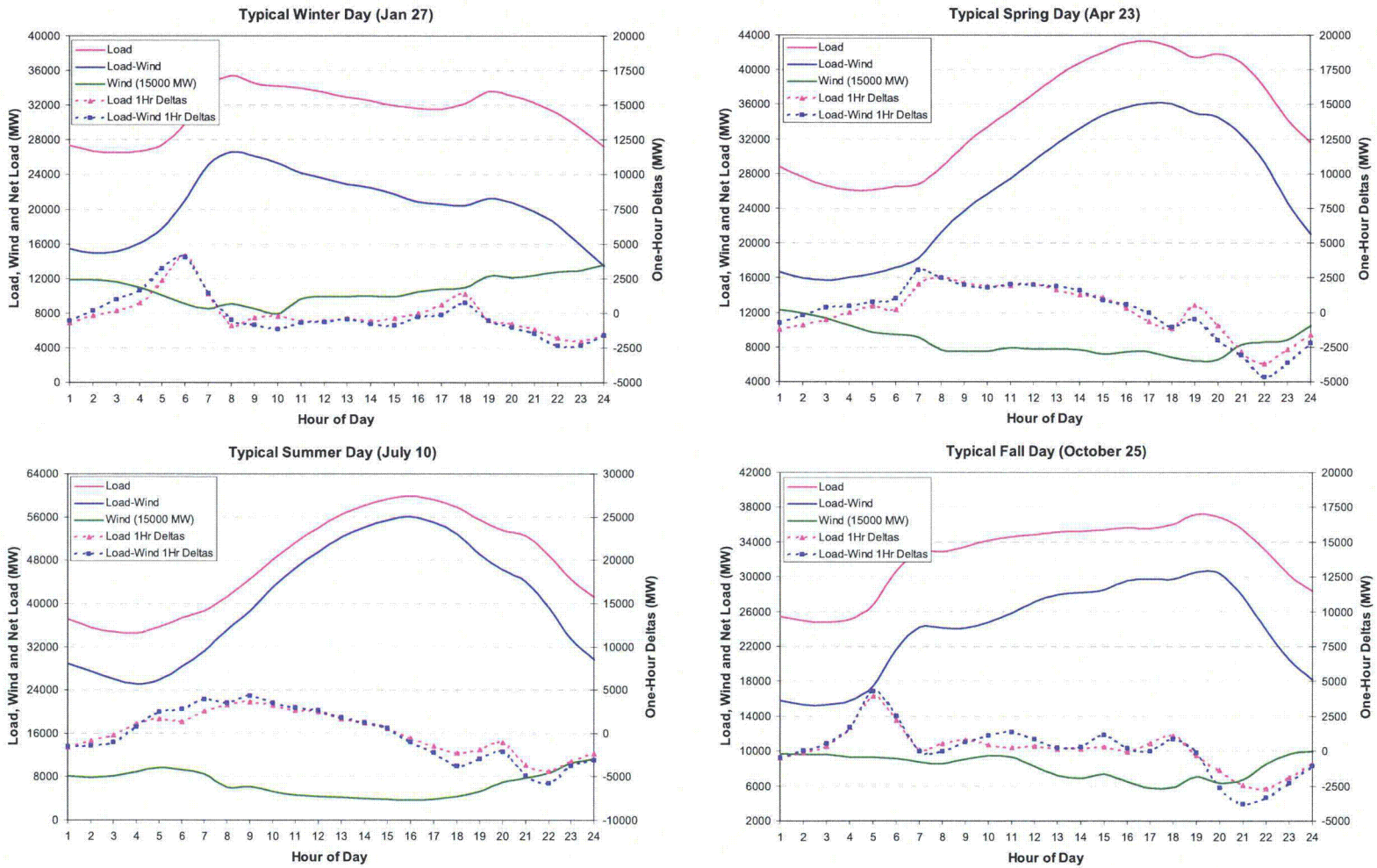

Figure 3-25 - Variability of load and net load with 15,000 MW of wind generation for typical seasonal days

3.4. Variability by Load Level

The ability of the system to accommodate net load variations is largely a function of the absolute net load level. System maneuverability tends to increase with the generation level because variations of a given magnitude are larger in proportion to the committed generators and units lower on the dispatch stack tend to be base load units that are less maneuverable. This section will examine the correlation of net load variability with load levels throughout the year. For clarity and brevity, most of the charts and discussion will focus on the largest wind generation scenario, 15,000 MW, but information on the other wind generation scenarios is included in Appendix C.3.

Figure 3-26 shows the cumulative distribution of wind generation and instantaneous wind penetration over the entire study year. The magenta trace is the total wind output for the 15 GW scenario, plotted against the left scale. The blue trace is the instantaneous wind penetration[1] plotted against the right scale. Both series of 8760 observations are sorted independently and plotted. Each point on the curves gives the number of hours of the year when wind output or wind penetration is at or above a certain value.

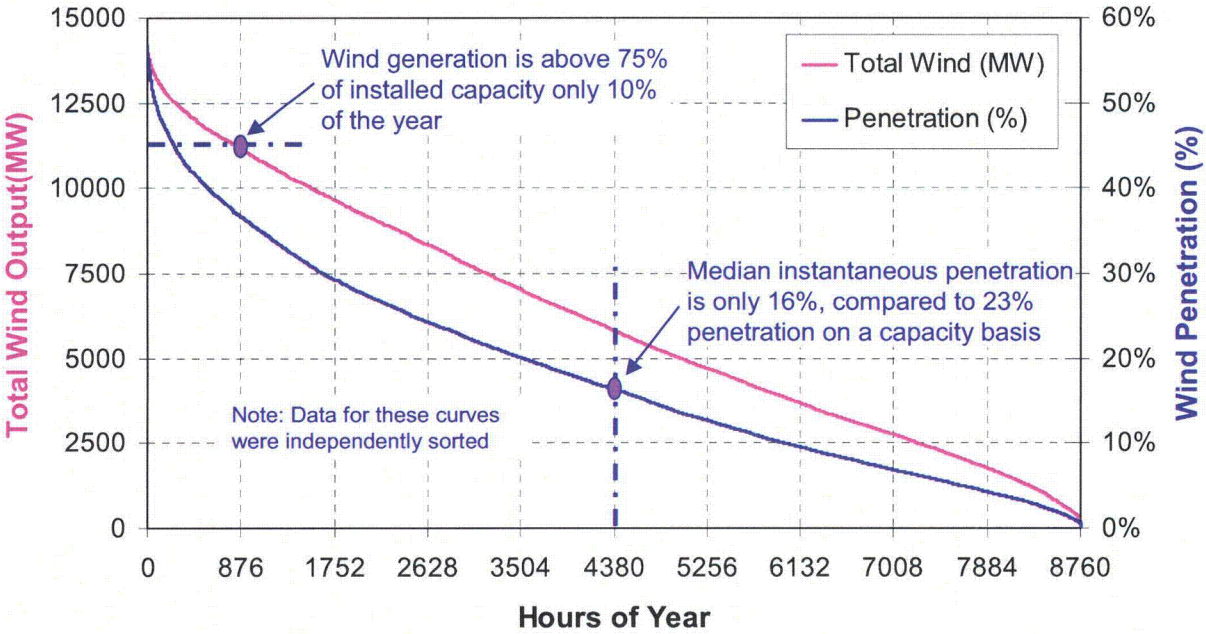

Figure 3-26 - Wind output duration and instantaneous penetration (15,000 MW)

For this wind generation scenario, there are a few hours of the year when the instantaneous wind penetration is over 50%. No doubt, this corresponds to minimum load periods, which tend to be operationally challenging (discussed later in this section).

[1] The instantaneous wind penetration is the wind generation at a particular hour divided by the load at that hour, expressed in percent.

Table 3-5 summarizes the maximum instantaneous wind penetration for all wind generation scenarios.

Table 3-5 - Maximum Instantaneous Wind Penetration for each Scenario

Wind Scenario (MW)	5000 MW	10,000 MW (1)	10,000 MW (2)	15,000 MW
Instantaneous Wind Penetration (%)	20%	39%	38%	57%

On a seasonal or monthly basis, there are considerable differences in wind duration and instantaneous penetration. Figure 3-27 and Figure 3-28 show duration plots for the peak load month, August, and the minimum load month, March for the 15-GW wind generation scenario. Additional duration plots are included in Appendix C.3.

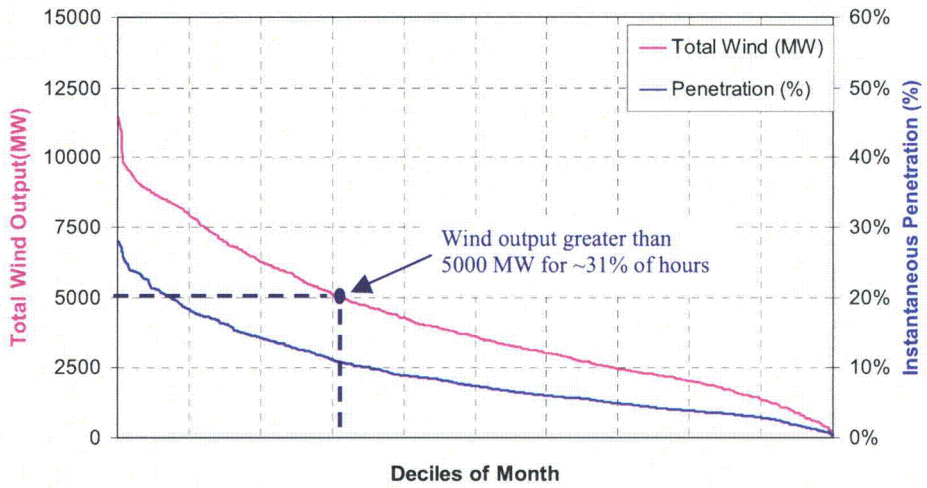

Figure 3-27 - 15 GW wind output duration and penetration for peak load month (August)

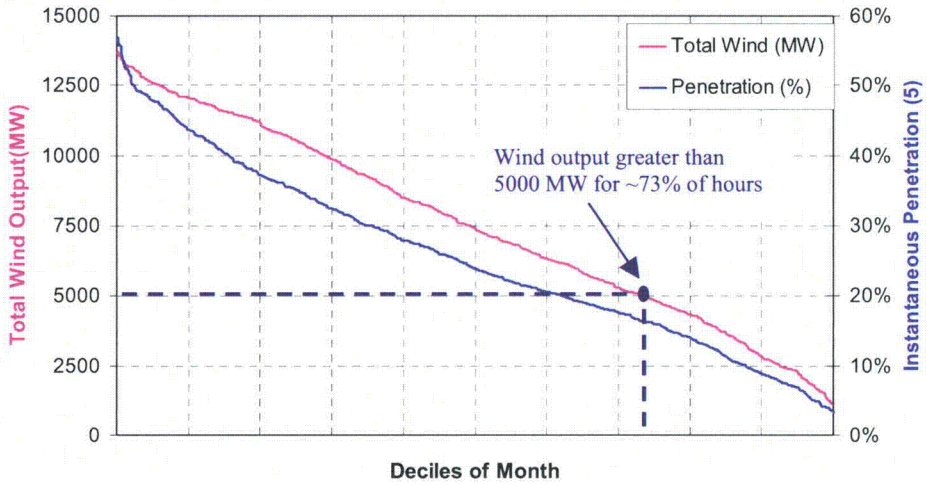

Figure 3-28 - 15 GW wind output duration and penetration for minimum load month (March)

The plots show that the instantaneous wind penetration is smallest at peak load (28%) and greatest at minimum load (57%), as expected. The load is greatest during the summer months and wind generation tends to be less during the mid-day peak load hours. In fact, total wind output is *less* than one-third rated capacity for about 70% of the hours in August. Conversely, at minimum load, the highest level of instantaneous wind penetration is seen, because wind output tends to be high in the very early morning hours when load is the lowest. For the month of March, total wind output is *greater* than one-third rated capacity for approximately 70% of the hours.

Considering the fact that wind penetration is higher at low load hours and lower at peak load hours, the question is, how does net load variability change with load level? The box and whisker plot in Figure 3-29 attempts to answer this question by charting load and net load variability at various load levels.

The chart is based on one-hour load and net load deltas (hour-to-hour changes) during the hours when the load level is in a particular decile. The top 10% of load hours (peak load) are in decile 1 and the bottom 10% (low load) are in decile 10, i.e. load level decreases from left to right. The length of the solid rectangular boxes represents a spread of one standard deviation (σ) around the mean of the deltas, and the dashed rectangular boxes represent a spread of 2.5σ. Hence, the longer the box, the greater the variability at that load level. The whiskers show the maximum up-ramps and down-ramps for the deciles.

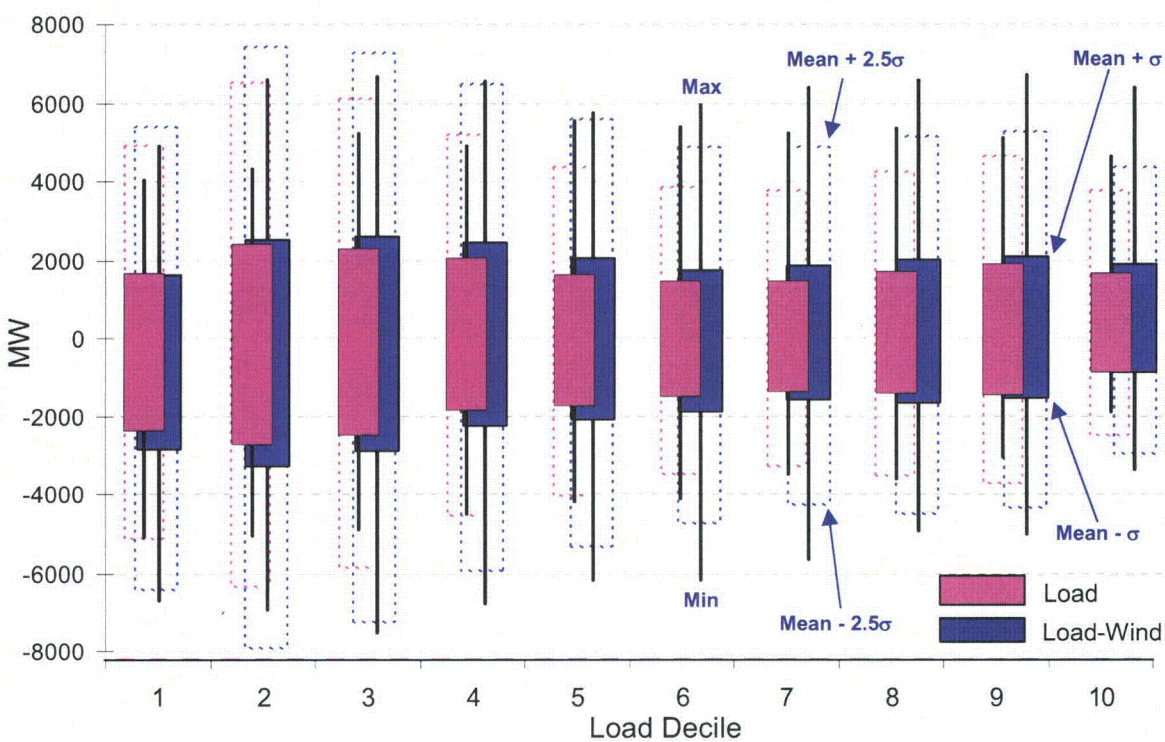

Figure 3-29 - Load and net load variability by load level for the 15 GW scenario

Considering the "whiskers" or max/min bars, it appears that wind generation increases the maximum up-ramps and (particularly) down-ramps at high and low load levels more than at mid-range load levels. The opposite seems to hold for variability. Comparing the magenta boxes (load-alone) to the blue boxes (net load with 15 GW of wind generation), there appears to be relatively little *incremental* variability due to wind output at the highest load levels and lowest load levels. Wind generation tends to have marginally more impact on variability at mid-range load levels. However, at low load hours, there are likely fewer dispatchable generators to accommodate the variability.

Figure 3-30 gives another view of the variability at different load levels by plotting the standard deviation of the one-hour deltas for load and net load.

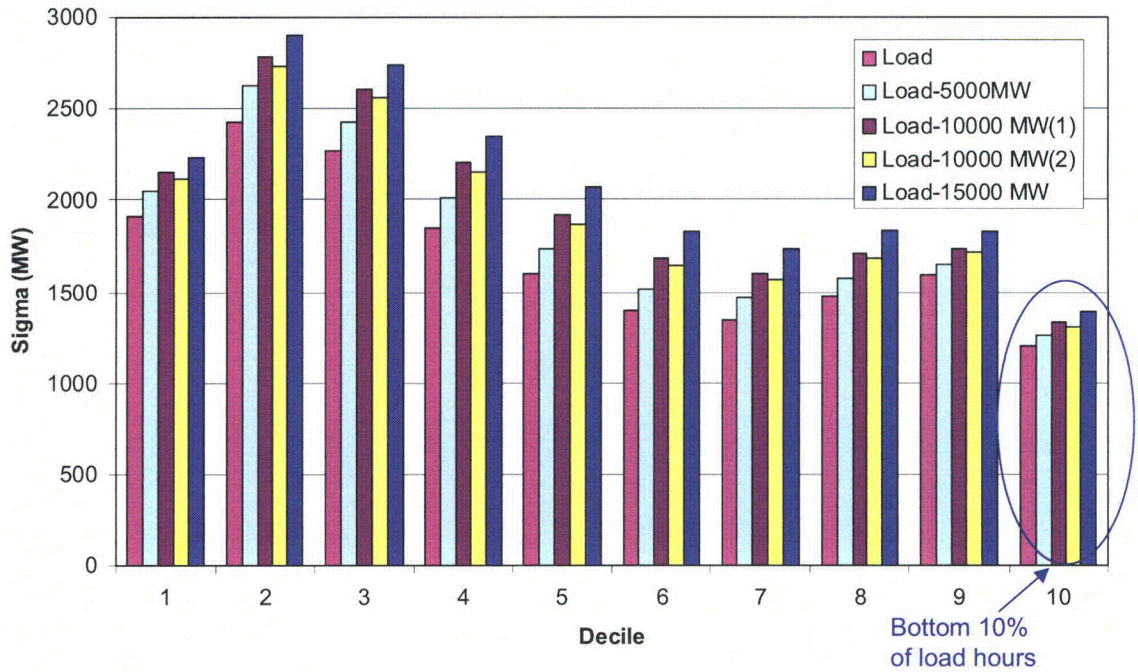

Figure 3-30 - Standard deviation of hourly deltas by load level

As wind penetration increases, the variability at the lowest 10% of load levels increases only slightly. As observed earlier, there are larger increases in variability at the mid-range load levels, but the low load period is operationally significant because flexible units might normally be de-committed during these hours.

Large amounts of wind generation online during low load hours would tend to push the "normal" minimum load point even lower, making the (economic) balance of generation mix even less flexible. Regardless of the capability of the system to maneuver at low load levels, there is potentially a point when the minimum net load is so low that non-conventional means may be needed to accommodate variability during these hours.

Figure 3-31 and Figure 3-32 illustrate the impact of increasing amounts of wind generation on net load, especially during low load hours.

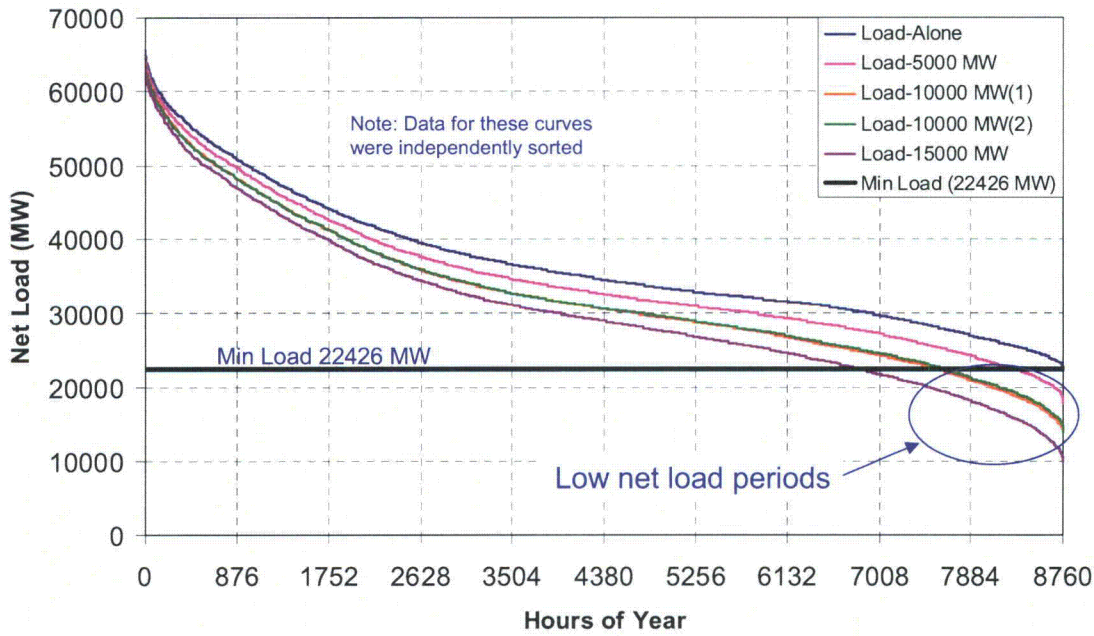

Figure 3-31 - Net load duration curves for various wind scenarios

Over the year, regardless of wind penetration, there are several hours when net load dips below the minimum load point (22,426 MW) for load alone. Admittedly, there is nothing inherently critical about this threshold. ERCOT may be able to operate their system well below this load level. However, it simply serves as a reference point for illustration. Figure 3-32 focuses on hours below the minimum load threshold.

For the 5 GW scenario, the minimum net load is 17933 MW. There are 470 hours when net load is lower than the minimum load point. Since the average wind output is double during low net-load hours, this represents about 10% of the wind energy. For the 15 GW scenario, the minimum net load is 9873 MW, a 56% reduction! Net load dips below the minimum load point for 1945 hours, representing 36% of the wind energy. Needless to say, curtailment of wind to hold the minimum load point would result in excessive energy loss. However, if the supply mix during these low load periods does not have adequate ramping capability to adjust for the wind variability, the reliable operation of the power system could be compromised. Mitigation measures to enable reliable operation with large wind penetration during low load hours are further discussed in Section 9.

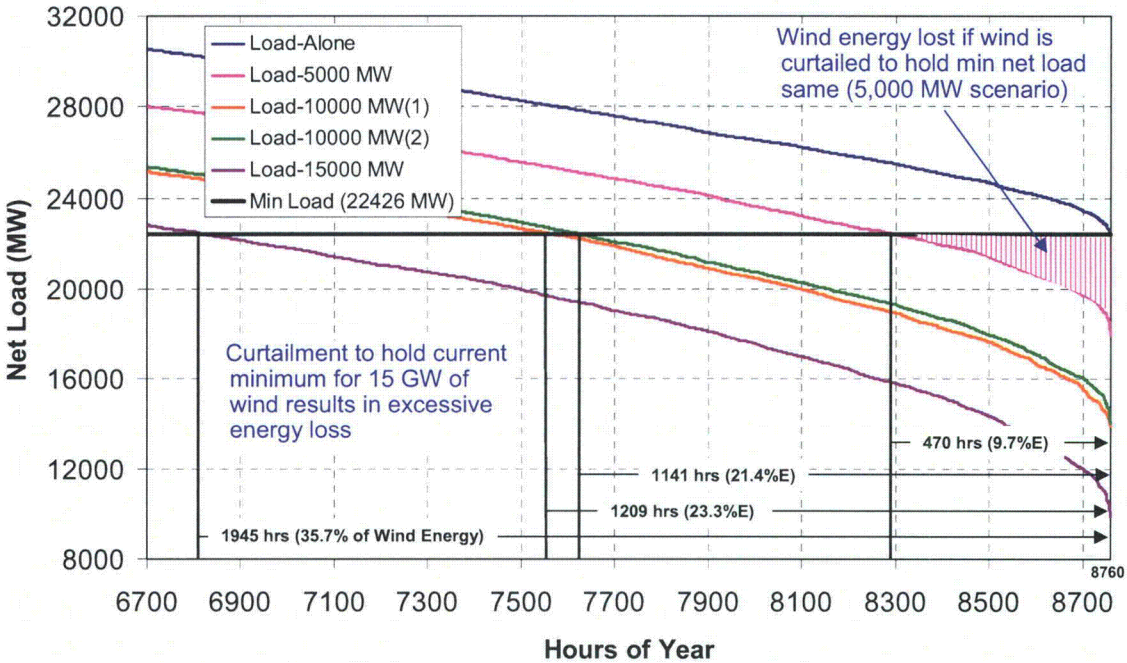

Figure 3-32 - Net load duration curves for various wind scenarios during low load hours

In summary, variability is relatively constant over the range of load levels, but tends to be greater during mid-range load levels than high and low load levels. Variability does increase with wind penetration but the increment tends to be less at high and low load levels. However, the low load periods are significant because net loads can be driven to extremely low levels with large wind penetration. The instantaneous wind penetration reaches 57% with 15 GW of wind and the minimum load point is reduced by 56%. Under these conditions additional measures may be needed to accommodate the net load variability.

3.5. Variability by Time-of-Day

Earlier sections have discussed broad trends in variability over various timeframes, across the year, and at different load levels. From a system operation point of view, broad trends in variability are not nearly as important as variability during particularly challenging periods. One such period, the minimum load, was discussed in the previous section. This section will discuss other challenging operating periods during the day created by large swings in net load.

In order to determine which are the "interesting" daily periods, average daily profiles for four seasonally representative months are created and overlaid with the hourly variability. Figure 3-33 shows these plots for load and net load with 15,000 MW of wind generation during January, April, July and October. Other plots are available in Appendix C.4.

The dashed magenta and blue curves are average daily load and net load, plotted against the left scale. Average daily profiles are created by averaging all similar hours during a month to create a 24-hour profile. The variability at each hour of the day, across the month, is captured by the box and whisker plot. The length of the rectangular boxes represents a spread of one standard deviation (σ) around the mean of the hourly change at a particular hour of the day. The whiskers show the maximum one-hour up-ramp and down-ramp over the month for a particular hour of the day.

Considering the relative length of the boxes in Figure 3-33, wind generation is a large contributor to variability over most of the day in the winter, particularly in the late afternoon and evening to early morning. Net load variability during the morning load rise period, is dominated by load changes. The largest one-hour net load rise is in late afternoon and the largest one-hour drop in the evening, both driven by large changes in wind production.

During the spring, wind output is a large contributor to ramping requirements during the morning load rise period and evening load drop-off. This can be more critical than an equivalent MW/hr rise in the summer, due to less generation committed. There are more extreme late evening load drops during the spring than winter, but wind generation tends to aggravate the one-hour drops even more.

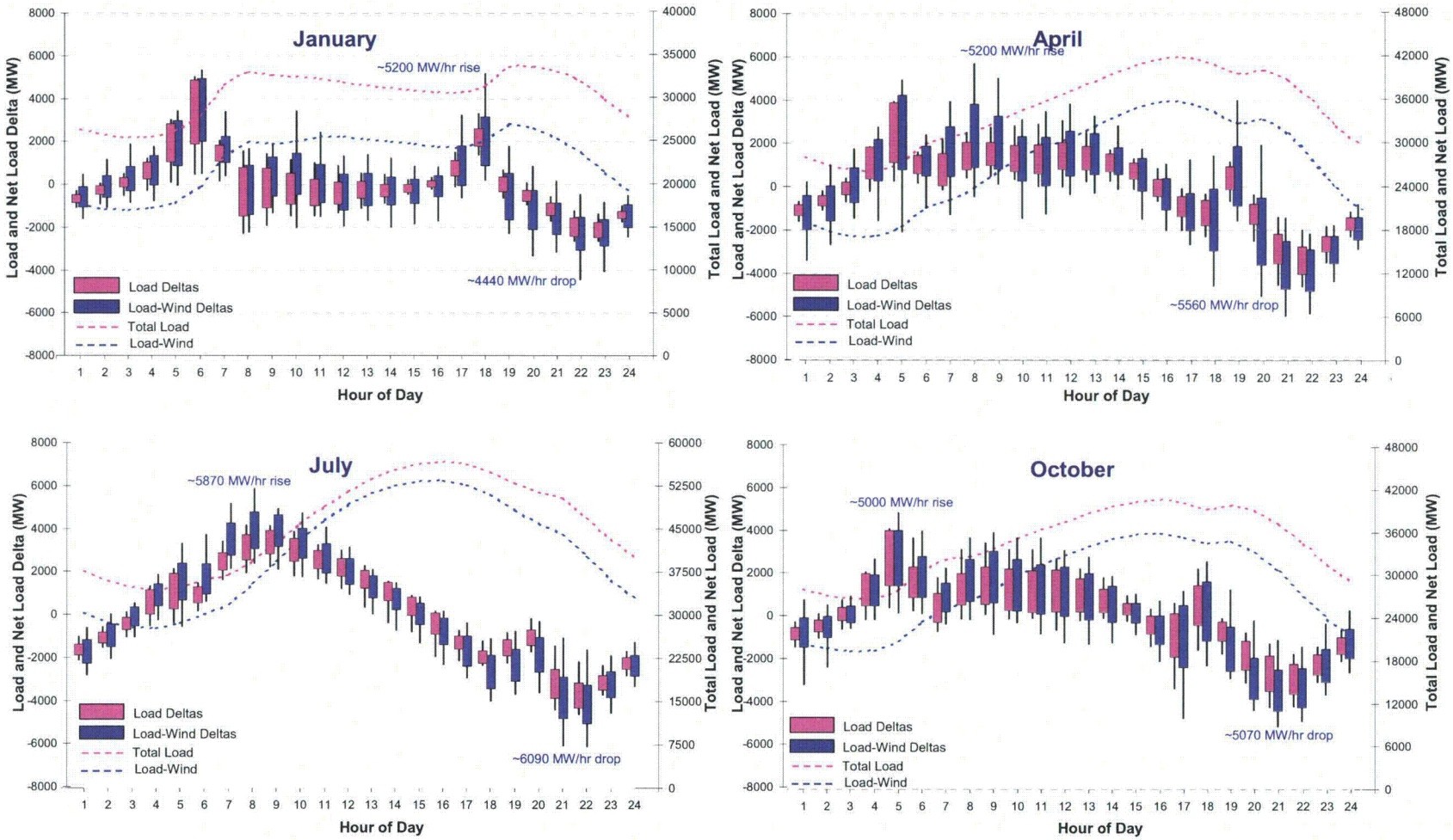

Figure 3-33 - Average daily profiles and hourly variability for load and load-15,000 MW of wind generation

In general, summer months experience less wind than other months, but output tends to drop faster in summer mornings and rise faster in the evenings than in other seasons (see Figure 3-3). With this in mind, it is not surprising that Figure 3-33 demonstrates that wind generation has the largest impact on net load variability during the early morning load rise period and evening load drop-off hours. The summer months also have the most extreme net load changes, which occur during the hours of greatest variability.

The profile of the typical fall month is similar to the typical spring month. Wind generation contributes to ramping requirements during morning load rise periods and evening load drop-off -- but to a lesser extent than the spring.

The charts in Figure 3-33 and discussion above, identify several daily periods of increased net load variability that merit closer examination. These include:

- Summer morning load rise: June – September, 7 – 11 AM
- Winter afternoon load rise: November – February, 4 – 6 PM
- Summer evening load drop: June – September, 8 PM – 12 Midnight

In addition, variability for spring morning load rise is plotted in Appendix C.4.

The following sections examine the net load variability during these periods, with particular emphasis on extreme ramps and trends for various scenarios.

3.5.1. Summer Morning Load Rise Period

The summer morning load rise period is designated as June to September, 7 – 11 AM. These daily hours are especially challenging because the load ramps are inherently steep and wind generation tends to be ramping down in the period (as shown in Figure 3-3). This anti-correlation only serves to aggravate the load-wind ramp, increasing variability and extreme ramps in the period. Figure 3-34 shows the distribution of hourly changes during the summer morning load rise period for load, and net load with 15 GW of wind generation capacity. The deltas for each five-hour morning load rise period from June to September were separated into 200-MW bins and plotted. Similar plots for the other wind generation scenarios are included in Appendix C.4.

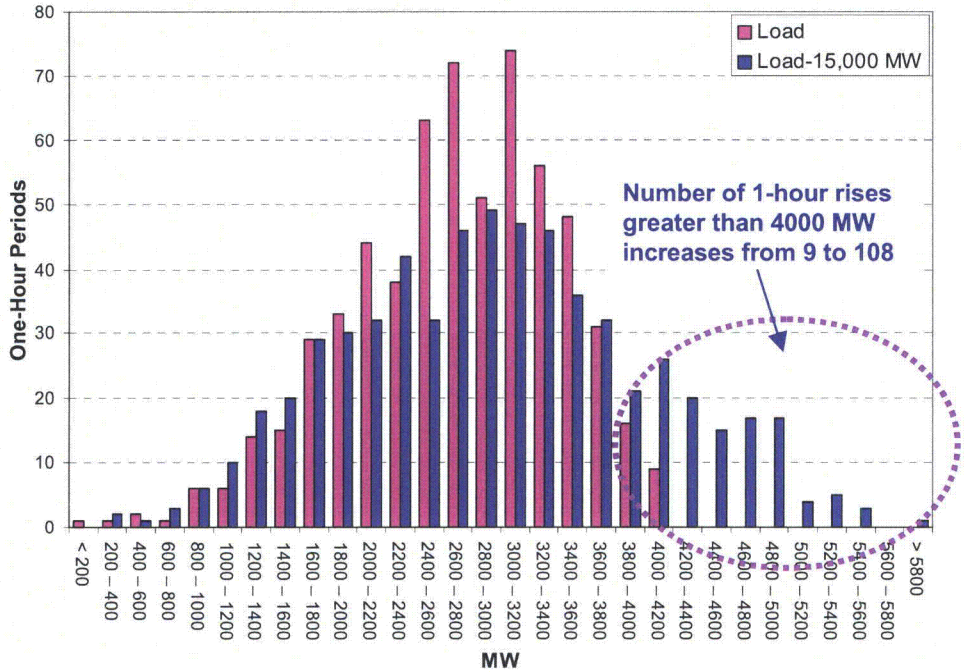

Figure 3-34 - Summer morning load rise hourly variability for load and net load (15 GW)

As expected, the distribution of hourly load changes is positive, because load is rising during the period. The median value is 2755 MW, which means that for half these periods the load is rising by over 2700 MW/hr. An additional 15,000 MW of wind generation increases variability in the period, creating more, and larger hourly up-ramps in net load. Where there were only nine hours when load rose by over 4000 MW/hr, there are 108 such instances with 15 GW of wind generation, and the maximum observed up-ramp increases by 41%.

Table 3-6 summarizes summer morning load rise variability statistics for the wind generation scenarios. By all measures, the observed variability increases linearly with wind, as shown in Figure 3-35, but the extrema tend to increase faster.

Table 3-6 - Summary of Summer Morning Load Rise Hourly Variability for Wind Scenarios

	Load	Load-5000 MW	Load-10,000 MW (1)	Load-10,000 MW (2)	Load-15,000 MW
Mean of Deltas (MW)	2694	2811	2919	2873	2963
σ of Deltas (MW)	729	808	923	894	1042
Max 1-Hour Drop (MW)	9	265	588	523	255
Max 1-Hour Rise (MW)	4160	4730	5479	5286	5871
Points ≥ ±2.5 * Load σ	0	2	27	14	53

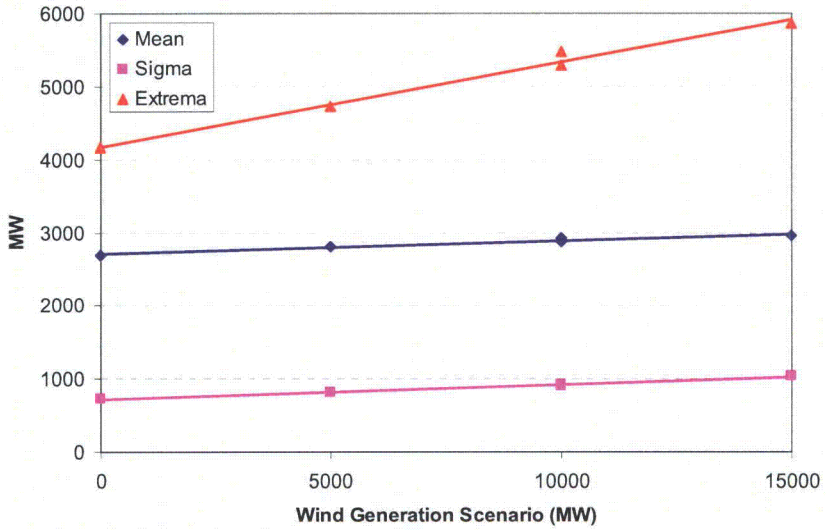

Figure 3-35 - Trend in summer morning load rise variability for wind scenarios

3.5.2. Winter Afternoon Load Rise Period

In the winter afternoon load rise period, designated as November to February, 4 – 6 PM, the load is rising while wind generation may be undergoing up-ramps or down-ramps. The distribution of hourly changes during these hours is shown in Figure 3-36 for load, and net load with 15 GW of wind generation capacity. The deltas for each three-hour afternoon load rise period from November to February were separated into 300-MW bins and plotted. Similar plots for other scenarios are included in Appendix C.4.

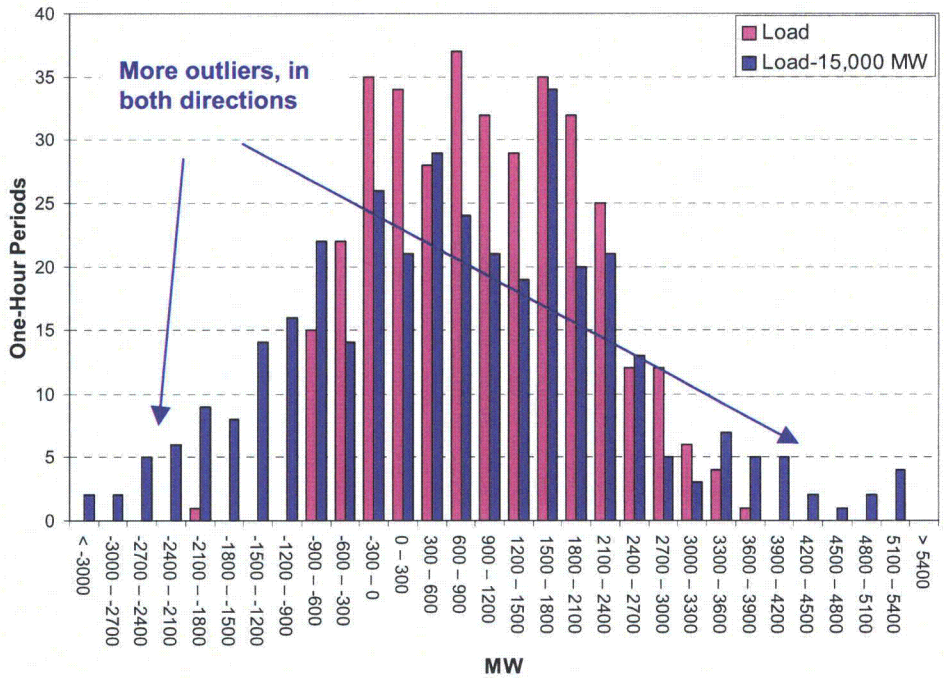

Figure 3-36 - Winter afternoon load rise hourly variability for load and net load (15 GW)

During this period, the hourly load changes are mostly positive (up-ramps), but with the incremental wind generation, there are additional large hourly changes in both directions. The number of one-hour rises greater than 3000 MW increases from 11 to 29 and the number of drops greater than 1500 MW increases from 1 to 32. Table 3-7 summarizes winter afternoon load rise variability for all the wind generation scenarios, and Figure 3-37 shows the trend with increasing wind output. Like the summer morning load rise period, the variability (sigma of the deltas) increases linearly, but the size of the extreme values tend to increase faster than the variability. Interestingly, the mean delta decreases, but this is due to the spread of net load deltas in the negative direction.

Table 3-7 - Summary of Winter Afternoon Load Rise Hourly Variability for Wind Scenarios

	Load	Load-5000 MW	Load-10,000 MW (1)	Load-10,000 MW (2)	Load-15,000 MW
Mean of Deltas (MW)	1018	895	776	823	722
σ of Deltas (MW)	1055	1232	1452	1405	1663
Max 1-Hour Drop (MW)	-1892	-1915	-2553	-2580	-3344
Max 1-Hour Rise (MW)	3678	4072	4694	4460	5190
Points ≥ ±2.5 * Load σ	1	6	12	10	19

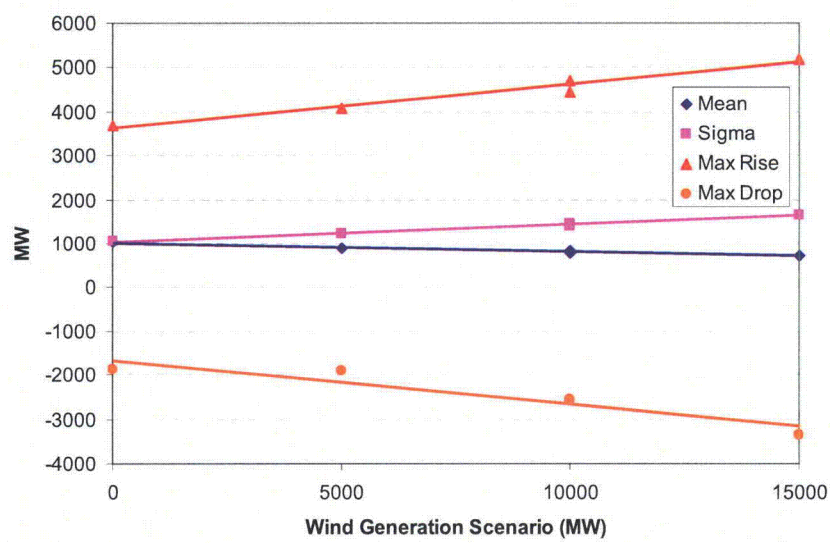

Figure 3-37 Trend in summer morning load rise variability for wind scenarios

3.5.3. Summer Evening Load Drop Period

Across the year, load generally drops in the evening while the wind generation tends to be ramping up. The charts in Figure 4-20 demonstrate that the net load variability increases and there are larger down-ramps. Since the largest one-hour net-load drops

occurs in the summer, variability in the 8 PM to 12 Midnight period from June to September is examined. The deltas for each four-hour evening load roll-off period from June to September were separated into 200-MW bins and plotted on a frequency histogram. Figure 3-38 shows this plot for load, and net load with 15 GW of wind. Similar plots for the other wind generation scenarios are included in Appendix C.4.

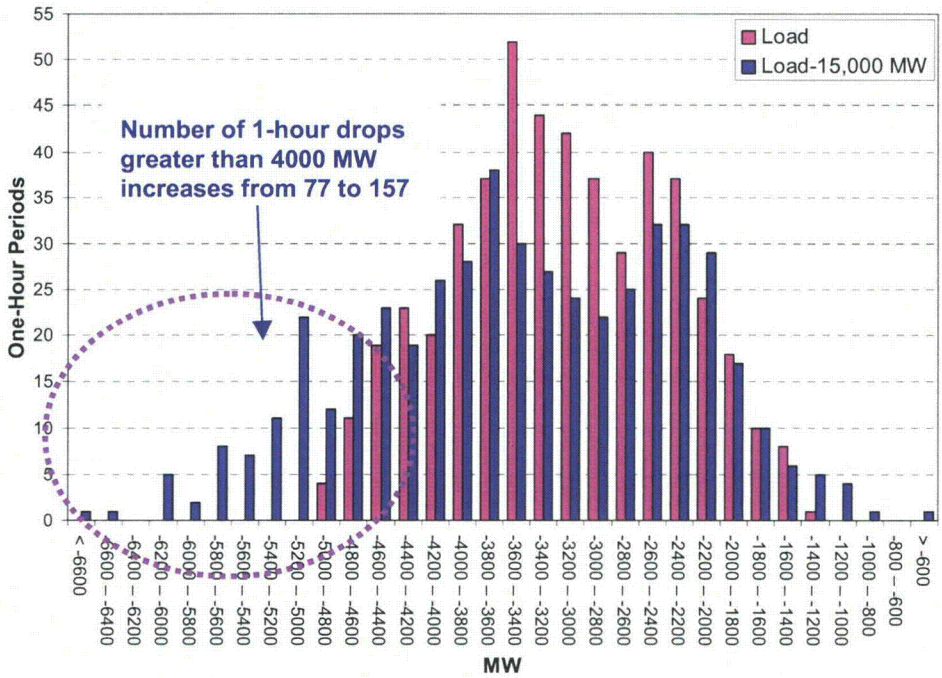

Figure 3-38 Summer evening load drop hourly variability for load and net load (15 GW)

As expected, the hour-to-hour load changes in the evening load-drop period are mostly negative and skewed to the left. With no wind, there are 77 periods (16% of the evening drop hours) when the load ramps down by more than 4000 MW/hr. With the addition of 15 GW of wind, there are 48 hours (or 32%) when net load-wind ramps down by 4000 MW/hr. Table 3-8 summarizes the evening load drop variability across all scenarios.

Table 3-8 - Summary of Summer Evening Load Drop Hourly Variability for Wind Scenarios

	Load	Load-5000 MW	Load-10,000 MW (1)	Load-10,000 MW (2)	Load-15,000 MW
Mean of Deltas	-3160	-3302	-3404	-3373	-3464
Std Dev (σ) of Deltas	795	927	1020	1025	1158
Max 1-Hour Drop	-4838	-5813	-6124	-6175	-6726
Max 1-Hour Rise	-1360	-1032	-837	-850	-565
Points ≥ ±2.5*Load σ	0	8	19	18	39

As wind penetration increases, the net load variability increases linearly, as shown in Figure 3-39. However the extreme values tend to increase faster than the variability, which is consistent with observations during other times of the day. A more complete discussion of extrema and their impact on operation requirements is included in Section 7.

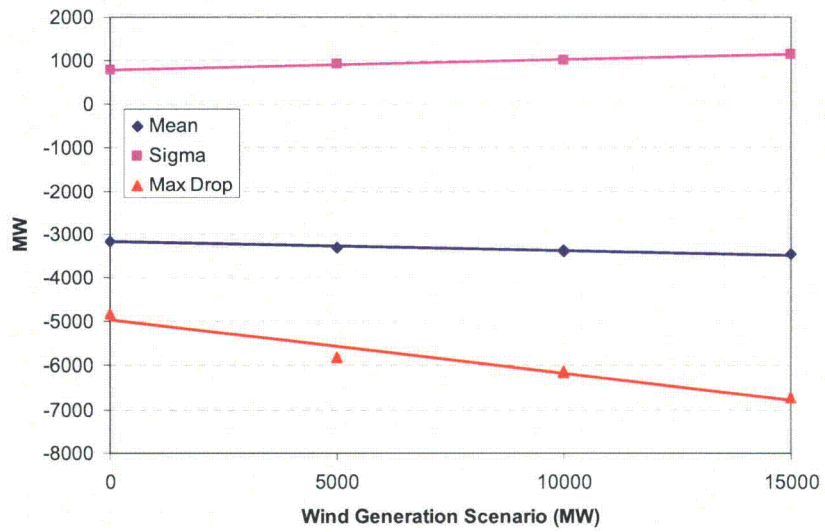

Figure 3-39 - Trend in summer evening load drop variability for wind scenarios

3.6. Summary

This section has discussed the variability of net-load (load-wind generation) from several different perspectives. The incremental variability due to wind has been assessed by comparing net load variability with load variability, rather than load and wind generation in isolation because experience has shown that some of the variation in load and wind output cancel each other. In order to perform credible analysis, load and wind generation time series must be time-synchronized to see the full impact of weather-related phenomena that affect both wind generation and load.

Over the months of the year, load and wind output vary considerably from day to day and throughout the day, but there is a distinct, observable diurnal cycle in the load. Wind output, on the other hand, does not exhibit strong periodic behavior, but correlation plots of load and wind series show that load peaks tend to coincide with wind generation valleys. The inverse-phase relationship appears to be stronger in the summer than during other seasons.

Other observations regarding load and wind coincidence include the fact that wind generation tends to drop sharply in the morning when load is rising quickly, wind generation generally increases sharply in the evening when load is dropping, and the winter afternoon load rise tends to coincide with a general increase in wind production, but there are times when wind is also ramping down in the period.

Using coincident load and wind generation time series, net load variability was examined in the one-minute, five-minute, fifteen-minute and one-hour timeframes. In all timeframes, incremental wind output linearly increased the overall net load variability (as measured by the standard deviation of the period-to-period changes, or deltas). The number and size of large and extreme deltas also increased with wind generation, but tended to grow faster than the variability.

A key observation is that in longer timespans (more than five minutes), net load variability is primarily driven by the long term ramp, but in shorter timespans there is an incremental component due to stochastic variation. The impact of the non-random ramp component can be seen in the frequency plots which become increasingly triangular in longer timeframes. With the same wind generating capacity, the incremental variability due to wind increases as the timespan becomes longer, but appears to taper off, and appears saturate at longer timeframes.

Seasonal trends in net load variability were examined using average yearly profiles and profiles of selected days. From an overall perspective, negative net load hour-to-hour changes (down-ramps) tend to be larger in the late spring, summer, and early fall, while the up-ramps are generally larger in late fall and winter. There tends to be larger differences between load deltas and net load deltas during spring and summer. The bottom line is that wind generation tends to have a greater overall impact on variability in the summer, late spring and early fall, but variations in winter and early spring may be more operationally significant due to the low net load levels.

Low load hours may present additional operational challenges because wind generation aggravates balance of generation ramp and range requirements. With regard to load level, variability is relatively constant, but tends to be greater during mid-range load levels than high and low load levels. Net load variability does increase significantly with wind penetration but the increment tends to be less at high and low load levels. However, low load periods are significant because net loads can be driven to extremely low levels with large wind penetration. The instantaneous wind penetration reaches 57% with 15 GW of wind and the minimum load point is reduced by 56%. Under these conditions additional measures may be needed to accommodate the net load variability.

From a system operation point of view, broad trends in variability are not nearly as important as variability during particularly challenging periods of the day. Considering time-of-day variability, wind generation is a large contributor to net load variability in the mornings and late evenings in most months (particularly in summer) and late afternoons during the winter. During the summer morning load rise period (June to September, 7-11 PM, wind generation increases variability in the period, creating more, and larger hourly up-ramps in net load. Where there were only nine hours when load rose by over 4000 MW/hr, there are 108 such instances with 15 GW of wind generation, and

the maximum observed up-ramp increases by 41%. The general trend is the same in the winter afternoon load rise period (November to February, 5-7 PM) and the summer evening load drop-off period (June to September, 9 PM-12 Midnight). By all measures, the observed variability increases linearly with wind, as shown in, but the extreme values tend to increase faster.

The results of this analysis are important for a general understanding of the overall impact of wind generation on system, but also to assess the acute operation issues that arise during particular hours of the day and times of the year. Net load variability and extreme net load changes (in different timeframes) directly impact the requirements for regulation and responsive reserves. These are further discussed in Sections 6, 7 and 8..

The next section discusses net load predictability (or forecast accuracy) which has implications for non-spinning reserve requirements.

4. NET LOAD PREDICTABILITY

Day-ahead predictability of net load is important to the unit commitment process. Inaccuracies (large forecast errors) may compromise reliability, increase operating costs and may require greater ancillary service procurement.

For the purposes of this study, "forecast error" is defined as forecast minus actual. Therefore positive forecast error (forecasted quantity greater than actual) is defined as *over-forecast* and negative forecast error (forecasted quantity less than actual) is defined as *under-forecast*. Over-forecasting of load may lead to more generation being committed than needed (which has potential economic consequences), while under-forecasting of load may lead to under-commitment, which is a potential reliability problem. Therefore, from a system operation point of view, under-forecasting of load and net load is a more serious issue.

Several statistics are used in this study to characterize forecast accuracy. They include:

- **Mean Absolute Error** (MAE) – measures the average magnitude of the forecast errors, without considering their direction; mean of the absolute value of the errors.
- **Root Mean Square Error** (RMSE) – characterizes forecast error by measuring the "average" of the square of the deviations. RMSE will always be larger than MAE because it penalizes large deviations more.
- **Standard Deviation of Errors** (Sigma) – measures the spread of forecast errors around the mean; similar to RMSE but tends to be smaller.

The next few sections will discuss individual wind forecast accuracy, overall trends in load and net load forecast errors, and load and net load forecast accuracy during various months/seasons of the year and periods of the day.

4.1. Overall Wind Predictability

Actual load data and day-ahead forecasts were supplied by ERCOT from operations records, and scaled up to represent the study year, as discussed in Section 2. However, there were no actual wind generation data for the CREZ scenarios, for obvious reasons.[1] Therefore wind production data from AWS Truewind represents "actual" wind generation data in this study. AWS Truewind also provided simulated day-ahead wind output forecasts to accompany the "actual" wind production data. These data comprise the wind generation forecast for this study. A fuller discussion of the wind production

[1] Some existing wind output data was made available from operations, but not nearly the quantity and quality needed for even the smallest (5000 MW) scenario.

data and day-ahead forecast synthesis methodology is included in Section 2.2.1 and Appendix B.

Using the wind production data and simulated day-ahead forecasts for each scenario, several 8760 series of forecast errors were created. These data were organized into 300 MW bins and plotted on a frequency plot. Figure 4-1 below shows the distribution of wind generation forecast errors over the study year.

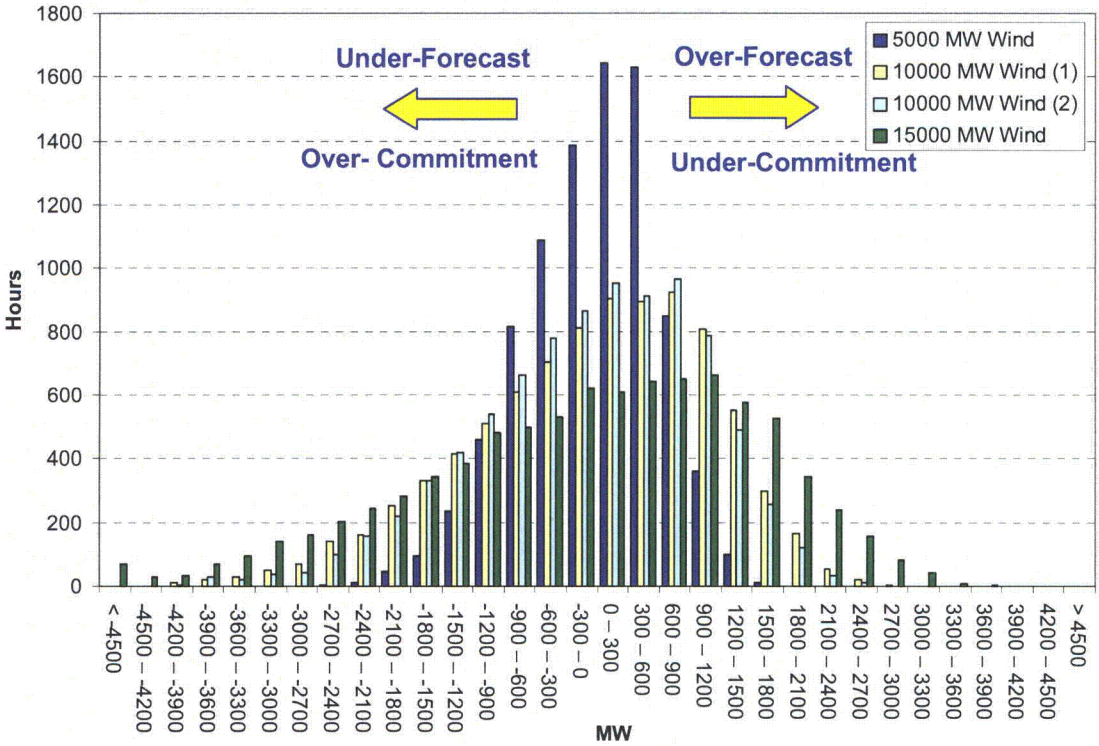

Figure 4-1 - Distribution of wind generation forecast errors over the study year

As wind penetration increases, the number and size of extreme forecast errors also increase. On both tails, there is a significant increase in extreme values going from the 10 GW case to the 15 GW case. The distribution of forecast errors becomes increasingly skewed to the left, which indicates that there is a clear tendency for the largest wind generation errors to be *under-forecast* errors. With 5 GW of wind generation capacity online, there are 30 under-forecast errors greater than 2000 MW, but with 15 GW online, there are 1164 such errors.

As discussed earlier, the real issue is whether forecast inaccuracies lead to unit under-commitment problems. Since wind generation is considered as negative load in the net load construct (load - wind), wind *under*-forecast errors actually manifest as *over*-forecast errors in net load. Therefore, the real operational concern is with wind generation *over*-forecasts, which ultimately show in net load as *under*-forecast errors. From the frequency plot, it appears that over-forecast is less of a problem in terms of

severity. The number of wind over-forecast errors greater than 2000 MW increases from 0 in the 5 GW wind generation capacity scenario to 634 with 15 GW.

Table 4-1 summarizes some key measures of forecast accuracy as well the extreme errors. By all measures, there is a clear trend of decreasing forecast accuracy (increasing error) as wind penetration increases.

Table 4-1 - Summary of Wind Forecast Accuracy over the Study Year

Wind Scenario	MAE (MW)	RMSE (MW)	Sigma (MW)	Max Neg Error (MW)	Max Pos Error (MW)
5000 MW Wind	511	639	638	-2529	1744
10,000 MW Wind (1)	935	1169	1167	-4264	3032
10,000 MW Wind (2)	876	1096	1093	-4028	2671
15,000 MW Wind	1294	1614	1611	-5921	4052

Figure 4-2 shows that the MAE and RMSE actually increase linearly with wind generation capacity, with RMSE increasing faster, as expected. The measures of absolute forecast error (MAE and RMSE) and the maximum positive and negative errors are plotted against the left (MW) scale. MAE and RMSE as a *percentage of rated capacity* are plotted against the right (%) scale. The size of the maximum (extreme) over-forecast and under-forecast errors also increase linearly with wind penetration, with the extreme negative forecast error growing faster than the positive one.

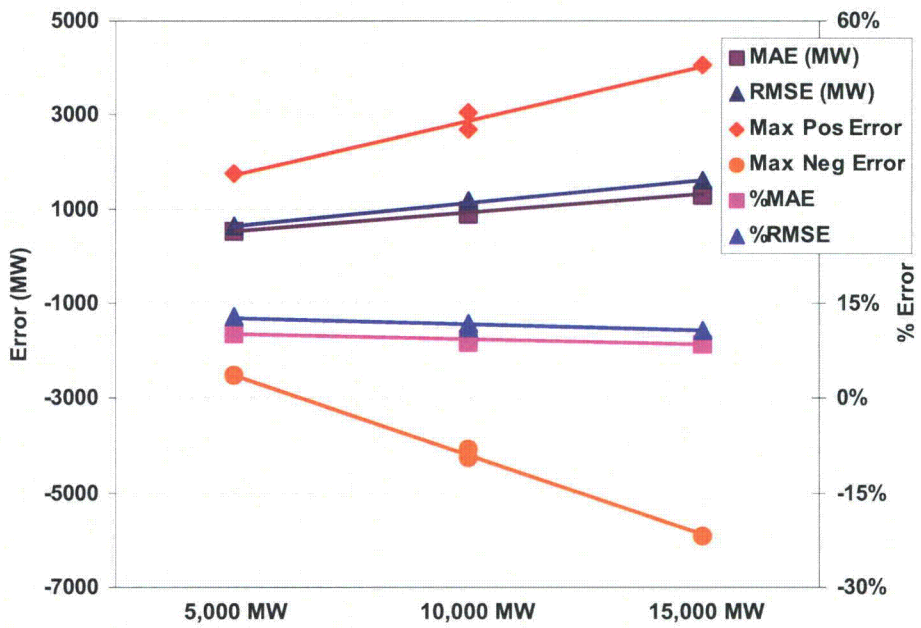

Figure 4-2 - Trend in wind forecast error accuracy and extreme errors

Interestingly, the percent error actually decreases with wind penetration, ostensibly because wind absolute error does not grow as fast as wind capacity. When capacity doubles from 5 GW to 10 GW, the absolute error does not double (increases 83%).

4.2. Overall Load and Net Load Predictability

Given day-ahead load forecasts and (simulated) next-day wind generation forecasts, next-day net load forecasts are generated by subtracting wind from load. These data are compared with the actual net load data to determine the net load forecast accuracy. In keeping with the defined convention, a positive forecast error is an over-forecast of net load and a negative forecast error is an under-forecast of net load. From an operations perspective, net load under-forecast errors are more significant because they can potentially lead to unit under-commitment.

Figure 4-3 shows the distribution of forecast errors, over the study year, for load and net load with 5000 MW and 15,000 MW of wind generation capacity. The first observation is that wind forecast errors do aggravate the overall net load forecast error, but this is more pronounced on the over-forecast side. The relative increase is greater around the inflection point, than on the tails of the distribution. Even so, there is still a definite increase in number of extreme errors as wind penetration increases. With no wind on the system, there are 210 instances where net load is over-forecasted by 4600 MW or more. With 15 GW of wind, this number grows to 316, a 50% increase, (but still less than 4% of all hours). On the negative side, the number of times when net load is under-forecasted at least 4600 MW goes from 26 with no wind, to 72 with 15 GW. Overall, there are more instances when load and net-load are over-forecasted than under-forecasted. The addition of wind skews the load-wind forecast toward the over-forecast side, because wind by itself tends to skewed toward being under-forecasted (as seen earlier in Figure 4-1).

Table 4-2 summarizes the broad measures of load and net load forecast accuracy, and Figure 4-4 plots the trend in overall error accuracy. In the plot, absolute error is on the left (MW) scale and error as a *percentage of the average net load* is on the left (%) scale. The plot demonstrates that there is a non-linear increase in absolute error and percent error as wind penetration increases. From the no-wind case to the 15 GW case, there is a 31% increase in MAE and a 23% increase in RMSE.

One non-intuitive observation is that the extreme positive forecast error actually *decreases* with additional wind generation., dropping by 5.4% from the no-wind case to the 15 GW case, in Table 4-2.

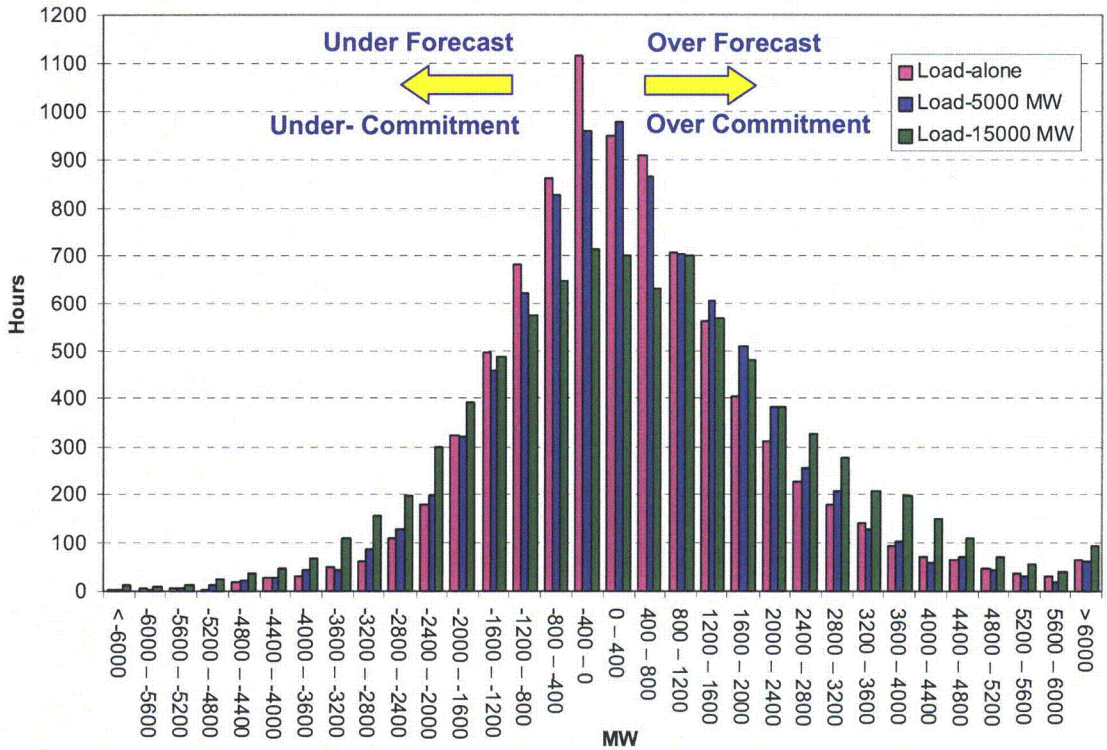

Figure 4-3 - Distribution of net load forecast errors over the study year

Table 4-2 - Summary of Net Load Forecast Accuracy over the Study Year

Scenario	MAE (MW)	RMSE (MW)	Sigma (MW)	Max Neg Error (MW)	Max Pos Error (MW)
Load-Alone	1296	1792	1755	-6291	10294
Load – 5000 MW	1338	1805	1762	-6574	9951
Load – 10,000 MW (1)	1505	1974	1928	-6724	9763
Load – 10,000 MW (2)	1467	1936	1887	-6803	9786
Load – 15,000 MW	1698	2199	2149	-7781	9765

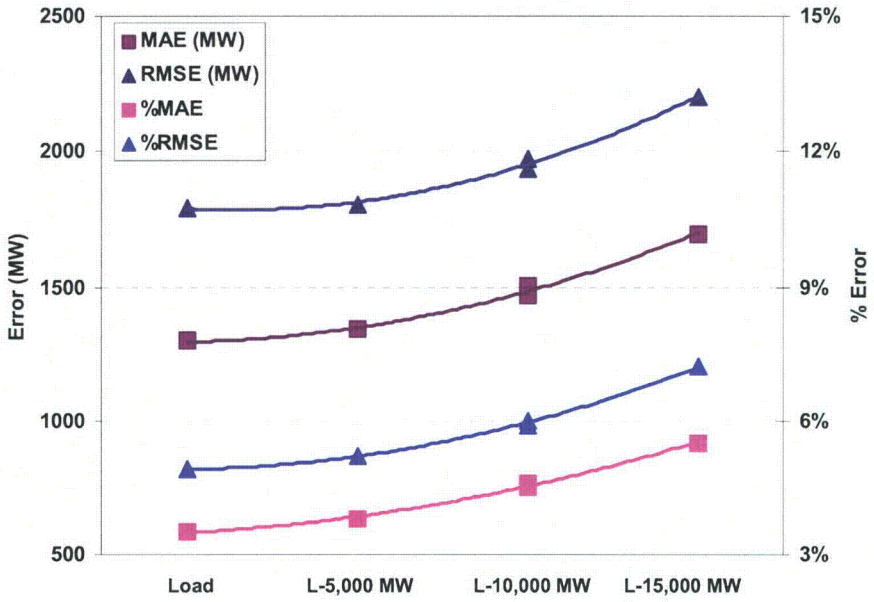

Figure 4-4 - Trend in net load forecast error accuracy

4.3. Net Load Forecast Errors by Time-of-Year

Load and wind generation vary over the year, from month to month and season to season. Therefore, one can reasonably expect some degree of variation in the ability to predict load and wind generation over the year. Figure 4-5 gives the profile of maximum daily load forecast errors, over the study year. This is to be compared with Figure 4-6 which plots the profile for maximum daily net load forecast errors for the 15 GW scenario.

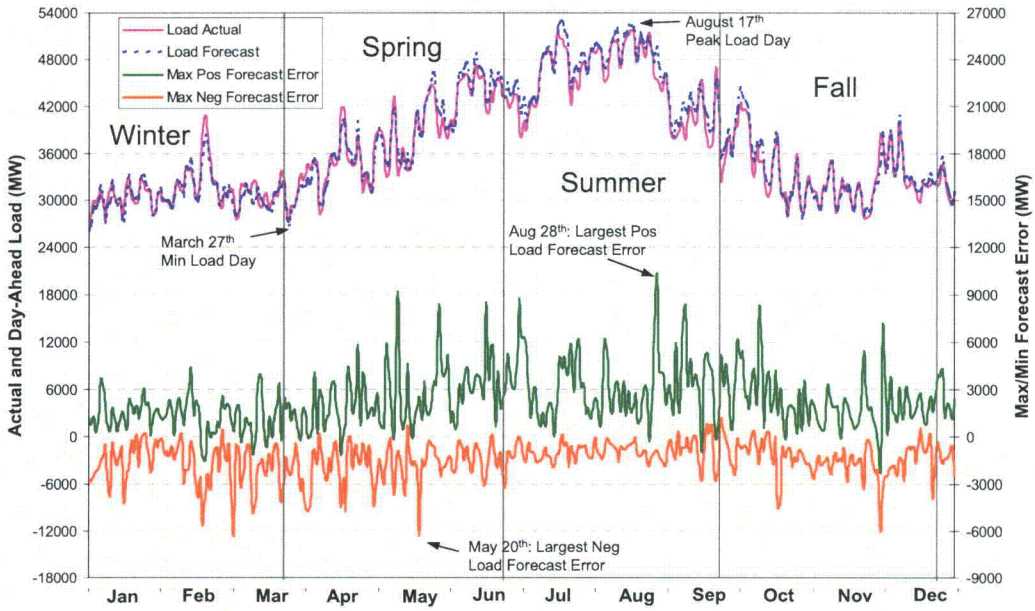

Figure 4-5 - Profile of maximum daily load forecast errors

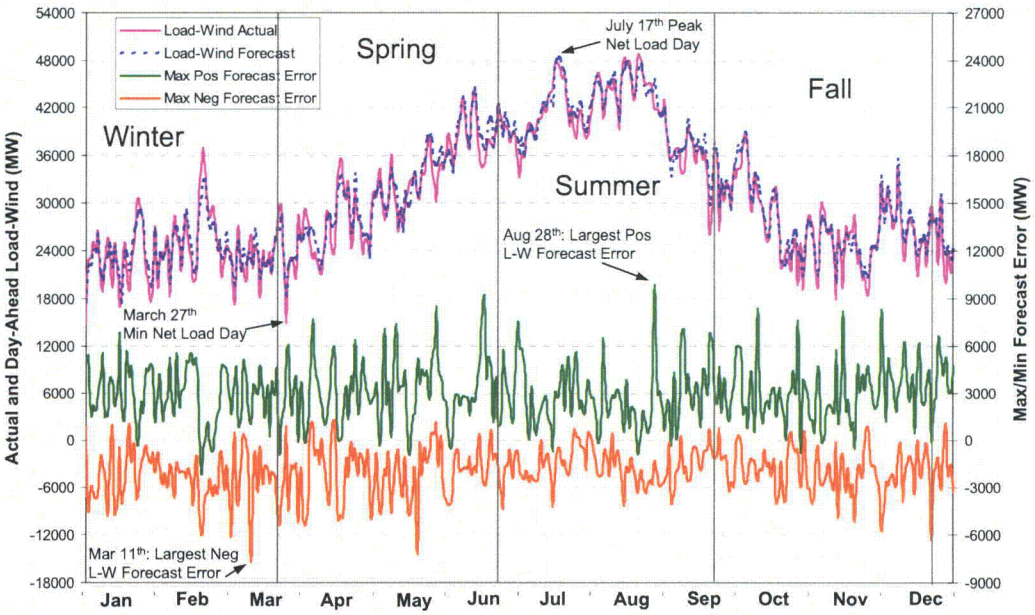

Figure 4-6 - Profile of maximum daily net load forecast errors (15 GW of wind)

The plots show *broad* trends in average daily forecast, and maximum daily forecast errors over the year, so by their very nature, they tend to mask the intra-day variability. Even so two general observations can be made regarding time-of-year forecast accuracy:

1. There is a greater tendency to accumulate large *load* over-forecast errors during the summer months and large load under-forecast errors during the winter months.
2. Extreme *net-load* forecast errors tend to be larger in non-summer months, than summer months.
3. Across the year net load forecast errors are generally larger than load forecast errors, but the increment may be greater for under-forecast errors in the summer.

These observations are confirmed and refined by additional analysis in the next sections.

4.3.1. Seasonal Forecast Errors

Figure 4-7 shows a scatter plot of load and wind generation forecast errors separated by season. Magenta diamonds represent load and wind generation forecast errors during winter hours, blue squares represent errors during spring hours, orange triangles represent summer hours, and green circles represent fall hours.

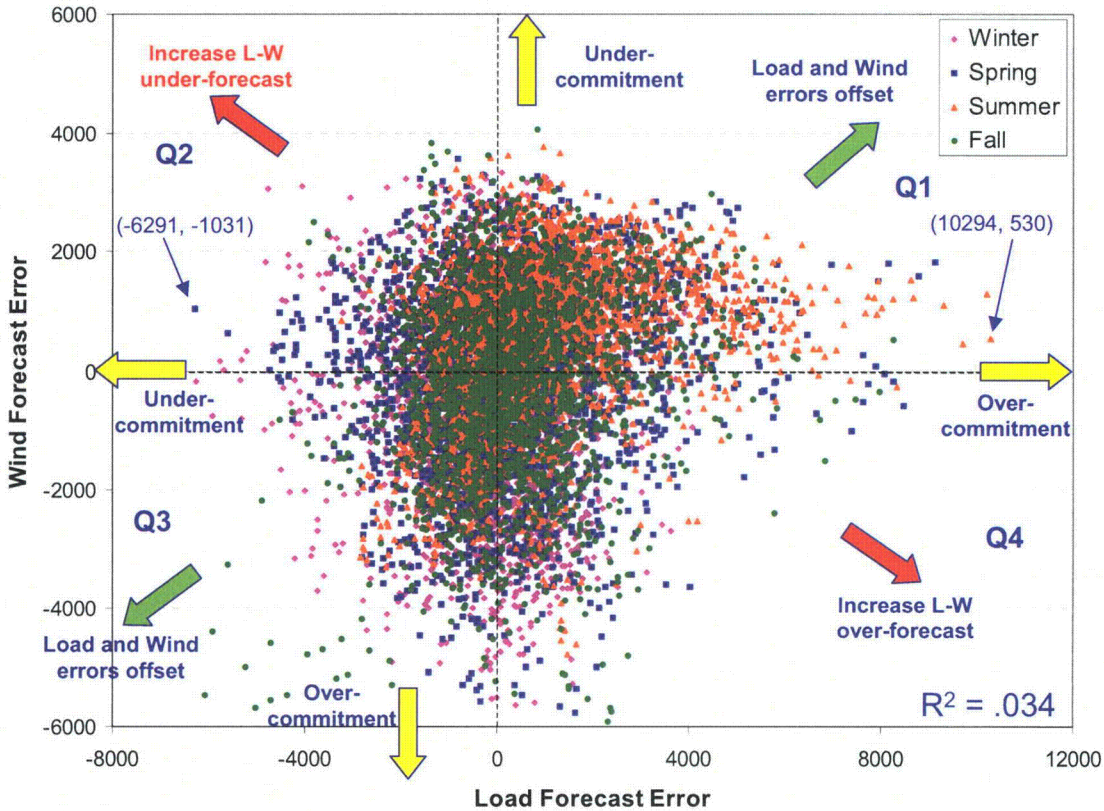

Figure 4-7 - Correlation of load and wind generation (15 GW) forecast errors by season

Overall, Figure 4-7 demonstrates that there is an extremely weak correlation between load forecast errors and wind forecast errors (R^2 = .034). This suggests that both errors are independent, not driven by the same factors, and are unlikely to coincide or reinforce each other. This exemplified by the data point in the first quadrant, Q1, corresponding to the largest load forecast error (10294 MW). During this same summer hour, the wind forecast error happens to be pretty modest (530 MW).

The scatter plot shows a very distinct spread in errors in the right-hand and downward directions. There are more large summer error-hours (orange triangles) along the positive x-axis (load over-forecast), than in other directions. Conversely, there are more non-summer error-hours along the negative x-axis (load under-forecast), than in other directions. This is completely consistent with the first observation made previously from the yearly profile of load forecast errors (Figure 4-5). The spread (and type) of points along the negative y-axis suggests that wind tends to be under-forecasted more in non-summer months, but as discussed below, this is may not be a significant operational issue.

The yellow arrows on Figure 4-7 show the forecast error directions that are consistent with unit commitment outcomes. For example, negative load forecast errors and positive wind forecast errors may individually lead to under-commitment of resources. On the other hand, positive load forecast errors and negative wind forecast are both consistent with over-commitment of resources.

The red diagonal arrows indicate the directions where load and wind errors combine (add) to increase net load forecast errors. All points in the second quadrant, Q2, represent hours during the year when load and wind errors combine to *increase* the net load *under*-forecast, which may lead to unit *under*-commitment problems. All errors in the fourth quadrant, Q4, potentially lead to over-commitment of resources -- so they are not as operationally significant (from a reliability standpoint) as errors in Q2.

The green arrows indicate directions in the off-diagonal quadrants, (Q1 and Q3), where load and wind forecast errors offset each other to reduce the net load forecast error -- so they are not generally as problematic as points in the diagonal quadrants.

In general, the points in Q2 and Q4 indicate that there are more extreme winter and spring errors (magenta diamonds, blue squares) than summer ones, *particularly in the under-commitment direction* (Q2). This is completely consistent with the second observation made earlier from the yearly profile of net load forecast errors (Figure 4-6). To expand on this point, Figure 4-8, separates the seasons into individual scatter plots and overlays the plots with equal-error lines. These are dashed lines that define the envelope where the sum of the load and wind forecast errors is the same.

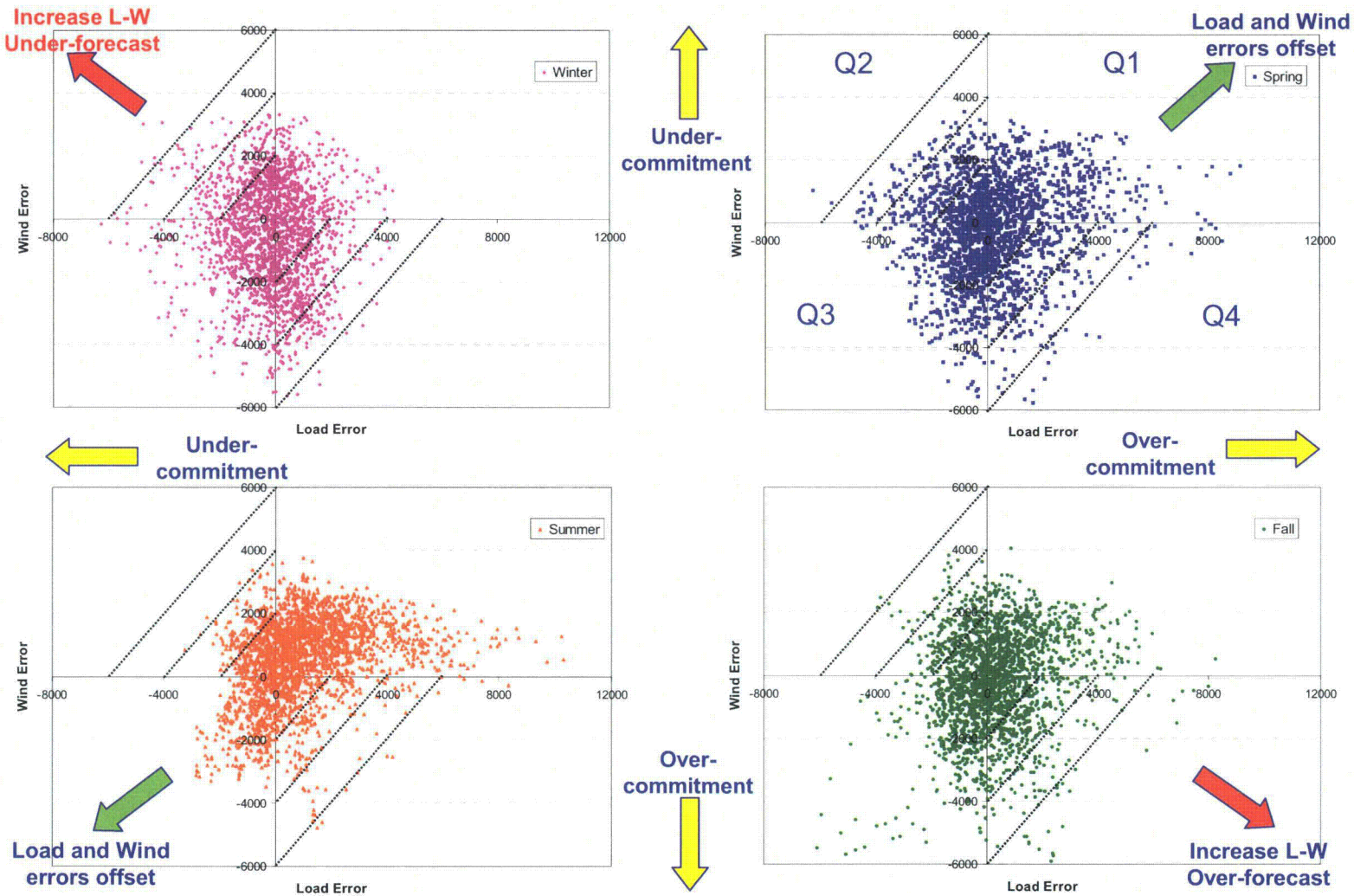

Figure 4-8 - Correlation of load and wind generation (15 GW) forecast errors in each season, with iso-error lines.

In Q2 and Q4, where load and wind forecast add, points outside the envelope lead to larger net load forecast errors, and points inside the envelope lead to smaller errors. For example, in Q2, which is consistent with net load under-commitment, very few points are beyond the 6000 MW bar, in all seasons. This means that in the winter, there are few hours when net load is under-forecasted by over 6000 MW, even less hours in spring and fall, and none in summer. In Q4, the pattern is weaker, but still discernable. This reinforces an earlier observation that it is improbable for the most severe load and wind errors to occur in the same hour -- or *the risk of simultaneous under-commitment error is small.*

Figure 4-9 shows time series plots and data on net load forecast accuracy during seasonally representative months, for the 15-GW wind generation scenario. The magenta trace is "actual" net load and the dotted blue trace is the day-ahead forecast. Both are plotted on the left scale. The orange trace is forecast error, plotted on the right scale. The plots and data confirm that *on average*, net load forecast accuracy is lower in the winter and spring months than during the summer.

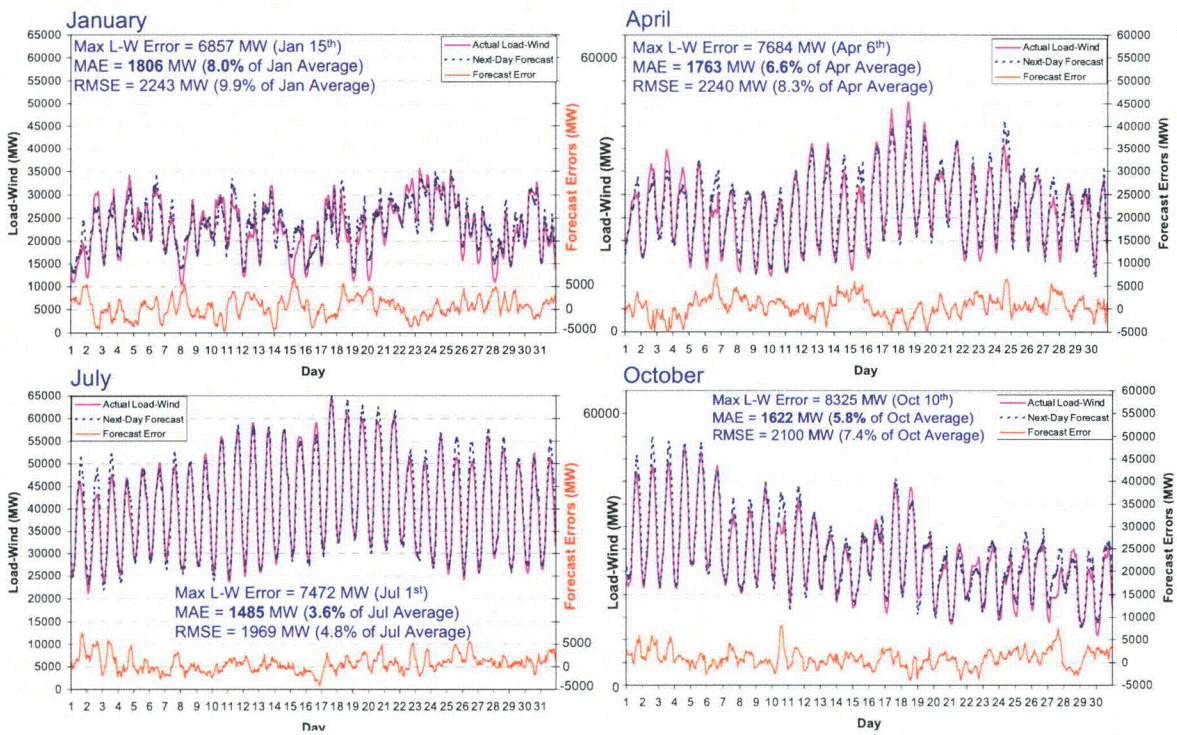

Figure 4-9 - Actual net load, day-ahead forecasts, and forecast error by seasonal month, 15 GW wind generation capacity scenario.

4.3.2. Forecast Errors for Selected Days

Based on Figure 4-6, there are some "interesting" days during the year where a closer examination of net load forecasts may give some additional insight. These include the days with the largest net load over- and under-forecast errors, the peak load day, minimum load day, and four typical, seasonally representative days.

Figure 4-10 shows the profile for the day on which the largest net load over-forecast occurs (August 28th), for the 15 GW wind generation scenario. The forecast error accumulates throughout the day, reaching a peak of 9675 MW (MAE is 4103 MW). However, the wind forecast error is consistently small, so the gross over-forecast is driven by the load forecast error.

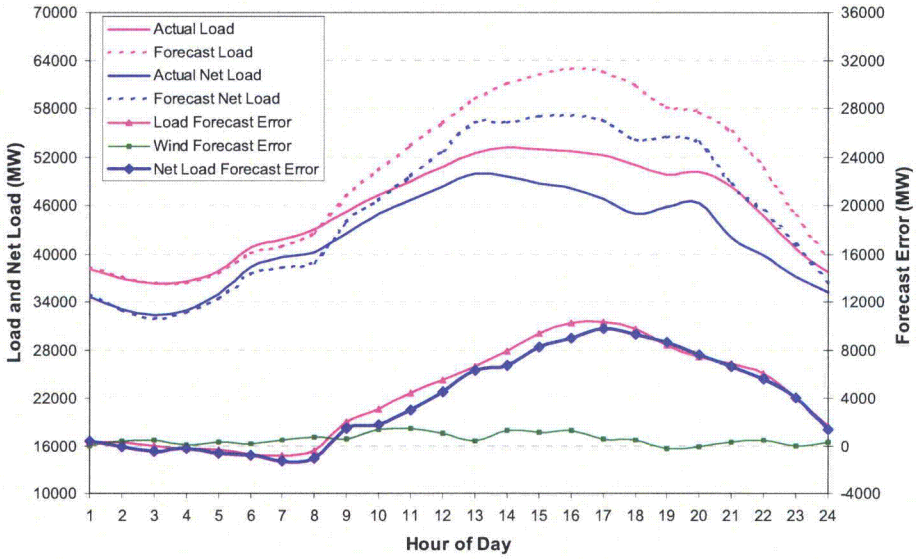

Figure 4-10 - Large positive net load forecast error day (Aug 28th), 15 GW wind scenario.

On the other hand, Figure 4-11 shows the profile for the day with the largest net load under-forecast error (March 11th), for the 15 GW wind generation scenario. In this case, the large net load under-forecast error (-7780 MW around 3 PM), is due to a simultaneous increase in wind over-forecast and load under-forecast errors at the time.

Figure 4-12 shows the daily profile for the peak load day (August 28th). This day is interesting if only for the lack of character. The load forecast is quite accurate, and the wind forecast error is uniformly small, creating relatively small net load forecast errors across the day. The largest forecast error is –2060 MW and the MAE is 886 MW.

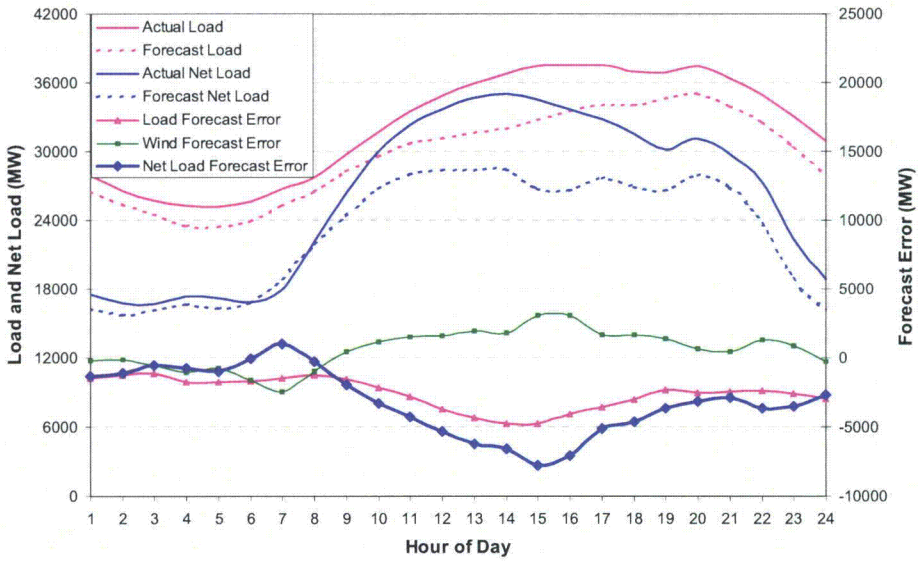

Figure 4-11 - Large negative net load forecast error day (Mar 11th), 15 GW wind scenario

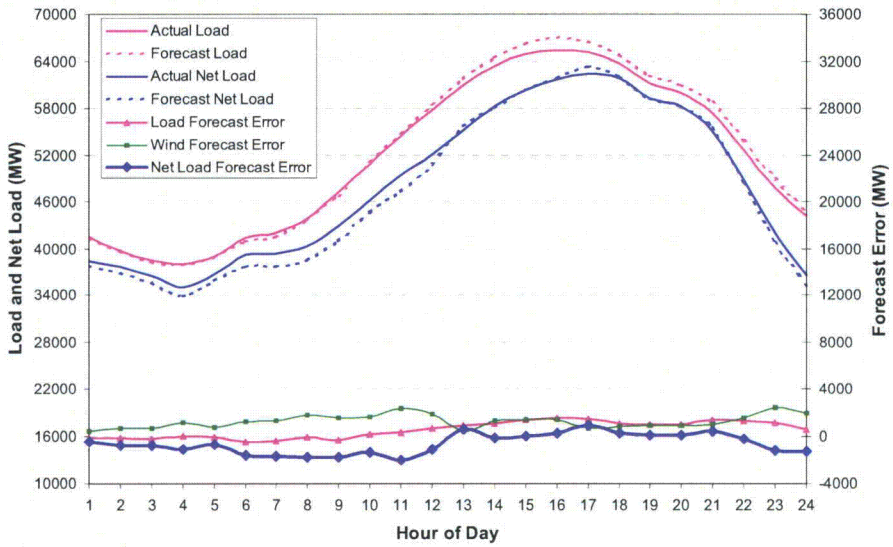

Figure 4-12 - Forecast errors for peak load day (August 17th), 15 GW wind scenario.

Figure 4-13 shows the minimum load day (March 27th). The plot exhibits some variation in net load forecast error across the day due to a combination of varying load and wind forecast errors. The largest over-forecast error, in the early morning, happens to coincide with the period when the least amount of resources are likely to be needed.

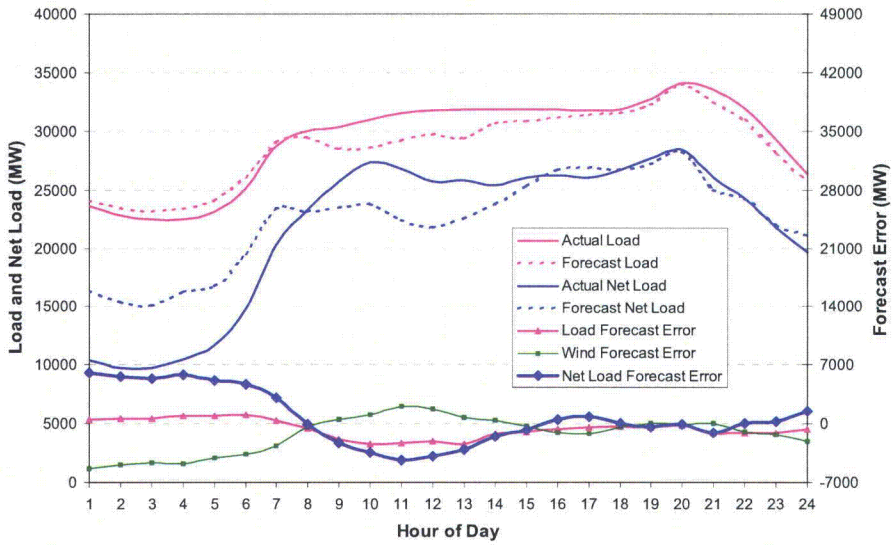

Figure 4-13 - Forecast errors for minimum load day (March 27th), 15 GW wind scenario.

The next four plots in Figure 4-14 show error profiles of typical days from each season. The representative seasonal days, January 27th, April 23rd, July 10th and October 25th were selected based on the fact that they did not significantly deviate from seasonal expected averages. On the plots, magenta traces are load-related, blue traces are net load-related, and the green trace is wind-related. Load and net load are on the left scale and the forecast errors are on the right scale. Note that some scales may vary among plots display purposes.

Since these typical plots are merely snapshots of the seasonal forecast accuracy, one should be careful when drawing broad inferences. However, from a macro perspective, the plots conform with the earlier observation that net load forecast errors show more separation from load forecast errors in winter, spring and fall days. To make any credible inferences about how forecast errors vary during the day, more data than just these four days need to be considered. Therefore, the next section will consider how forecast errors vary during the day, (hour to hour), across the entire year.

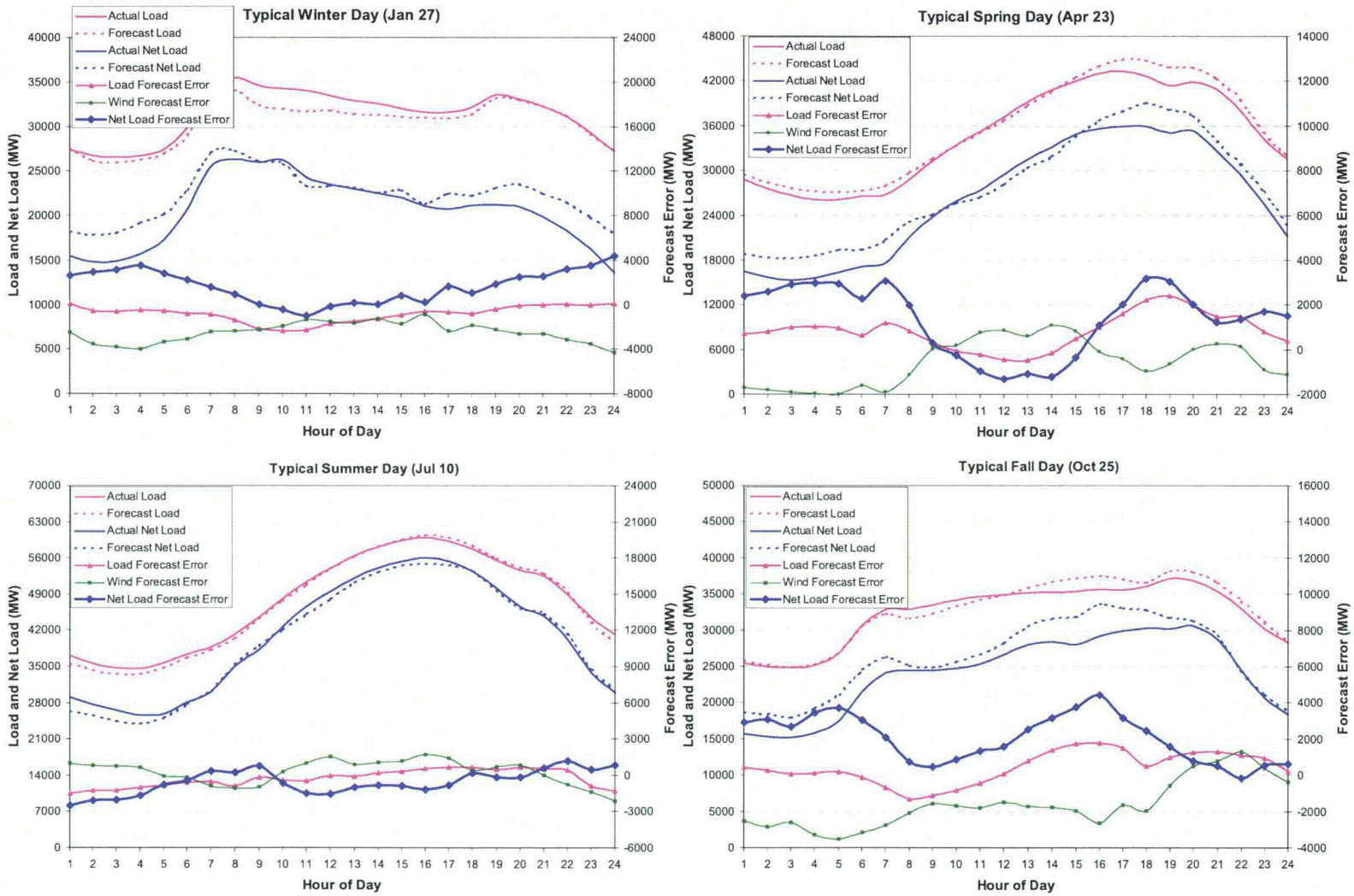

Figure 4-14 - Forecast errors for four seasonally representative days, (15 GW scenario)

4.4. Net Load Forecast Errors by Time-of-Day

From a system operation perspective, it is very important to understand the net load predictability during challenging periods of the day, such as when the system is stressed or resources are likely to be low. Since day-ahead forecast error is a key input to the unit-commitment decision-making process, this discussion is germane to the evaluation of non-spinning reserve requirements (further discussed in Section 8).

The time-of-day forecast errors will be examined in two ways: first, the daily time of extreme forecast occurrence will be examined over the twelve months and then the daily average error profile will be discussed in each season.

4.4.1. Timing of Forecast Errors

This section discusses the pattern of extreme forecast error occurrence over the hours of the day and months of the year. The data are presented in 24×12 surface plots using color intensity to represent the magnitude of the forecast errors.

The data for the surface plots were extracted from the forecast error time series. For each month of the year, the maximum positive and negative forecast errors where selected for each hour of the day. For example, in the month of January, there are thirty-one 6 AM hours (one for each day). Only the maximum errors from each of the 31 forecast errors was selected for the surface plot. Repeated for each month, this resulted in 24 positive error observations for each of the twelve months, and 24 negative error observation.

The next few surface plots illustrate the timing of positive and negative forecast errors, which highlight periods with the greatest risk of over- and under-commitment.

Figure 4-15 shows the surface plot for positive (over-commitment) load forecast errors. The legend indicates the level of the forecast error during a particular period. Periods with the largest errors are colored in red and orange. From the pattern, the largest load over-forecasts typically occur in late afternoons during the summer months. This is consistent with earlier observations.

With 15 GW of wind generation capacity (see Figure 4-16), there is generally an *increased* risk of over-commitment in mornings and afternoons during fall and winter. The risk is simultaneously reduced in the mid-summer afternoons.

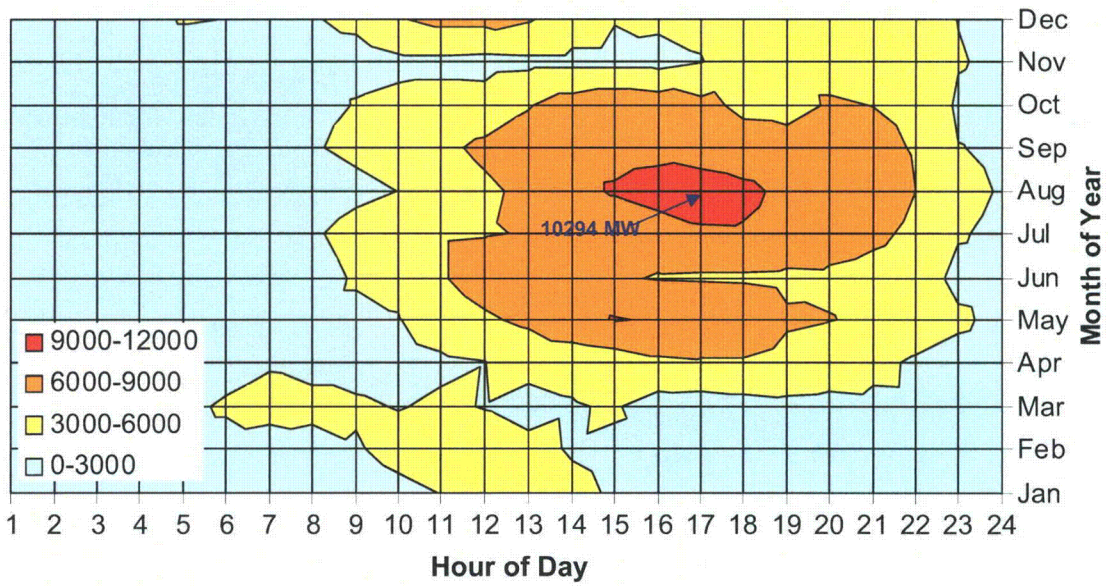

Figure 4-15 - Timing of maximum positive load forecast errors (over-commitment)

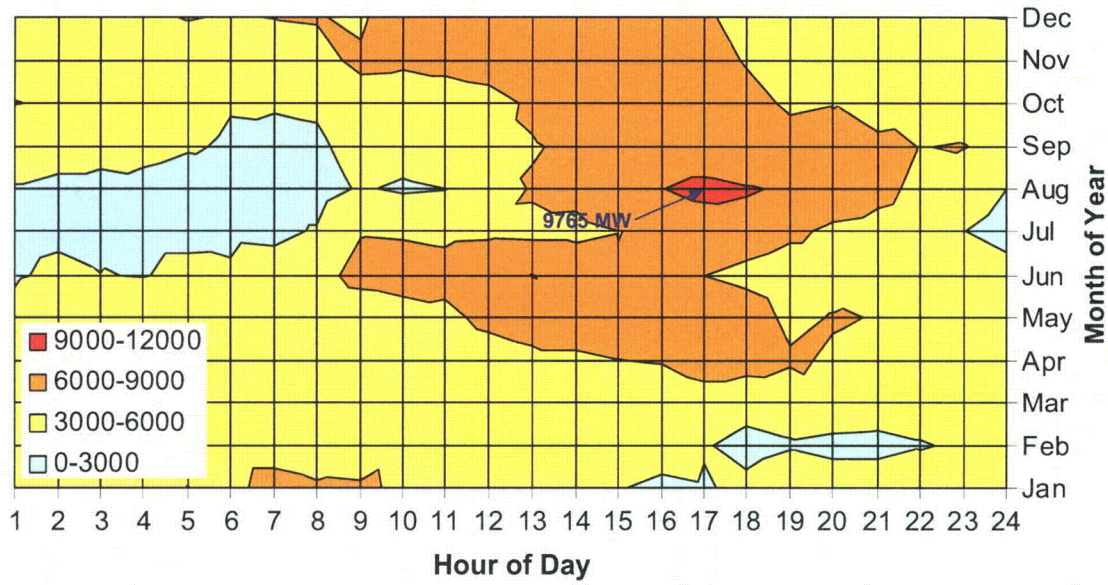

Figure 4-16 - Timing of maximum positive net load forecast errors (over-commitment), 15 GW wind generation capacity scenario.

Figure 4-17 shows the surface plot for negative (under-commitment) load forecast errors. With no wind on the system, the periods with the greatest risk of under-commitment are in the afternoon to early evening during winter and spring (red and orange areas). When 15 GW of wind generation is added, Figure 4-18 shows that the pattern of net load forecast errors changes appreciably. The extreme net-load under-forecasts (orange and

red) are now much more spread over the day, and the magnitudes are greater (more red). The periods with the greatest risk of under-commitment occur in winter and spring.

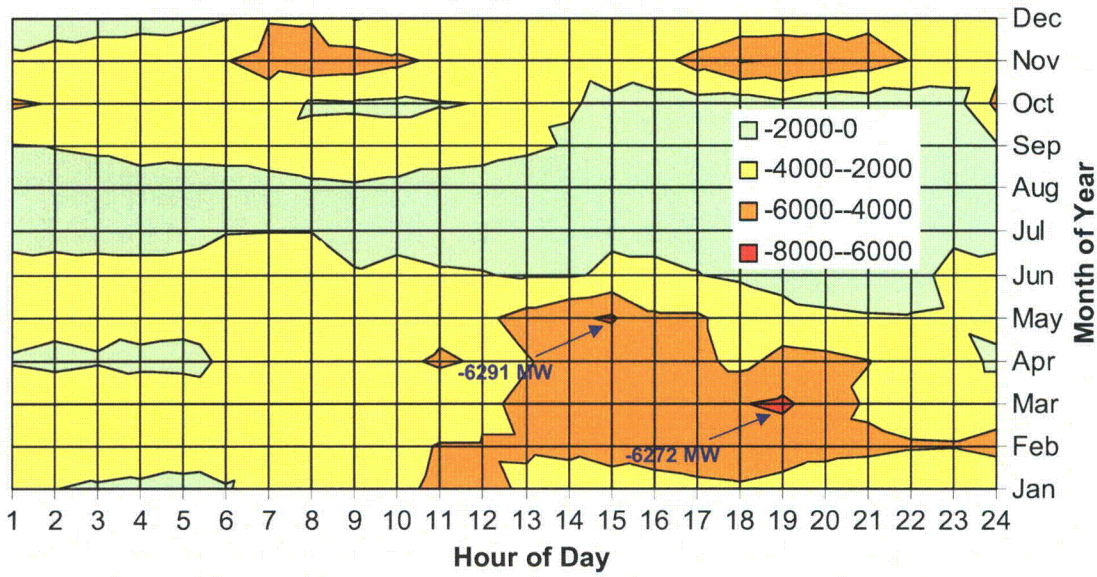

Figure 4-17 - Timing of maximum negative load forecast errors (under-commitment)

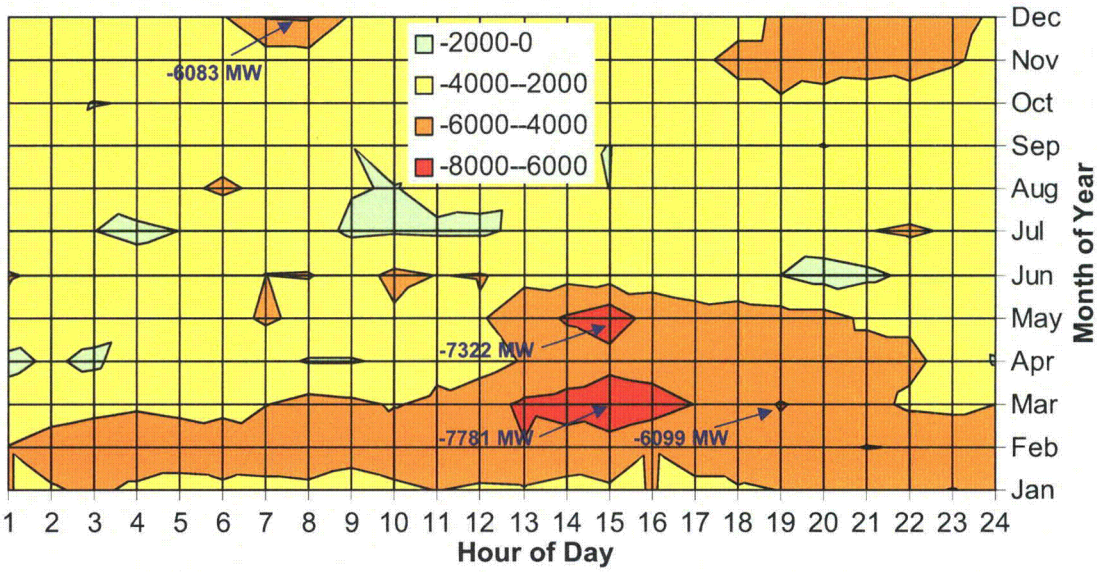

Figure 4-18 - Timing of maximum negative net load forecast errors (under-commitment), 15 GW wind generation capacity scenario.

The difference between Figure 4-17 and Figure 4-18 is the timing of the incremental large net load forecast errors due to wind, i.e. it highlights periods with incremental risk of under-commitment due to wind. This is shown in Figure 4-19 below. The pattern indicates that 15,000 MW of wind generation capacity would cause the risk of under-commitment to generally increase across all hours of the day and months of the year, with particularly acute increases in some periods. These include evening hours in summer and fall and early morning hours in the winter. This hourly risk is investigated further using daily profile plots in the next section.

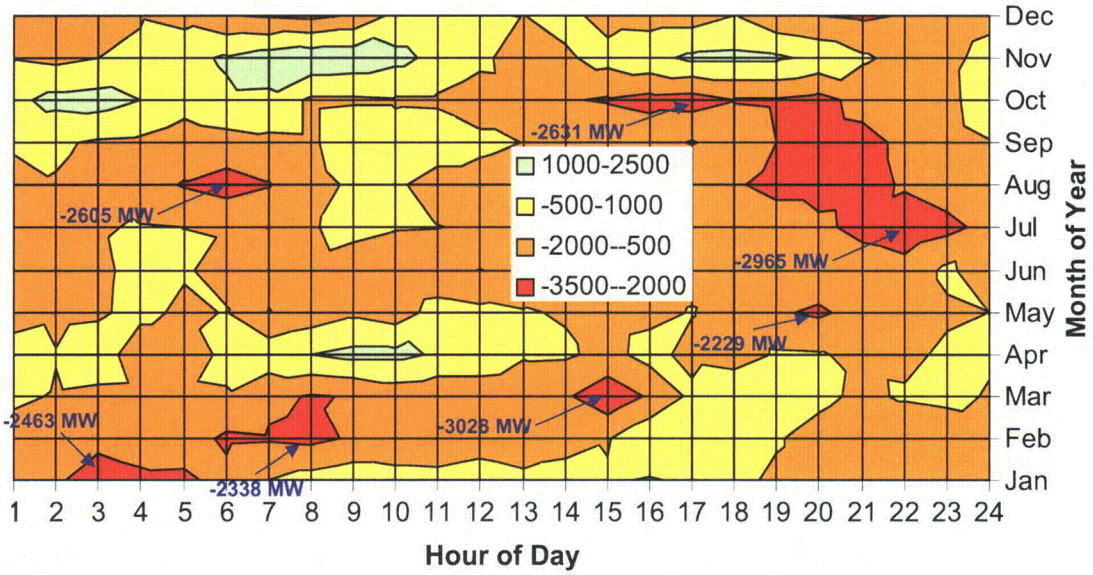

Figure 4-19 - Incremental maximum net load under-forecast errors due to wind

4.4.2. Daily Profiles of Forecast Errors

In order to assess how forecast error varies throughout a typical day, average daily profiles for four seasonally representative months are created and overlaid with the hourly forecast errors. Figure 4-20 shows these plots for load and net load with 15,000 MW of wind generation during January, April, July and October. Other plots, including complete traces of all profiles and forecast errors are available in Appendix D.

The dashed magenta and blue curves are average daily load and net load, plotted against the left scale. Average daily profiles are created by averaging all similar hours during a month to create a 24-hour profile. The forecast error at each hour of the day, across the month, is captured by the box and whisker plot. The length of the rectangular boxes represents a spread of one standard deviation (σ) around the mean of the day-ahead forecast error for a particular hour of the day. The whiskers show the maximum over-forecast and under-forecast errors over the month, for a particular hour of the day.

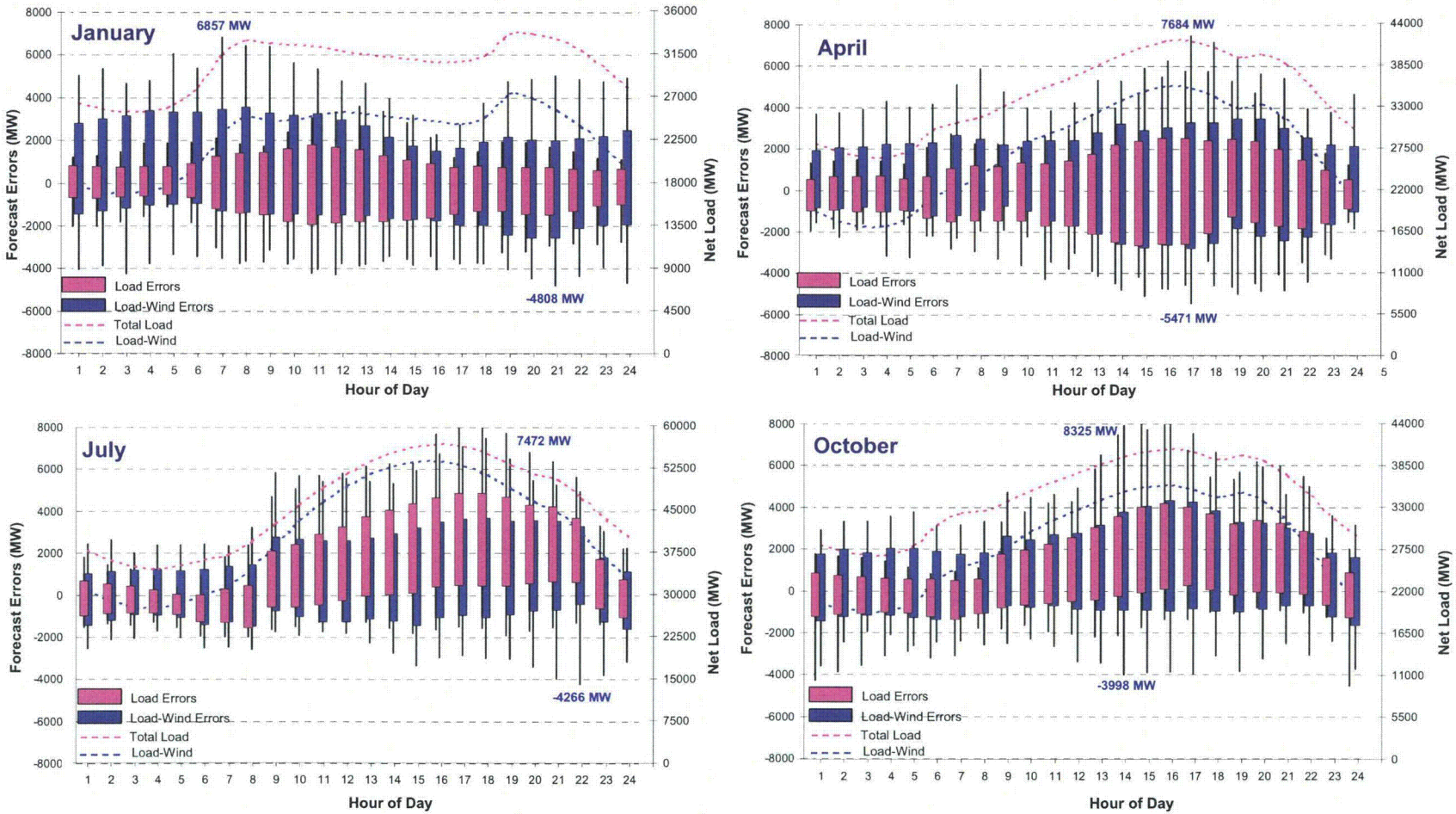

Figure 4-20 Average daily profiles and predictability for load and load-15,000 MW of wind generation (net load).

The length of the boxes in Figure 4-20 indicate the spread in forecast error, or the general forecast accuracy at a particular hour of the day. Considering the relative length of the magenta (load) and blue (net load) boxes, wind generation reduces forecast accuracy over most hours of the day, but particularly in early morning and late evening hours during winter, spring and fall.

Considering the trend in the average (center of the boxes), during the morning hours (corresponding with load-pickup), net load tends to be generally over-forecasted relative to load (positive bias). But during late afternoon to evening hours in summer and fall, net load tends to be under-forecasted relative to load (negative bias).

The whiskers in Figure 4-20 show the maximum positive and negative forecast errors. Considering the relative length of the whiskers for the load and net load boxes, we see that wind generation can drive extreme forecast errors in both directions. The late evening hours in summer and fall tend to see incrementally large net load under-forecast errors. This is consistent with the observation from the incremental surface plot in Figure 4-19. Large under-forecast errors during these hours may lead to under-commitment of resources, however, these are typically the hours when resource needs are low.

There are also incrementally large net load under-forecast errors in the early afternoon (peak) hours during the summer, (and fall to some extent). Note that the spread of the net load forecast errors (or general forecast accuracy) is not dramatically different from load alone, but there are significantly larger under-forecast errors with wind. This may potentially lead to under-commitment of resources during peak load times when they are most needed.

4.5. Summary

The predictability of net load is important to the unit commitment process because large errors in the day-ahead forecast may compromise reliability, increase operating costs and require greater ancillary service procurement.

Forecast error (forecast – actual) is defined as positive for over-forecast and negative for under-forecast. Over-forecasting may lead to more generation being committed than needed (which has potential economic consequences), while under-forecasting may lead to under-commitment, which is a potential reliability problem. From a system operation standpoint, under-forecasting is a more serious issue.

Considering wind generation in isolation, as penetration increases, the number and size of extreme wind forecast errors also increase. The distribution of forecast errors becomes more skewed to the left with additional capacity, which indicates that there is a clear tendency for wind generation to be under-forecasted. However, wind generation *under*-forecast errors show up in net load as *over*-forecast errors, which may lead to over-commitment (rather than under-commitment) problems.

Overall Net Load Trends - With coincident load and wind, there is an overall trend of decreasing forecast accuracy (increasing error) with increasing wind penetration. The incremental wind forecast errors tend to skew the net load forecast error toward the positive (over-commit) side. The size of the extreme forecast errors also increase with wind penetration, but the negative errors tend to grow faster than the positive ones.

Seasonal Trends - Seasonal trends in predictability were initially studied by comparing the profile of maximum daily load forecast errors with maximum daily net load forecast errors over the study year. The analysis revealed that

1. There is a greater tendency to accumulate large *load* over-forecast errors during the summer months and large load under-forecast errors during the winter months.
2. Extreme *net-load* forecast errors tend to be greater in non-summer months.
3. Across the year net load forecast errors are generally larger than corresponding load forecast errors, but the incremental increase may be greater for under-forecast errors in the summer.

These observations become even more pointed when the correlation of all load and wind forecast errors is examined by seasons. Overall, there is an extremely weak correlation between the errors, which suggests that both errors are independent, not driven by the same factors, and are unlikely to coincide or reinforce each other. Further inspection of the pattern of errors over different seasons led to the conclusion was that it is improbable for the most severe load and wind errors to occur in the same hour -- or *the risk of simultaneous under-commitment error is small.*

The scatter plots confirmed the earlier observation about net loads, (from the profile of maximum errors) -- on average, net load forecast accuracy is lower (errors are larger) in the winter and spring months than during the summer.

Time-of-Day Trends from Extreme Error Profiles - The time-of-day pattern for forecast errors was first investigated by looking at the time of occurrence of daily extreme errors across the months. The results showed that with no wind, the largest load *over*-forecasts typically occur in late afternoons during the summer months. With 15 GW of wind generation capacity, there is generally an *increased* risk of over-commitment mornings and afternoons in fall and winter. The risk is simultaneously reduced in the mid-summer afternoons.

Considering under-forecast errors, with no wind, the periods with the greatest risk of *under*-commitment are in the afternoon to early evening hours during winter and spring. With a large penetration of wind generation resources, the risk of net load under-commitment is more spread over the day, and the magnitudes are greater, particularly in spring afternoons.

The difference between negative load forecast errors and negative net load forecast errors gives the *incremental* risk of under-commitment due to wind generation. The resulting pattern indicates that the incremental risk (over load-alone) is increased across all hours of the day and months of the year, with particularly acute increases in some periods -- *evening hours in summer and fall and early morning hours in the winter.*

Time-of-Day Trends from Forecast Accuracy Profile - When the hourly risk is further investigated from the overall error profiles using box plots, the results conform with earlier observations. Wind generation reduces net load forecast accuracy (increases errors) over most hours of the day, but particularly in early morning and late evening hours during winter, spring and fall. With regard to time-of-day trends, there three major observations:

1. Across all seasons, during the morning load rise hours, net load tends to be generally over-forecasted relative to load (positive bias). These are the periods when ramping requirement is high, so resource over-commitment should not lead to reliability issues.
2. Late evening hours tend to have lower net load forecast (relative to load) and incrementally larger extreme net load under-forecast errors, which may lead to under-commitment of resources. However, these are typically the hours of the day when resource needs are low.
3. During afternoon to early evening (peak) hours during summer and fall, there are incrementally larger net load under-forecast errors (relative to load. The size of these errors, relative to load errors, are such that they may potentially lead to under-commitment of resources during peak load times when they are most needed.

5. PRODUCTION SIMULATION ANALYSIS

5.1. Introduction

An economic simulation was performed on the ERCOT system in order to determine the operational impact of various levels of wind generation on the balance of the system generation. In addition to seeing how thermal generation production might be expected to shift, the key values determined were the hourly spot prices, or marginal cost of energy, and the hourly value, or opportunity cost, of spinning reserves. The spinning reserve cost was used as a surrogate to estimate the impact of wind generation on the cost of ancillary services in general. Another key value determined was the amount of capacity available for regulation services. As more wind generation enters the system there is a tendency for less thermal generation to be committed, thereby reducing the amount of generation that would naturally be available to provide ancillary services.

Although these results were available as a natural by-product of the simulation, the primary purpose of the simulation analysis was NOT to determine the economic value of the wind generation but rather to determine the operational impact on the balance of the system. What type of generation is displaced, coal or gas? What is the impact on emissions? What is the spot price impact of introducing a large amount of "price takers" to the system? What is the ramping rate and range of the balance of the system for regulation services? These are the types of results addressed in the remainder of this section.

The operational analysis was performed using the GE Multi Area Production Simulation program (MAPS). This program has been used for years throughout North America to assist planners, developers and regulators in the analysis of electric power systems. MAPS is a highly detailed model that calculates hour-by-hour production costs while recognizing the constraints on the dispatch of generation imposed by the transmission system. When the program was initially developed over thirty years ago, its primary use was as a generation and transmission planning tool to evaluate the impacts of transmission system constraints on the system production cost. In the current deregulated utility environment, the model has been useful in studying issues such as market power and the valuation of generating assets operating in a competitive environment. The unique modeling capabilities of MAPS include a detailed electrical model of the entire transmission network, along with generation shift factors determined from a solved ac load flow, to calculate the real power flows for each generation dispatch. This enables the user to capture the economic penalties of redispatching the generation to satisfy transmission line flow limits and security constraints. The chronological nature of the hourly loads is modeled for all hours in the year. In the electrical representation, the loads are modeled by individual bus. In addition to the traditional production costing

results, MAPS can provide information on the hourly spot prices at individual buses and flows on selected transmission lines for all hours in the year.

In this particular analysis the transmission constraints were ignored. The study was designed to examine the impact of the intermittent and uncertain characteristics of wind assuming that sufficient levels of transmission were available. The base year of interest was 2008. Chronological regional load data for 2006 were scaled up to the 2008 projections. These loads were then paired with generation outputs from various wind plants throughout the system based on actual 2006 hourly meteorological data, as has been described previously. It was important to have load and meteorological data from the same time frame in order to capture the correlation between them. Wind generation penetration levels of 5,000 MW, 10,000 MW and 15,000 MW were examined, with two slightly different 10,000 MW scenarios being considered. For each wind site two separate profiles were developed. The first profile estimated the hourly production that would be expected at each wind plant based on the actual meteorological data that had occurred. The second profile was an unbiased (mean, or 50% confidence level) wind generation forecast, representing a day-ahead forecast made on the previous day. These profiles are referred to as the "State-of-the-Art", or S-o-A forecast and were used in the day ahead commitment process.

5.2. Simulation Results

The bars in Figure 5-1 show the generation by type for the various wind generation scenarios. These results are based on the 2008 (study year) simulation using a state-of-the-art wind generation forecast for the day ahead commitment. Only the generation types that changed are shown. These include combined cycle units (CC), peaking gas turbines (GT), steam coal units (STCOAL) and steam natural gas fired units (STNG). The wind generation is also shown for each scenario. As can be seen, the major generation displacement occurred on the combined cycle units. There was slight impact on the other types, with gas turbines increasing slightly for the 5,000 MW and 10,000 MW wind generation capacity scenarios.

One of the key factors examined was the impact of wind generation on the commitment and dispatch of the balance of the system. Figure 5-2 shows the hourly unit commitment by unit type for the peak load week in mid August assuming zero wind generation. The unit commitment took into account the operational characteristics of the individual generators, including minimum down time, start up costs and their ability to contribute to the spinning reserve. The combined cycle, steam gas and gas turbine varied the most throughout the week.

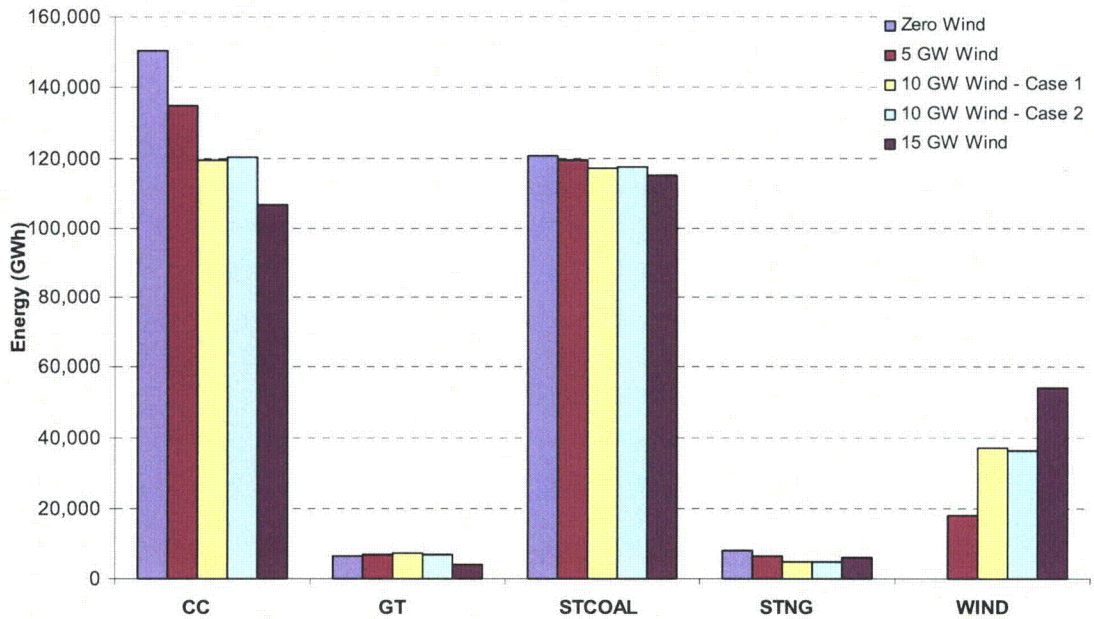

Figure 5-1 - Generation by type.

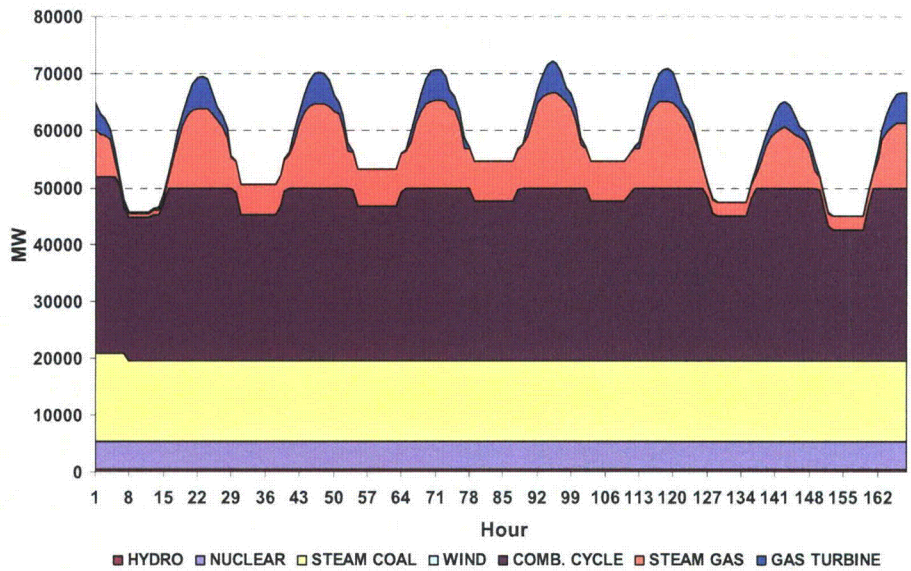

Figure 5-2 - Commitment for peak load week, zero wind generation.

The hourly dispatch for this week is shown in Figure 5-3. Here can be seen some variation in the hydro operation and more significant variation in the combined cycle and steam gas units. As will be shown later, this hourly unit commitment and dispatch information was used with the unit's ramping capability to determine the ramping (MW/minute) and range (MW) capability of the system on an hourly basis. This was then compared to the hourly regulation requirements of the system. Of particular

importance was how this ramping and range capability changed as increasing amounts of wind generation were added to the system.

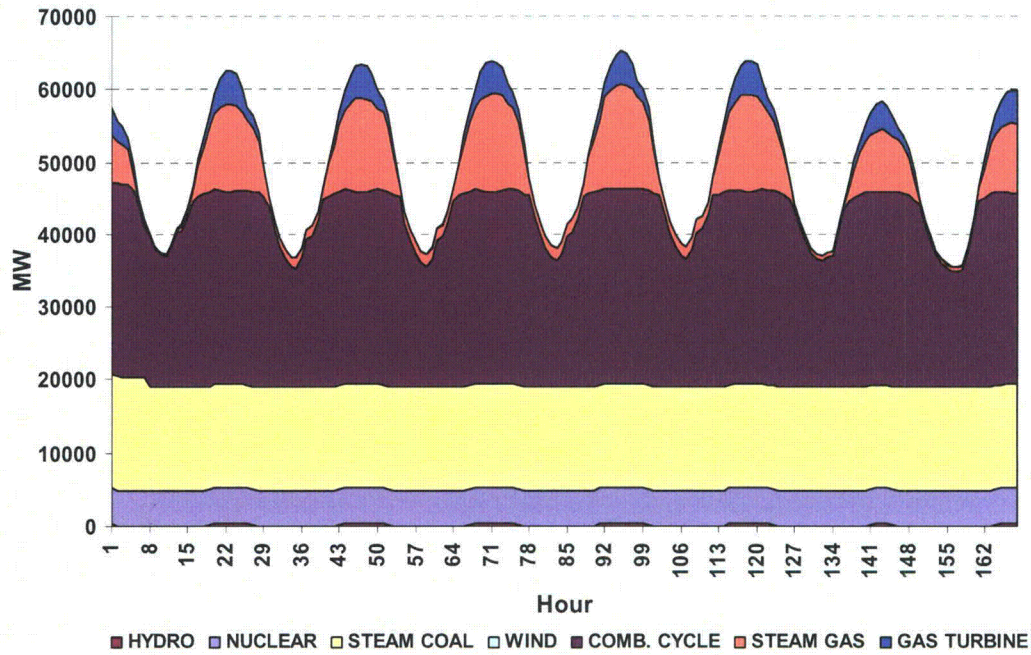

Figure 5-3 - Dispatch for peak load week, zero wind generation.

The plots in Figure 5-4 and Figure 5-5 show how the commitment and dispatch for this week change when 15 GW of wind generation capacity is added to the system. In this week it appears that the wind generation displaced peaking capacity on peak and combined cycle generation in the off-peak hours.

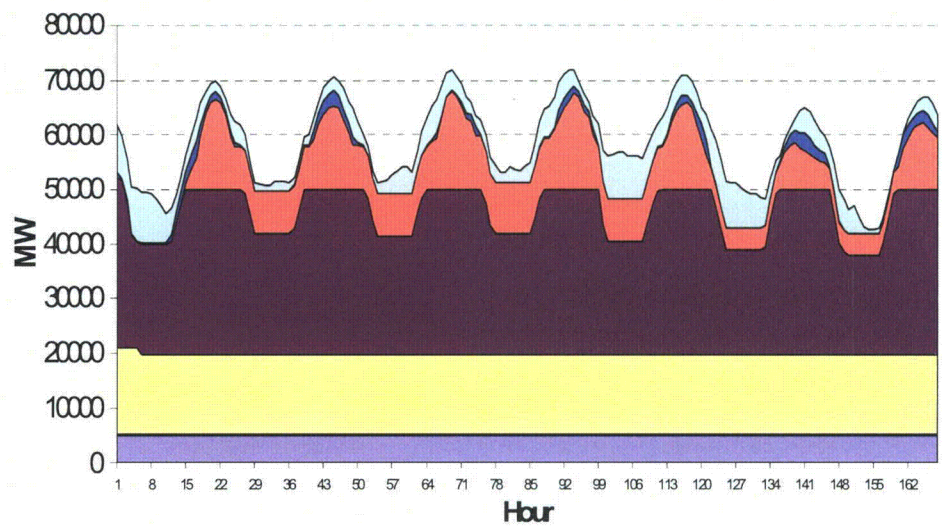

Figure 5-4 - Commitment for peak load week, 15 GW wind generation. (Same legend as Figure 5-3 applies)

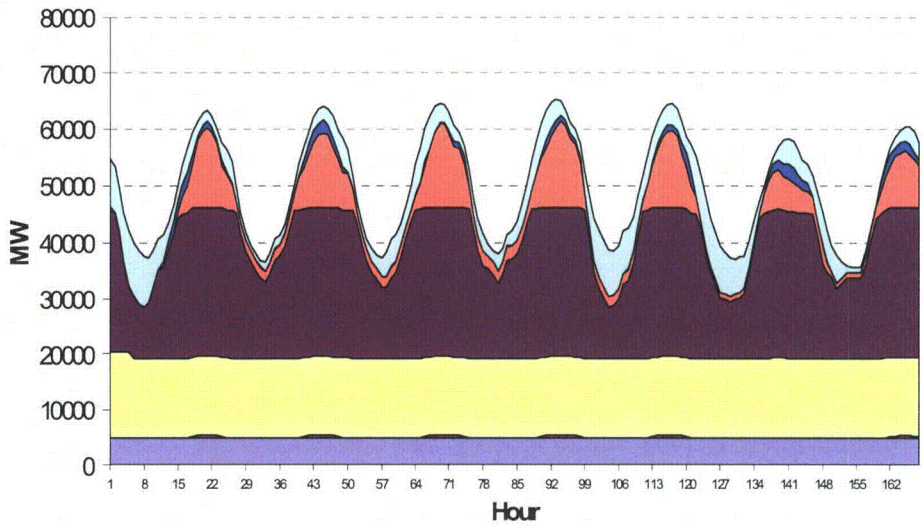

Figure 5-5 - Dispatch for peak load week, 15 GW wind generation capacity. . (Same legend as Figure 5-3 applies)

The next set of figures examines the system commitment and dispatch during the week with the highest amount of wind generation in early April. Figure 5-6 and Figure 5-7 show the hourly commitment and dispatch for this week for the zero wind generation scenario. Most of the variability in the loads is handled by the combined cycle generation. Figure 5-8 and Figure 5-9 show the impact of 15 GW of wind generation capacity added to the system. The committed combined cycle capacity is reduced to almost zero in some overnight periods and even the coal fired generation shows some deep turn downs in the overnight dispatch.

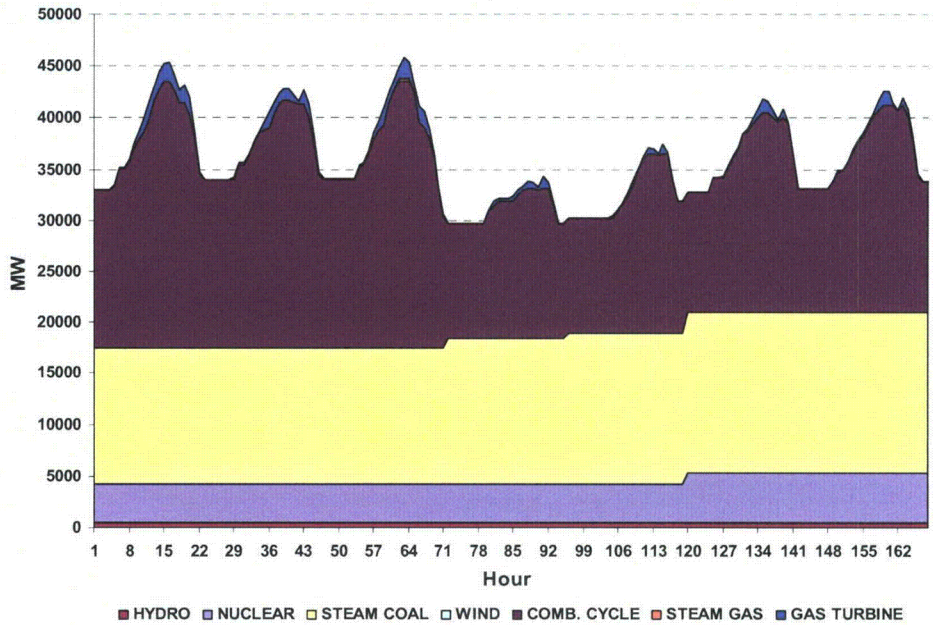

Figure 5-6 - Commitment for peak wind generation output week, zero wind generation.

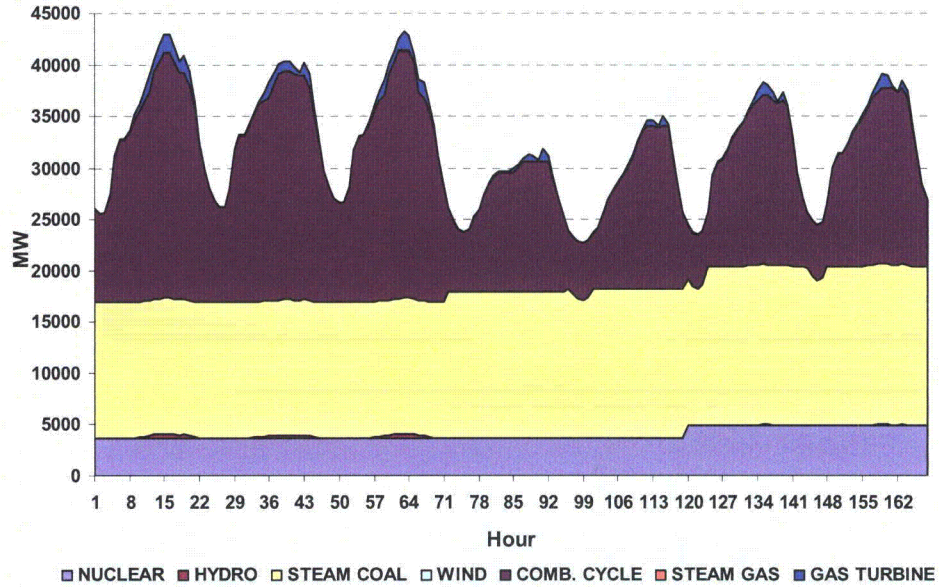

Figure 5-7 - Dispatch for peak wind generation output week, zero wind generation.

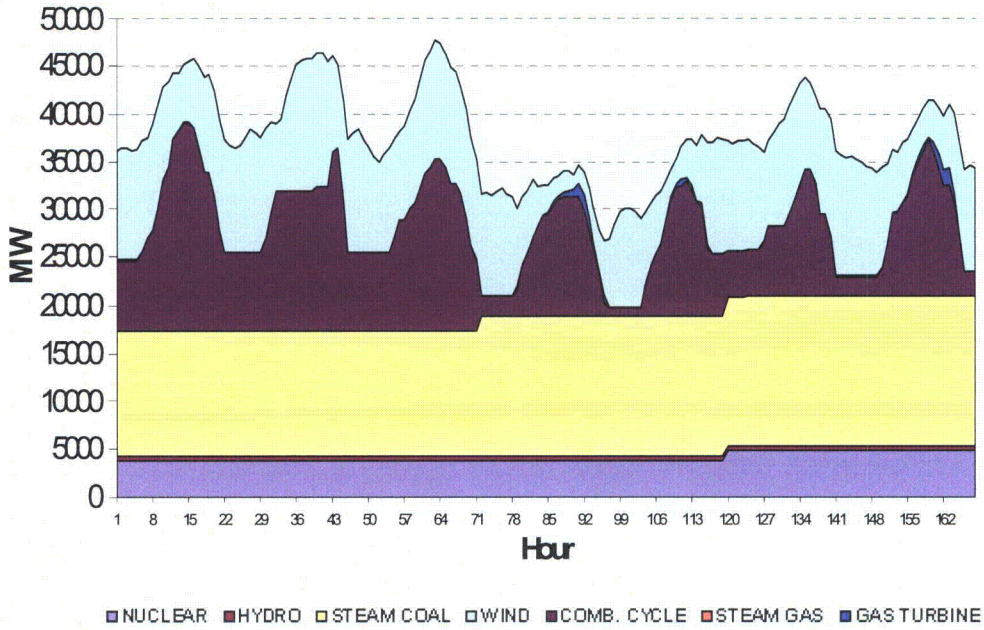

Figure 5-8 - Commitment for peak wind generation output week, 15 GW wind generation capacity.

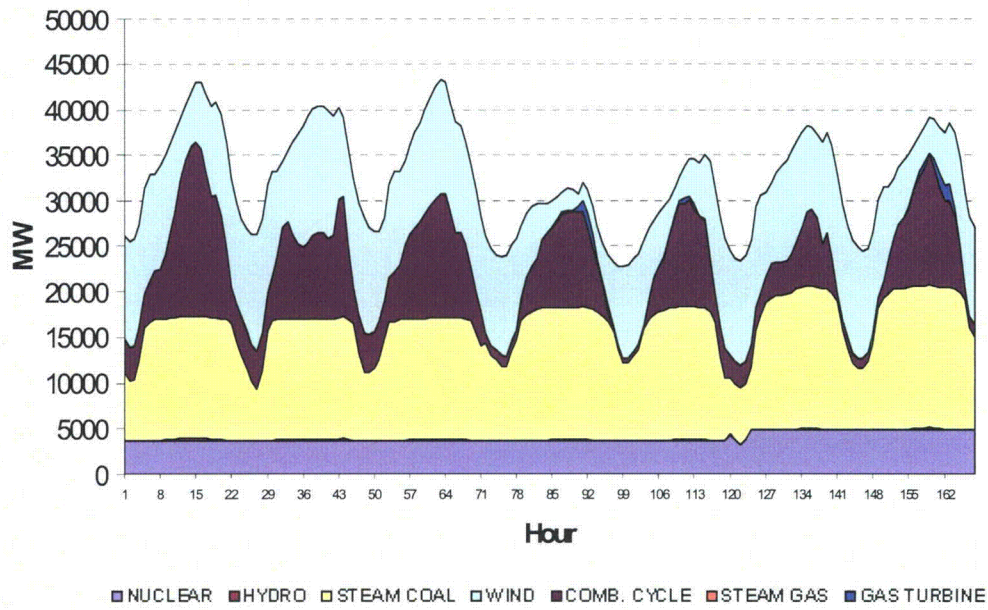

Figure 5-9 - Dispatch for peak wind generation output week, 15 GW wind generation.

The bars in Figure 5-10 show the reductions in the system production cost expressed on a megawatt hour of wind generation basis for the various wind scenarios. Based on this chart, the value of the wind does not drop significantly up through penetrations of up to 15 GW. These bars are consistent with the earlier chart showing that combined cycle generation bore the brunt of the displacement across all scenarios.

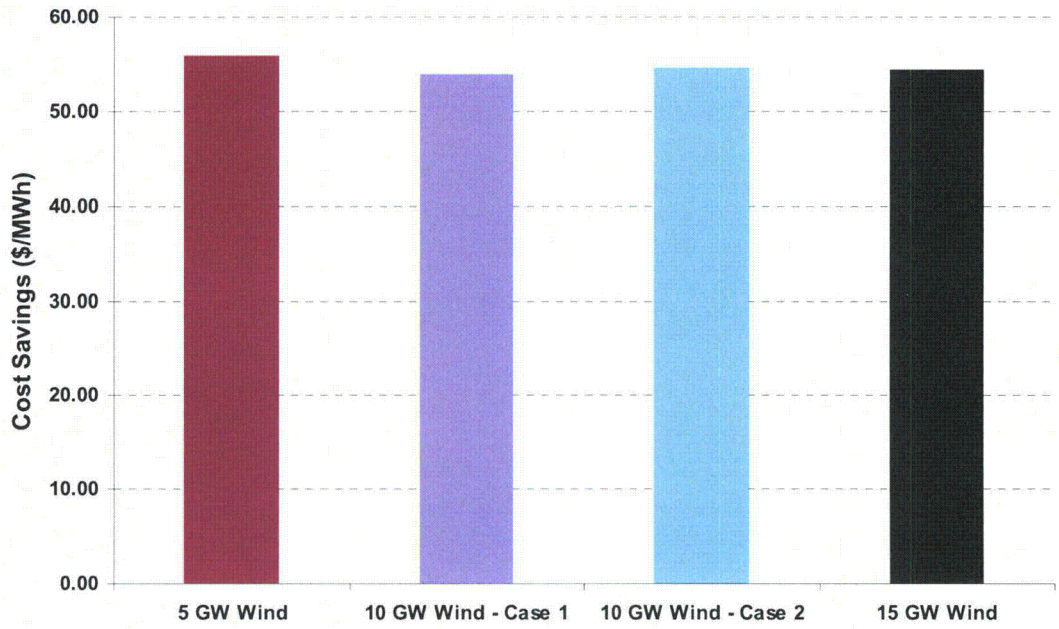

Figure 5-10 - Production cost reductions due to wind generation.

The charts in Figure 5-11 show how the total annual emissions decline as the wind generation penetration is increased.

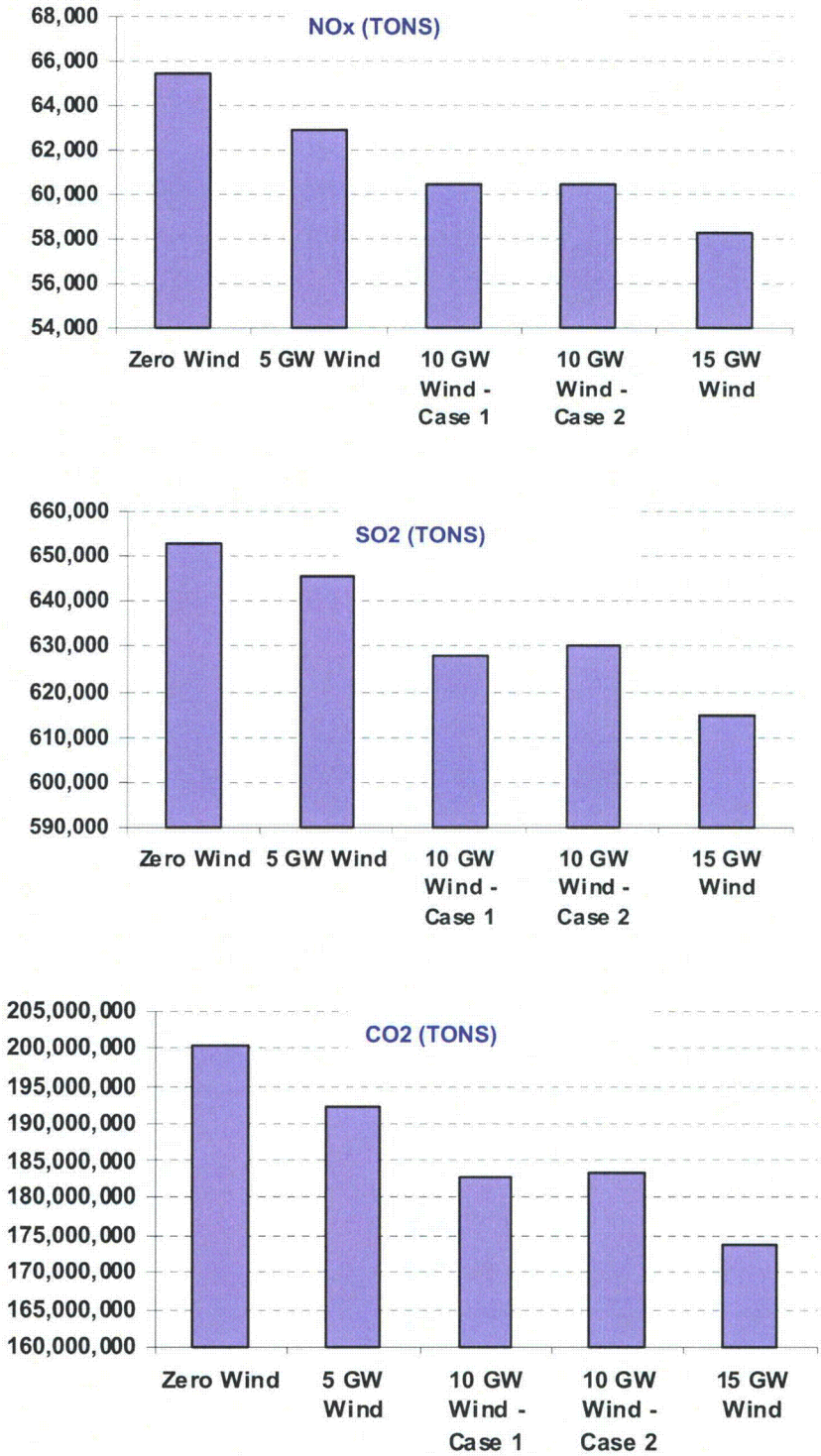

Figure 5-11 - Total annual emission.

5.3. Spot Price Impact

The curves in Figure 5-12 show the impact of increased wind generation on the system spot price, or incremental value of energy in $/MWh. The values were calculated on a chronological, hourly basis assuming a state-of-the-art wind generation forecast. They were then sorted individually for the plot.

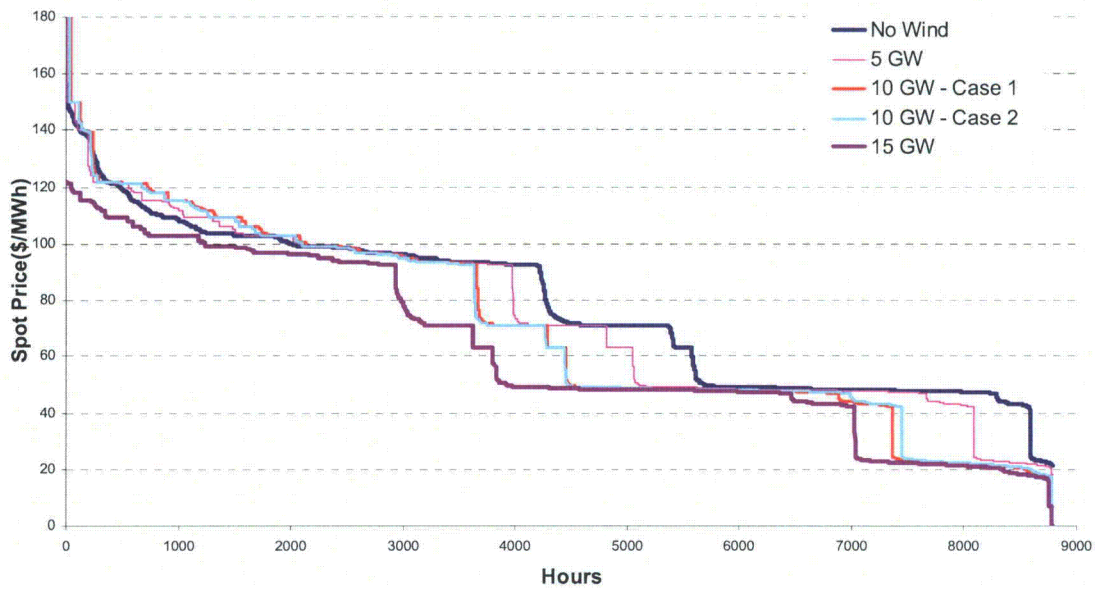

Figure 5-12 - Energy spot prices.

In general, as the wind generation penetration increases it displaces the higher cost thermal generation and reduces the overall cost of energy. In some cases the spot prices are slightly higher due to the imperfections in the state-of-the-art forecast used.

The curves in Figure 5-13 examine the impact of wind generation forecast on the resulting spot prices for the 15 GW penetration scenario. The perfect forecast drops slightly below the zero wind scenario for the first 3500 hours and then increases the separation for the rest of the curve. The spot prices calculated with the state-of-the-art forecast are slightly lower and then drop after about 3000 hours. The "no forecast" case totally ignores the wind generation in the day ahead forecast and therefore significantly over-commits the system. This results in the spot prices dropping significantly all of the time.

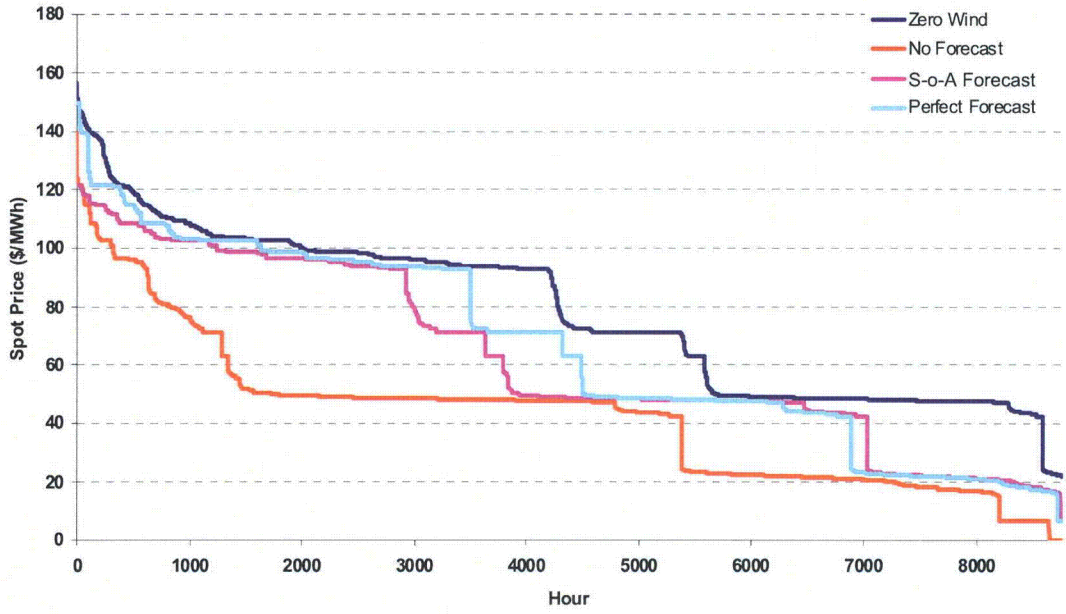

Figure 5-13 - Wind forecast impact on energy spot prices.

6. REGULATION REQUIREMENTS ANALYSIS

Section 3 provides the results of an extensive analysis of load and net load variability, over various timeframes, independent of specific ancillary services definitions or system operating practices. This section specifically analyzes the regulation ancillary service, as defined by ERCOT for use in the new nodal market structure.

This section includes extensive analysis of the deployed regulation for each of the wind generation scenarios, and correlation to temporal factors. The adequacy of ERCOT's present methodology to determine the amount of regulation to procure is assessed, and some improvements are suggested. Using production simulations for each scenario described in Section 5, the flexibility of the dispatchable generation fleet to provide the required regulation capability is assessed. Also using the production cost simulation results, the costs of procuring the regulation service are estimated.

6.1. Regulation in the Nodal Market

ERCOT plans to shift from a zonal market to a nodal market in 2009. In this transition, the methods of system operation and the nature of the regulation ancillary service will change. This study solely analyzes regulation as defined for the nodal market. However, there are details of the nodal market with regard to regulation that are still subject to refinement.

The ERCOT nodal market will use five-minute dispatch cycles. The dispatched generation setpoint for each period is the instantaneous value of load (or net load) at the beginning of the period, plus a heuristically-determined "tuning factor" times the expected change of net load over the period as determined by the short-term load forecast. The tuning factor will be between zero and one, and may vary with time of day and season.

Analysis of actual regulation requirements under the nodal market was beyond the scope of this study, as ERCOT has not yet made determination of the tuning factors that will be used. Any speculative choices made regarding the tuning factors are most likely to not be the same as the final values, and defining a quasi-optimal selection of tuning factor levels for different seasons and times of day would have required significant additional study outside of the study scope.

At the direction of ERCOT, the tuning factor was assumed to be zero. It is expected that optimizing the tuning factors on an hourly and seasonal basis will reduce the amount of regulation required to provide load-following service during periods of large system ramps (up or down). By proceeding with this analysis with the tuning factor set to zero, the study has purposely foregone an exact reflection of regulation requirements in the nodal market. But, by so doing, have allowed the development of an unbiased analysis of

the incremental amounts of regulation required with increasing amounts of wind generation capacity on the system. The results of this study should not be considered as an absolute prediction of regulation requirements in the nodal market. But, this limitation does not invalidate what are the key results from this study - the incremental regulation requirements resulting from additional wind generation capacity. It is important that results shown in this report are not compared with historical zonal regulation requirements.

In this study, regulation has been defined to be the deviation of the net load from the economic dispatch setpoint, unadjusted by the short-term net load forecast. as illustrated in Figure 6-1. Up-regulation (indicated in this report as +REG) is the positive difference between actual load and dispatched generation output, and is used when load exceeds the generation . Down-regulation (indicated in this report as –REG) is used when load is less than the dispatched generation output. Throughout this report, up-regulation is shown as a positive number and down-regulation is shown as a negative number.

Figure 6-2 shows the regulation deployments using the nodal algorithm, for one typical day (April 1). The regulation is strongly influenced by the load ramp rate, with large up-regulation requirements during periods of load rise, with little or no down-regulation required for the same period, and large down-regulation requirements during load drop. The impact of load ramp rate has a greater influence on regulation than does the random variation of load.

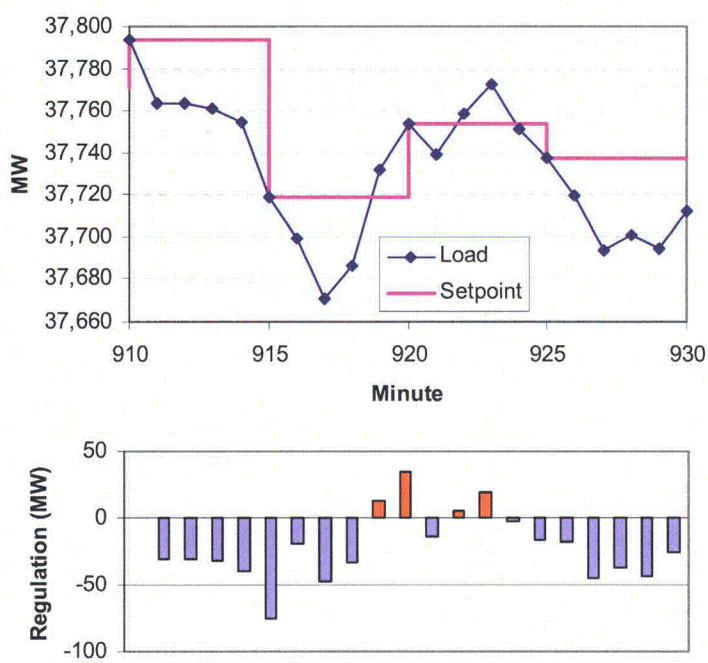

Figure 6-1 - Illustration of regulation as defined for the ERCOT nodal market

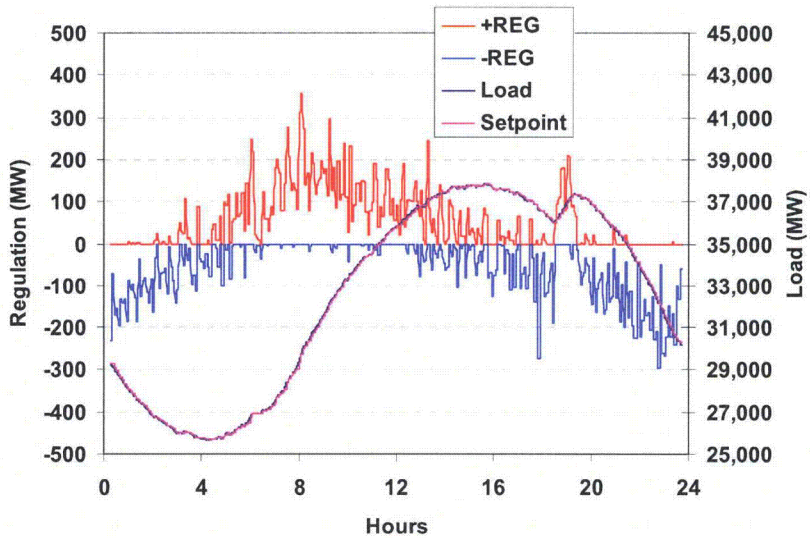

Figure 6-2 Regulation deployments for the same spring day as Figure 6-1.

6.2. Impact of Wind on Regulation

The nodal regulation algorithm was modeled on a minute-by-minute basis for the entire "study year", and for the "prior year, for each of the wind generation scenarios. Figure 6-3 plots the maximum up-regulation and down-regulation[1] requirements for each hour in a 100-hour (approximately four day) sample from January of the study year. Similar plots for the months of April, July, and October, representing the seasons of the year, can be found in Appendix E.1. In these plots, the lines above zero represent up-regulation, plotted as a positive number, and the lines below zero represent down-regulation, plotted as a negative number. These plots illustrate several observations which can be made regarding the impact of wind generation on regulation deployments, which are:

- The general nature of the regulation requirement is not greatly altered by the addition of wind generation.
- Some extrema are driven entirely by the wind. An example is seen at Point A of the expansion in Figure 6-3, where there is no significant peak in regulation requirements at this hour without wind generation, and the peak becomes progressively more significant as wind generation is added.
- The largest peaks in the plot are driven by the load behavior such as at Point B, and addition of wind makes only a very incremental increase in severity.

[1] Maximum in the absolute value sense. Because the down-regulation is recorded as a negative number, the most severe down-regulation requirement is, mathematically speaking, the minimum regulation.

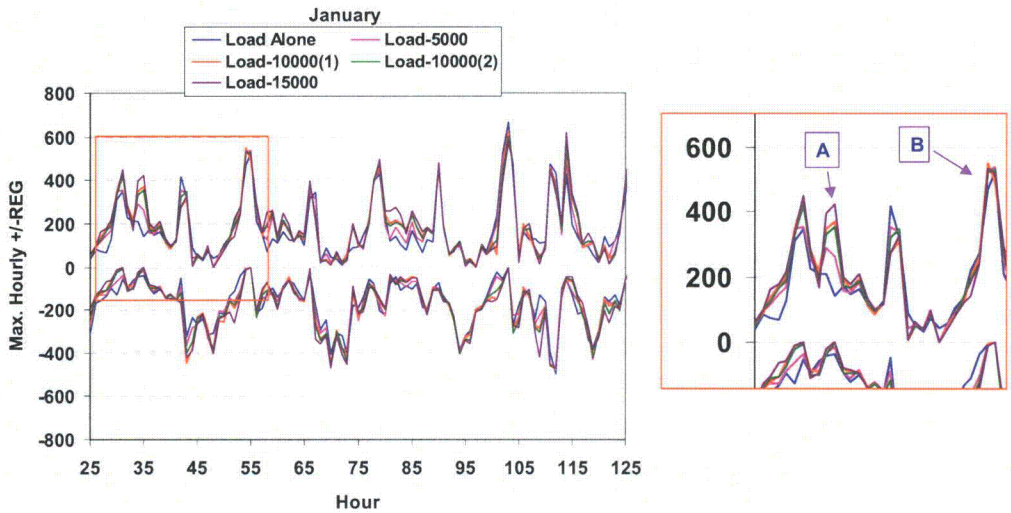

Figure 6-3 ***Maximum hourly regulation deployments for a 100-hour sample from January of the study year, for the wind generation scenarios. (Plot to the right is an expansion of the boxed area shown in the plot on the left).***

6.2.1. Statistical Description of Regulation Deployment

The cumulative distributions of hourly regulation maxima shown in Figure 6-4 to Figure 6-9 illustrate the incremental impact of increased wind penetration on regulation deployments. Figure 6-5 and Figure 6-8 expand the plot for the lower values of maximum regulation that pertain to 90% of the annual hours. Most important to system operations are the extreme values of regulation deployment[2]. Figure 6-6 and Figure 6-9 expand the cumulative distribution plots for the most severe 100 hours, or 1.14% of the year, and indicate that the increase in extreme regulation deployments between zero and 15,000 MW of wind is on the order of 100 MW. Throughout all of these plots it can be seen that the impact of wind penetration on regulation is quite incremental, and approximately proportional to the amount wind generation capacity of the scenario.

It should be noted that the cumulative distributions, plotted in Figure 6-4 to Figure 6-9, use data separately sorted and ranked for each scenario. Therefore, points at the same location on the independent axis (x-axis) are not necessarily associated with the same hour in the year. Another way to view the relative impact of wind penetration on regulation requirements is by the frequency distribution of changes in regulation

[2] In this report, the difference between net load and dispatch setpoint are always considered "deployed" regulation, even if this amount exceeds the procured regulation service for that hour. In such a case, when the procured regulation reserves are exhausted, responsive reserves are used to fulfill the regulation deployment required.

requirements, due to wind, on an hour-by-hour basis. Such a distribution is plotted in Figure 6-10, and statistics of the hour-by-hour comparison are summarized in Table 6-1.

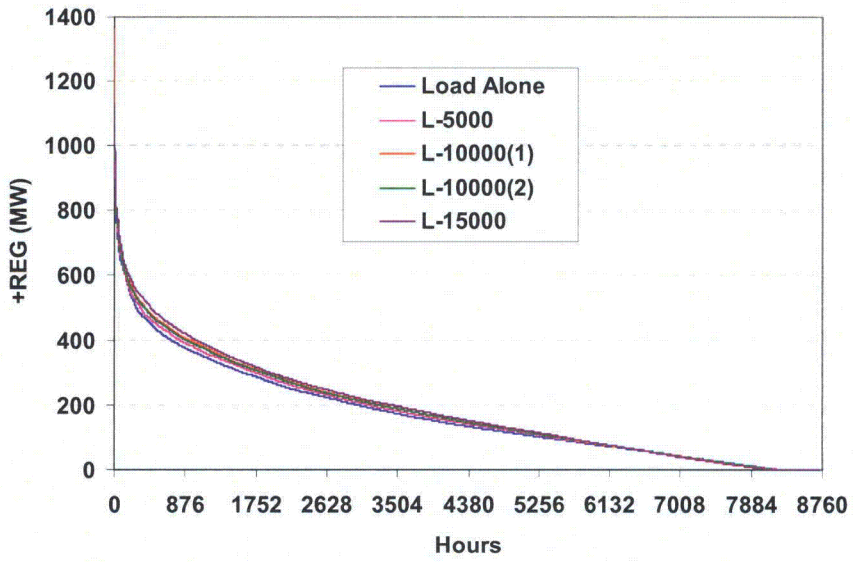

Figure 6-4 Cumulative distribution of hourly up-regulation maxima.

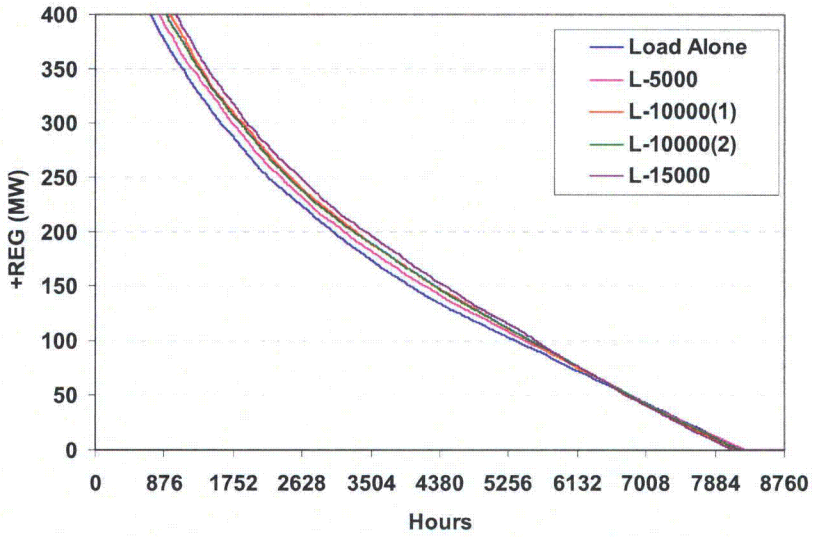

Figure 6-5 Expansion of Figure 6-4 for the range of 0 to 400 MW up-regulation.

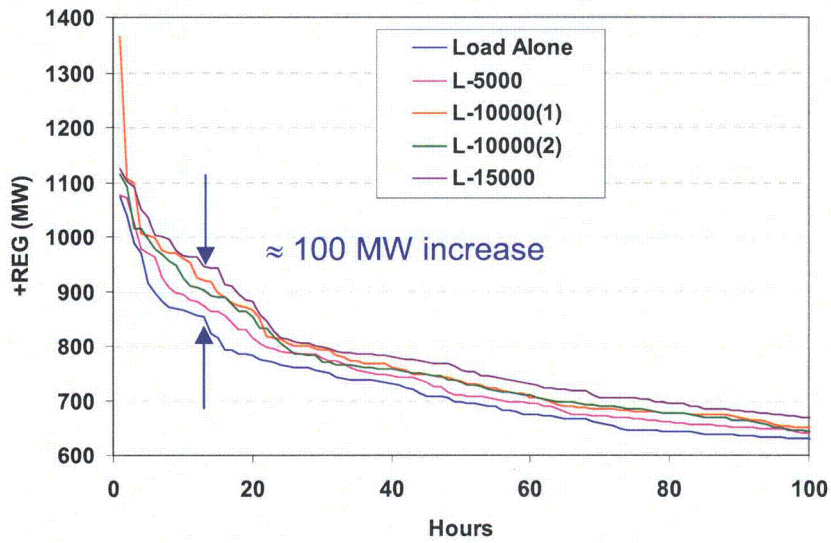

Figure 6-6 ***Expansion of Figure 6-4 for the 100 hours with the greatest up-regulation deployments***

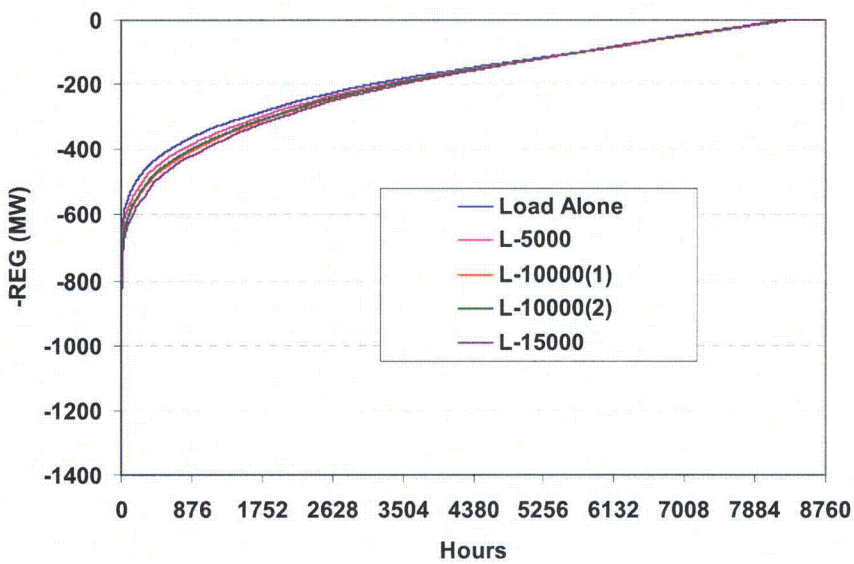

Figure 6-7 ***Cumulative distribution of hourly down regulation maxima.***

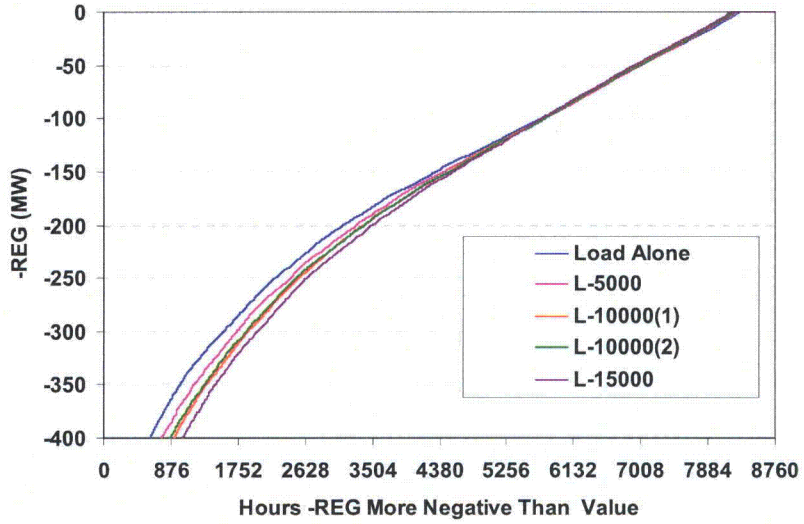

Figure 6-8 ***Expansion of Figure 6-7 for the range of 0 to 400 MW down-regulation.***

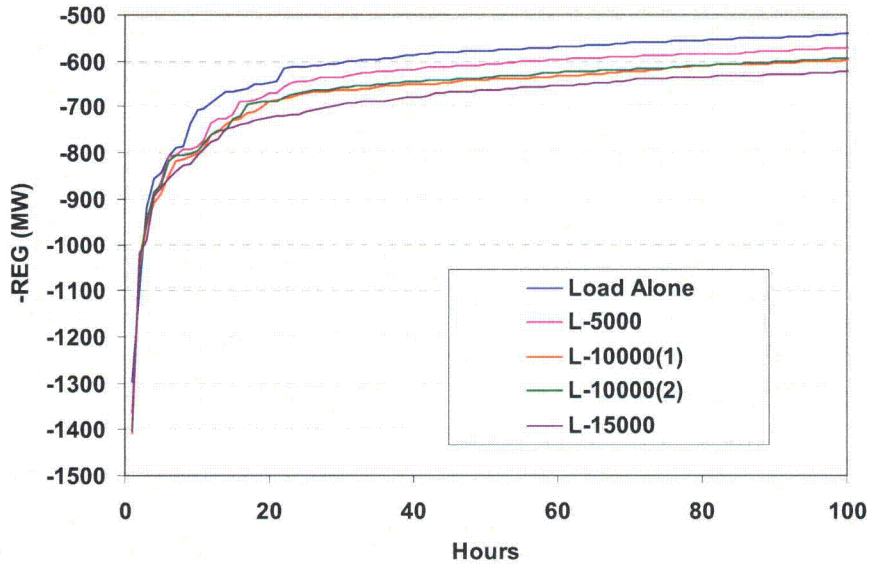

Figure 6-9 ***Expansion of Figure 6-7 for the 100 hours with the most severe down-regulation deployments***

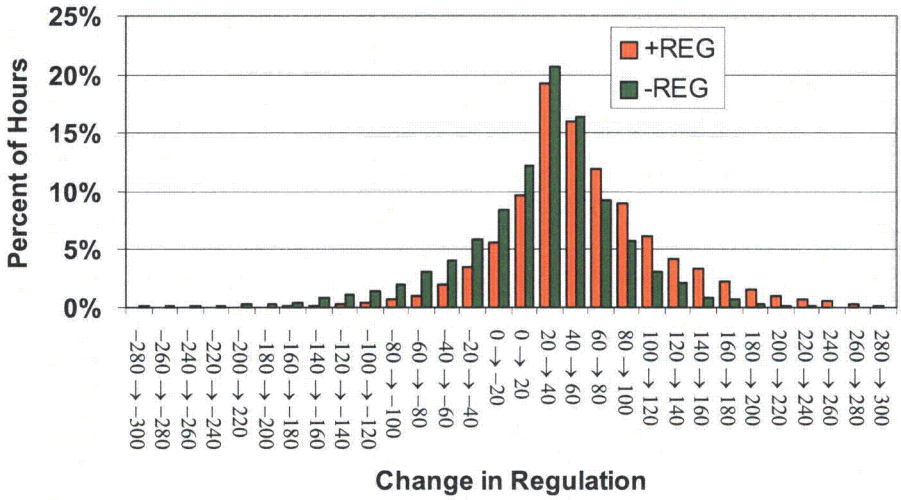

Figure 6-10 ***Frequency distribution of changes in hourly maximum regulation deployments between the 15,000 MW wind scenario and the zero wind scenario.***

Table 6-1 ***Statistical Summary of Changes in Hourly Maximum Regulation Deployments, Between No Wind to 15,000 MW of Wind Generation Capacity***

	+REG	-REG
Mean	17.7	-18.2
Sigma	64.9	65.1
Maximum	444.2	265.3
Minimum	-287.2	-453.1

There are a number of observations which can be made with regard to this frequency distribution and statistical summary:

- For any given hour, the magnitude of regulation can be either increased or decreased by having more wind capacity in the system.
- The mean increase in absolute value of hourly regulation extrema is approximately 18 MW for both up- and down-regulation.
- The mode (value range with the highest frequency) is a positive value for both the up-regulation and the down-regulation, even though the down-regulation is analyzed as a negative number. This means that a small increase in up-regulation, and a small decrease in down-regulation absolute value, are the most common changes caused by wind.

- The standard deviation of the relative regulation change is nearly equal for both up- and down-regulation, but there is a very obvious skew in the distributions toward the direction of increased regulation requirements (positive for up-regulation, and negative for down-regulation as a negative value).
- The most severe changes are symmetrical for up-regulation and down-regulation. The maximum up-regulation is nearly equal to the minimum, or most negative (most severe) down regulation. Also, the greatest changes in the direction of most severity were about 150%-170% of the greatest change toward reduced regulation severity (minimum, or most negative, change for up-regulation and maximum, or most positive change for down-regulation).

6.2.2. Regulation Service Procurement

ERCOT presently procures regulation services based on statistical analysis of historical deployments. For each month, procurements are determined for each hour of the day, with the same daily procurement pattern applying to all days of the month. Historical deployments considered are for the same hour of day in the prior month, and for the same month in the prior year. To perform the statistical analysis, ERCOT starts by determining the maximum regulation deployment within 5-minute periods for the hour in consideration. Maximum deployment data for the hour are combined for all days in the month, yielding a total of 336 to 372 periods (12 periods per hour times the number of days in the month). The 98.8th percentiles of these points are determined for the data pools for the same month in the prior year and for the prior month, and the greater of these is used as the basis for regulation procurement.

Thus, the statistical description of regulation deployments in terms of the 98.8th percentile is most relevant, and is indicative of the changes in regulation service procurements which will need to be made with increased wind penetration.

Table 6-2 summarizes the average, 98.8th percentile[3], and extrema[4] of the 5-minute regulation deployments for each wind generation scenario. The 98.8th percentile data

[3] This value is the average of the 98th percentiles of the maximum regulation in five-minute periods for each hour for each month, which is a metric indicative of the annual average amount of regulation service that would need to be procured. The process for determining this value is as follows: 1) Maximum up-regulation, or most negative down-regulation, is determined for each five minute period. 2) The 98th percentile of these maxima are determined for each hour-of-day within a month (population of 336 to 372 samples). 3) The average of the 98th percentiles are determined for all hours-of-day within the month (24 values). 4) The annual weighted average of the months, weighted by the number of days per month, yields the final value.

[4] Mathematically, the maximum of the up-regulation deployments and the minimum of the down regulation deployments.

increases, relative to the zero wind case, by 20.7% and 23.1% for up-regulation and down regulation, respectively. Interestingly, this correlates closely with the relative increase in net load variability as presented in Section 3. Also of note is the fact that the regulation extrema do not increase as much as the mean and 98.8th percentile values. This implies that the distributions are better behaved with increasing wind, with outliers less severe relative to the magnitude of the mean and 98.8th percentile.

Table 6-2 - Deployed Regulation Statistics

Up-Regulation

Wind (MW)	Average Max of 5-min Periods	% Change	98th Percentile of 5-min Periods	% Change	Maximum	% Change
0	73.8 MW		232.1 MW		1072.5 MW	
5,000	78.1 MW	5.8%	247.0 MW	6.4%	1075.9 MW	0.3%
10,000 (1)	82.5 MW	11.7%	265.2 MW	14.2%	1105.6 MW	3.1%
10,000 (2)	81.4 MW	10.2%	261.5 MW	12.7%	1112.7 MW	3.7%
15,000	86.1 MW	16.5%	285.8 MW	23.1%	1124.9 MW	4.9%

Down-Regulation

Wind (MW)	Average Min of 5-min Periods	% Change	98th Percentile of 5-min Periods	% Change	Minimum	% Change
0	-74.3 MW		-233.0 MW		-522.2	
5,000	-78.6 MW	5.8%	-246.7 MW	5.9%	-538.9	3.2%
10,000 (1)	-83.0 MW	11.7%	-262.7 MW	12.8%	-554.9	6.3%
10,000 (2)	-81.5 MW	9.7%	-260.4 MW	11.8%	-565.9	8.4%
15,000	-86.6 MW	16.5%	-281.2 MW	20.7%	-566.4	8.5%

6.2.3. Temporal Trends

Figure 6-11 shows plots of the maximum and 98.8th percentile of regulation deployments for four months of the year, representing each season. The solid lines represent the 98.8th percentile of the maximum regulation deployments for the five-minute periods, with the magenta line representing load alone, and the blue line representing the net load for the 15,000 MW wind scenario. The dotted lines represent the extrema for the two scenarios plotted here.[5] Plots above zero indicate up-regulation, and plots below zero represent down-regulation, plotted as a negative number.

The contour plots in Figure 6-12 and Figure 6-13 compare the temporal characteristics of the up-regulation deployment 98.8th percentiles for no wind and the 15,000 MW wind scenario, respectively. The x-axis indicates the hour of day, and the y-axis indicates the month of year. The colors, according to the legend, indicate the 98.8th percentile of the

[5] For plotting clarity, only the maximum (15,000 MW) and zero wind penetration results are shown in many plots of this report. These results bracket the results for all the scenarios, and results of this study show the intermediate scenarios providing results which are generally proportional to the wind penetration.

maximum regulation deployments in all the 5-minute periods for the particular hour, over all the days in the month. Figure 6-14 and Figure 6-15 are equivalent contour plots for down-regulation. Appendix E.2 provides these contour plots for all wind scenarios.

The temporal characteristics of the differences in 98.8th percentile regulation deployments, between zero and 15,000 MW of wind scenarios, are shown in Figure 6-16 and Figure 6-17.

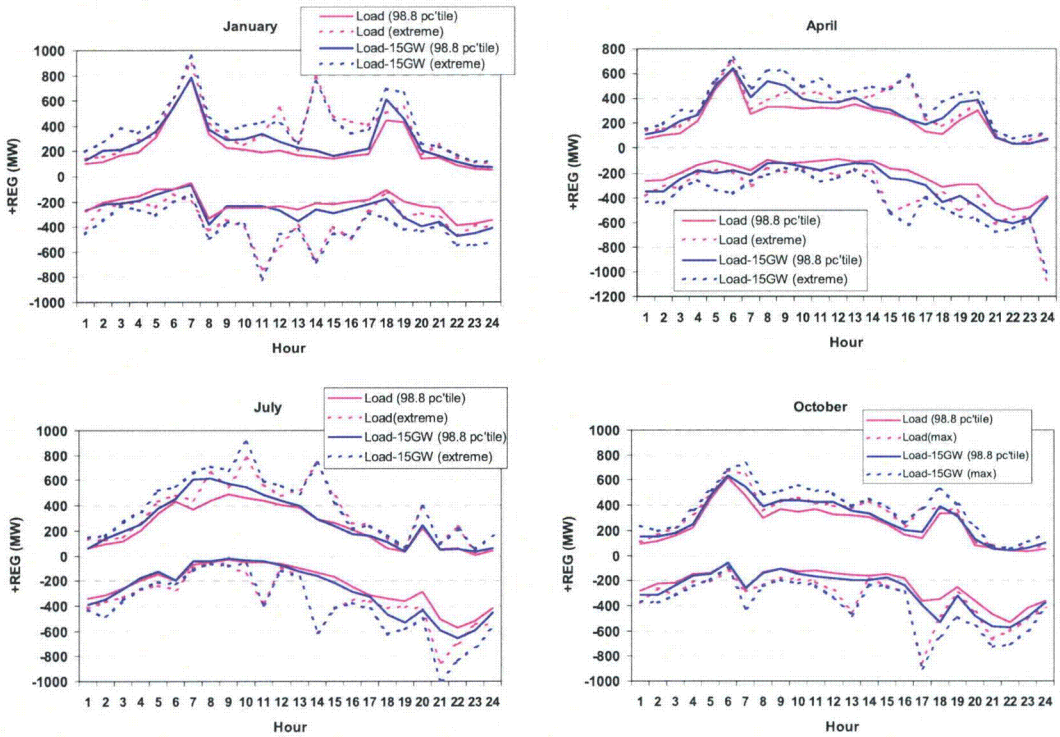

Figure 6-11 - Maximum and 98.8th percentile regulation deployments by hour of day for months representing the four seasons.

Regulation procurements are currently based on the greater of the 98.8th percentile of deployments for the same month in the prior year and the prior month in the same year. Because wind generation capacity is presently increasing very rapidly in ERCOT, the prior month value may be controlling most of the time if measures are not taken to adjust the prior year data for the wind capacity growth. Basing regulation procurement only on the prior month, by default, may result in under-procurement in months where the regulation requirements exceed the prior month. A methodology adjustment to account for year-to-year wind capacity additions is discussed later in Section 6.3.2.

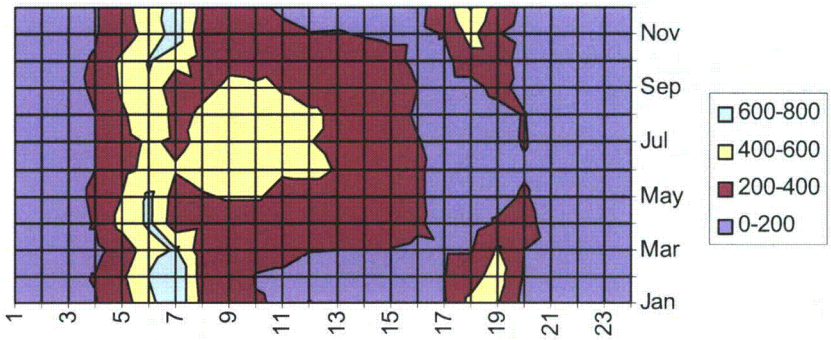

Figure 6-12 ***98.8th percentile of up-regulation deployments for the zero wind scenario.***

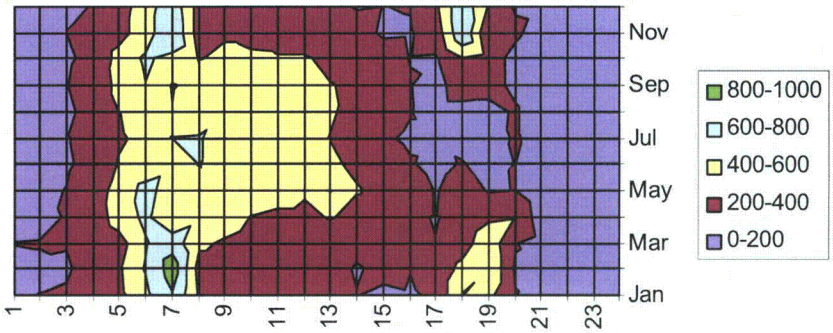

Figure 6-13 ***98.8th percentile of up-regulation deployments for the 15,000 MW wind scenario.***

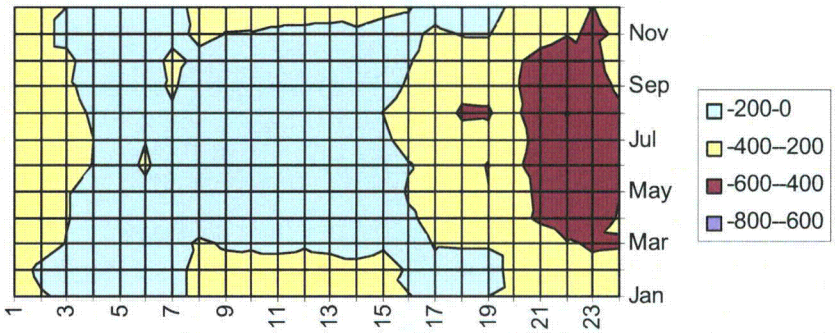

Figure 6-14 ***98.8th percentile of down-regulation deployments for the zero wind scenario.***

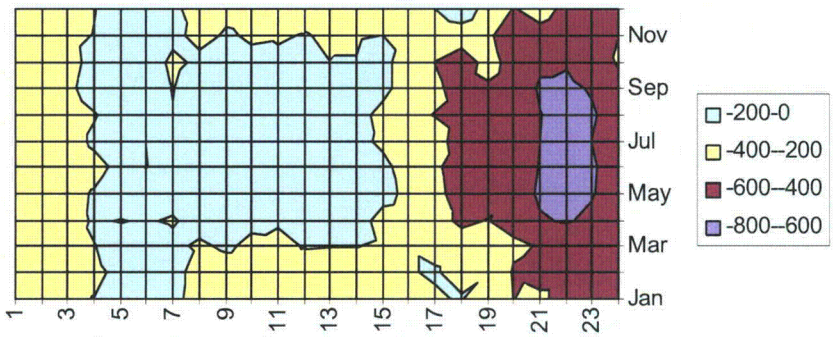

Figure 6-15 ***98.8th percentile of down-regulation deployments for the 15,000 MW wind scenario.***

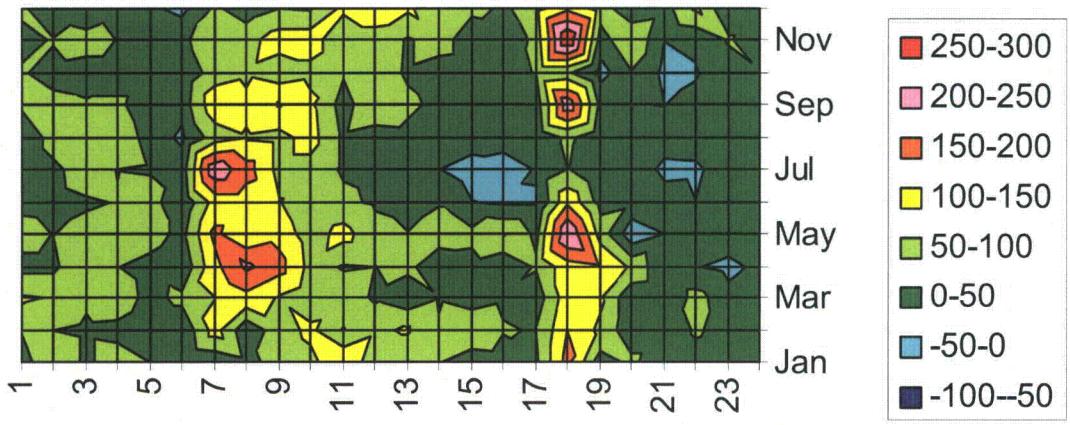

Figure 6-16 ***Difference in 98th percentile of up-regulation deployments between 15,000 MW wind scenario and zero wind scenario.***

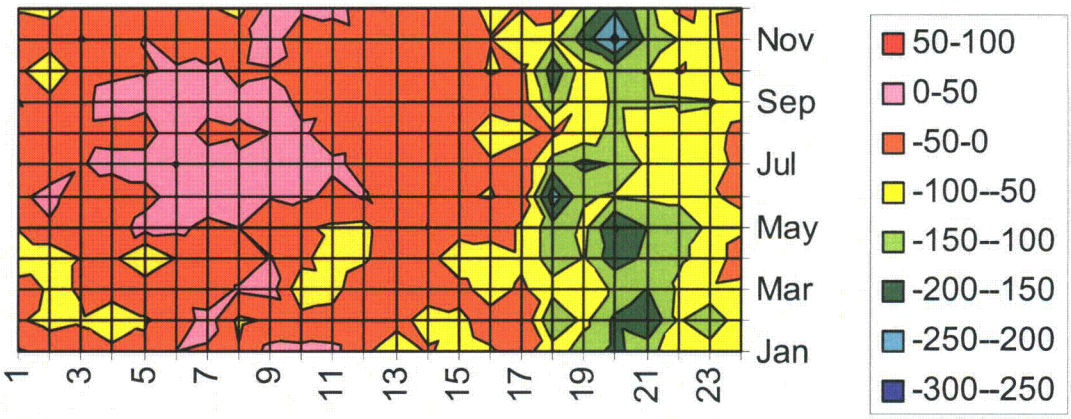

Figure 6-17 ***Difference in 98th percentile of down-regulation deployments between 15,000 MW wind scenario and zero wind scenario.***

The following observations regarding the changes in the 98.8th percentile of regulation deployments, due to wind, can be derived from these plots:

- Up-regulation requirements are most significantly increased during the morning load rise period, particularly during spring and summer, when winds tend to drop.
- Up-regulation requirements also increase significantly during the evening, for all seasons except summer.
- Down-regulation deployments increase during the evening, all year round.
- Down-regulation requirements tend to decrease, with increasing wind, during the morning hours, particularly during the period from late spring through early fall.

The relative changes in regulation are not consistent over the temporal space. Selected periods of significant regulation change are plotted as a function of the wind penetration in Figure 6-18.

The relative changes in regulation deployments vary greatly for different time periods. However, all the changes are nearly perfectly linear with wind capacity. This attribute can be applied to adjusting ERCOT's regulation procurements during periods of significant year-to-year wind capacity growth. This is discussed later in Section 6.3.2.

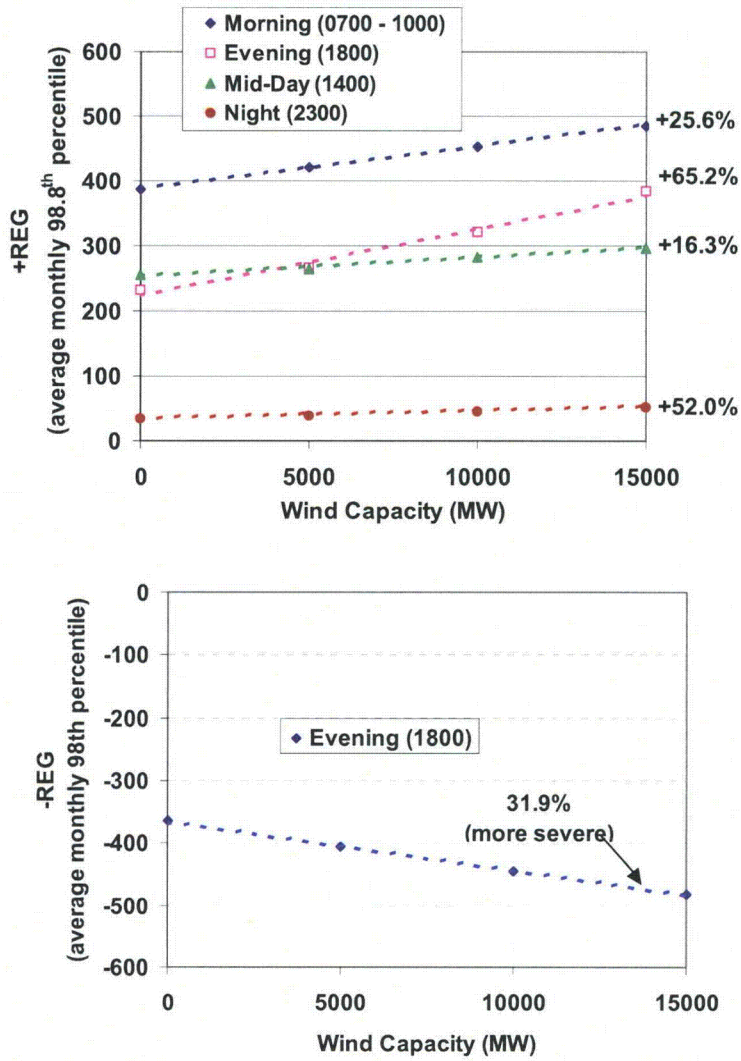

Figure 6-18 ***Regulation deployment (average 98.8th percentile) as a function of wind generation capacity.***

6.2.4. Comparison of Regulation Deployments in 10,000 MW Scenarios

This study considered two 10,000 MW wind generation scenarios, with different allocations of generation capacity to the CREZs. The first 10,000 MW case, denoted as the 10,000(1) scenario, has 1,500 MW of wind generation in CREZ 4, located in the Texas Panhandle. The second 10,000 MW case, denoted as the 10,000(2) scenario, substitutes 1,500 MW of wind generation in CREZ 24, located on the coast of South Texas, for the CREZ 4 generation. Table 6-3 compares the regulation deployments for these two scenarios. These results indicate that the improved geographic diversity of the wind generation portfolio, in the 10,000(2) scenario, slightly decrease regulation service requirements. Figure 6-19 and Figure 6-20 show the temporal distribution of the regulation deployment differences.

Table 6-3 Comparison of Regulation Deployments for the 10,000 MW Wind Generation Capacity Scenarios

	Case 10,000(1)	Case 10,000 (2)
Up-Regulation (MW)		
Mean	82.5	81.4
Sigma	64.9	64.1
98.8th Percentile	265.2	261.5
Maximum	1105.6	1112.7
Down-Regulation (MW)		
Mean	-83.0	-81.5
Sigma	63.7	63.1
98.8th Percentile	-262.7	-260.4
Maximum	-554.9	-565.9

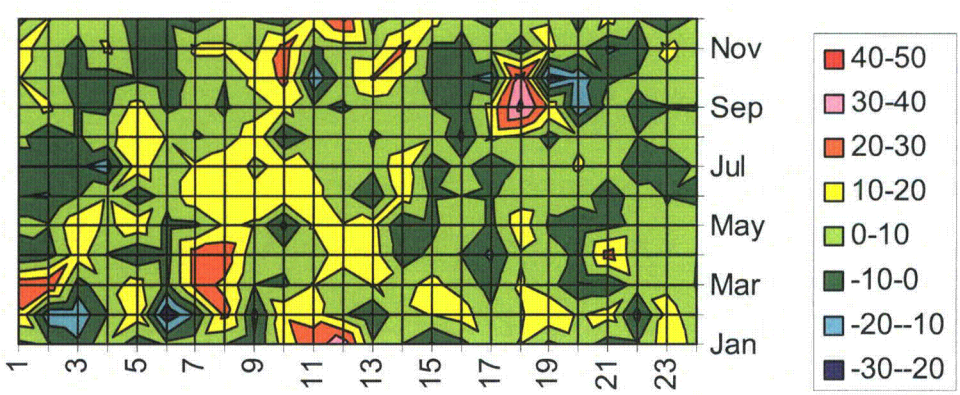

Figure 6-19 Difference in up-regulation (Case 10,000(1) minus Case 10,000(2))

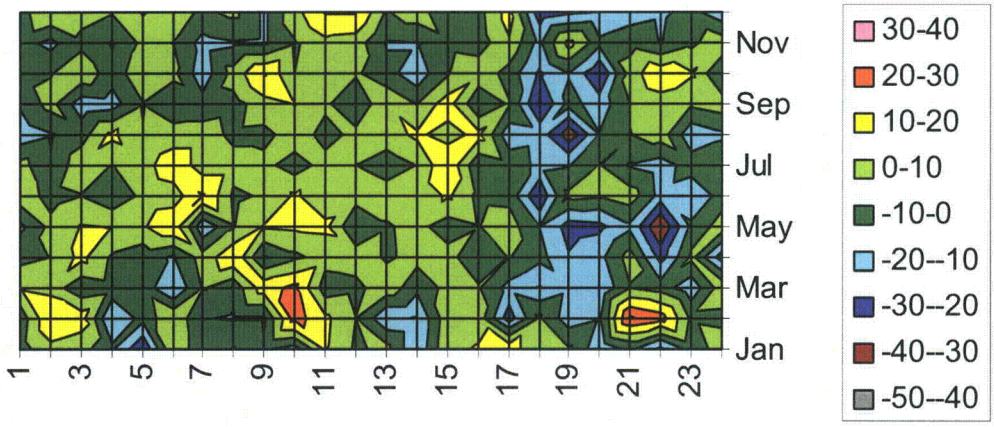

Figure 6-20 Difference in down-regulation (Case 10,000(1) minus Case 10,000(2))

6.2.5. Correlation of Regulation to Wind Generation Output

The previous correlations of regulation are to temporal parameters; hour of day and month, for various levels of wind generation capacity. In this section, regulation deployments are correlated to the real-time output of the wind generation portfolio for the respective hour. The analysis focuses on the incremental regulation requirement for the 15,000 MW wind generation capacity scenario, compared to the zero-wind capacity scenario.

The incremental hourly maximum up-regulation and down-regulation deployments are plotted as a function of the average wind generation output for the respective hour in Figure 6-21. Note that, in a given hour, wind generation output may increase or decrease regulation requirements. Figure 6-22 plots the maximum of the absolute value of up- and down-regulation for each hour, plotted versus wind generation output. The solid line in this plot is a quadratic curve fit of the scattered points, indicating that the impact of wind on regulation is most pronounced at the mid levels of output of the installed capacity (15,000 MW in these plots).

Figure 6-23 plots a typical wind turbine's power output versus wind speed characteristic, as well as a probability density function for wind speeds at a typical site. When the output of the entire wind generation portfolio is midway between zero and the rated capacity, most wind turbines are operating on the steep portion of the wind turbine output curve, where small wind velocity changes yield large power changes. This amplifies variability in output due to wind variations, and is the probable explanation for the increased incremental regulation requirements at mid-levels of wind generation output.

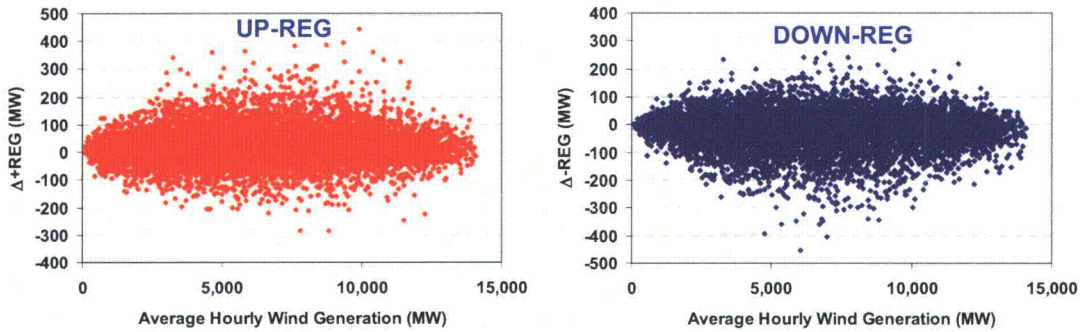

Figure 6-21 ***Incremental hourly maximum up- and down-regulation due to wind, versus average hourly wind generation output***

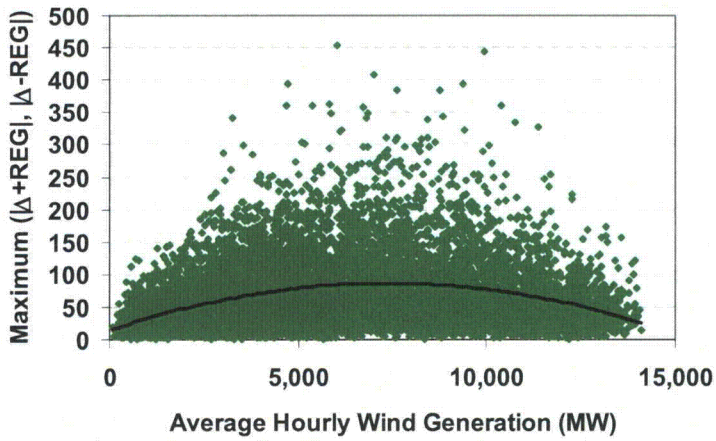

Figure 6-22 ***Incremental hourly maximum -regulation due to wind, versus average hourly wind generation output. Maximum of up- and down-regulation.***

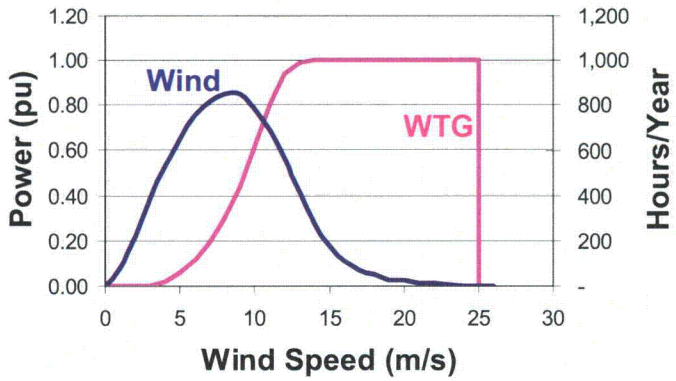

Figure 6-23 ***Typical wind turbine power output curve and wind probability density function for a typical wind plant site.***

Figure 6-24 shows a very strong correlation between the incremental regulation maximum, due to wind, and the long-term ramp rate of the wind generation output. The wind ramp rate used here is the delta between successive hours' integrated wind power output (current hour minus previous hour). As discussed earlier, the ERCOT definition of regulation results in the regulation requirements being strongly affected by the ramping of the net load, and the wind output is one component of the net load. The solid lines in these plots indicate the amount of power change in one five-minute dispatch period, which is the hourly ramp rate divided by twelve. The plotted points clearly trend along these lines. This correlation is applied later in Section 6.3.2 to possible improvements to the regulation procurement methodology.

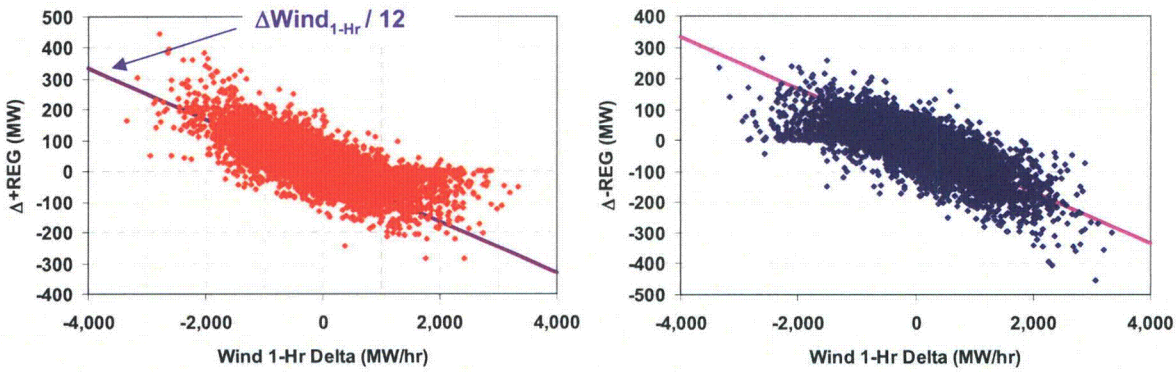

Figure 6-24 Incremental hourly maximum regulation versus wind generation ramp rate.

6.3. Adequacy of ERCOT Regulation Procurement Methodology

Regulation procurements were calculated for each hour of each month of the study year using regulation deployments calculated for the prior month of the study year and the same month of the prior year, applying ERCOT's present methodology. This process was performed for each wind scenario, with the installed wind generation capacity assumed to be constant from year to year. Deployments for each hour and month were compared to the procurements to determine the adequacy of the methodology with increased, but constant (steady-state), wind penetration. Later, in Section 6.3.2, suggestions will be given for modifying the regulation procurement process to properly account for year-to-year wind generation capacity increases when penetration is increasing rapidly.

Figure 6-25 plots up-regulation procurements and deployments over a fifty-hour interval, illustrating several under-deployment periods. Figure 6-26 compares up-regulation deployments and procurements, for scenarios with 15,000 MW of wind generation and

without wind generation. This example shows periods where the addition of wind generation results in an under-procurement, and other periods where the margin between wind procurement and wind deployment is increased. Similar plots for example periods in each season are in Appendix E.3.

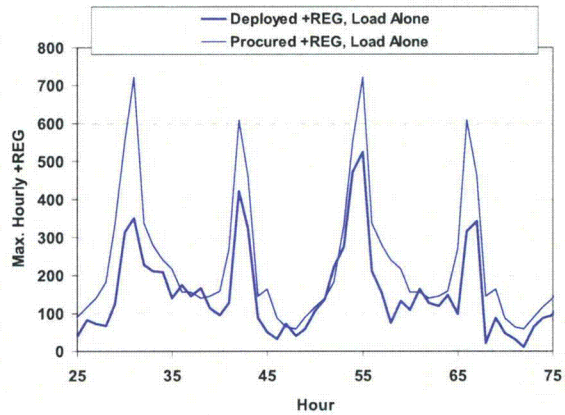

Figure 6-25 Illustration of up-regulation procurement and deployment

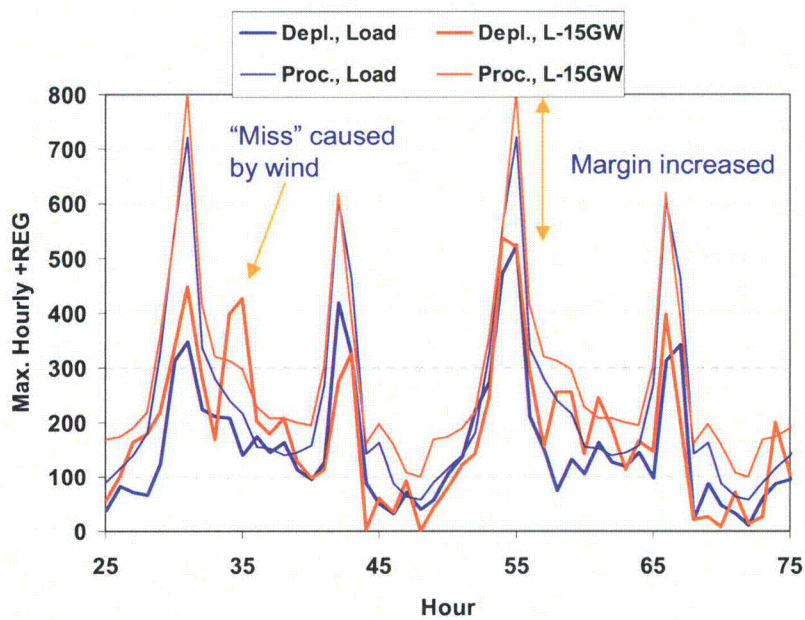

Figure 6-26 Up-regulation deployments and procurements, with 15,000 MW of wind generation and without wind generation, for an example period.

Figure 6-27 plots the mean and maximum regulation procurement and deployment as a function of the installed wind capacity. Again, it is seen that results are nearly perfectly linear. The slope of the extreme procurements are greater than that of the extreme deployments, meaning that the under-deployment gap narrows with more wind capacity.

(Note that down regulation is considered to be a negative number, so minimum down-regulation is a more severe requirement.)

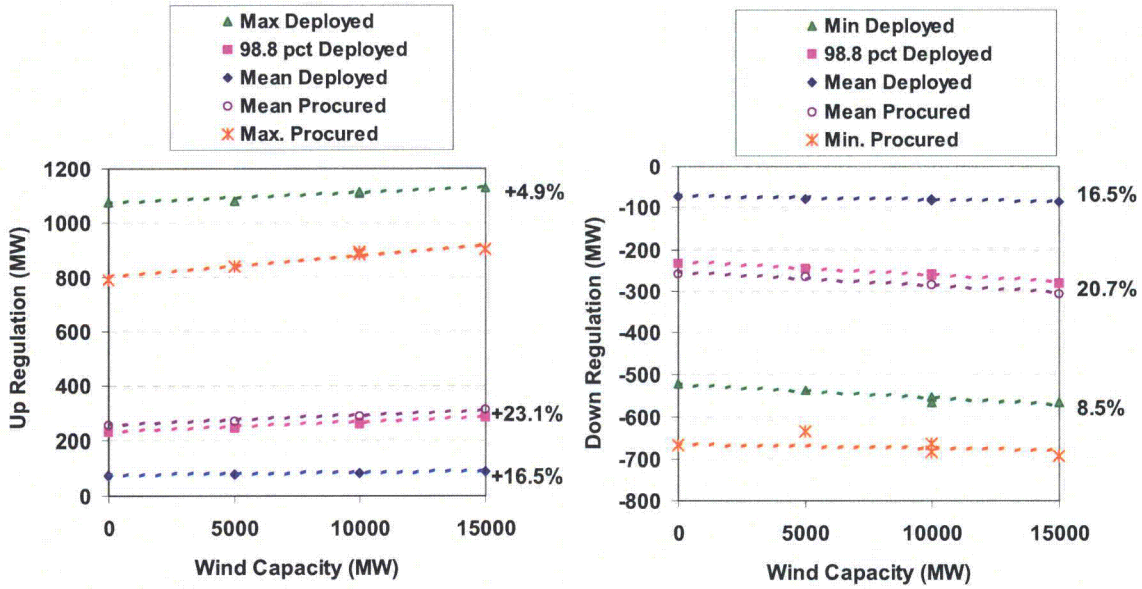

Figure 6-27 Regulation procurement and deployment as a function of wind capacity.

6.3.1. Analysis of Under-Procurements

The adequacy of the regulation procurement methodology can be quantified by analysis of the under-procurements — periods where the algorithm does not procure sufficient regulation services to cover the regulation deployment. There are various metrics that can be placed on under-procurement that indicate the frequency and the severity of the under-procurements. It should be noted that the procurement methodology is not intended to be perfect; procurement of sufficient regulation such that deployment needs are always met would be uneconomical. Instead, the responsive reserve service is relied upon to cover infrequent excesses, with the expectation that an unusually large regulation requirement will not coincide with a worst-case generation trip. ERCOT has determined that procuring sufficient regulation service for 98.8% of the five-minute periods reduces the risk to an acceptable level.

Table 6-4 summarizes regulation under-procurement metrics for the wind generation scenarios. The data columns are explained as follows:

> **Percentage of Periods** – Percentage of five-minute periods in the study year with regulation requirements exceeding the amount procured.
>
> **Total MWh Under-Proc.** – Sum of the products of amount that regulation requirements exceed procurement for each period, times the duration of each period, (1/12 of one hour for each period). Periods where regulation requirements do not exceed the procured value count as zero.

Average Under-Proc. – Average amount of the under-procurement, considering only periods where regulation requirements exceed procurement.

RMS of Under-Proc. – Root-mean-square of under-procurements, considering only periods where regulation requirements exceed procurement. This value of this metric is that it gives greater weighting to larger under-procurements, which tend to be more operationally significant.

Extreme Under-Proc. – The most severe under-procurement (maximum of up-regulation under-procurements, and minimum of down-regulation under-procurements, with down-regulation expressed as a negative number).

The results in this table indicate that ERCOT's current regulation procurement methodology provides essentially equivalent accuracy with, or without, significant wind penetration. The very slight increase in under-procurement rate for up-regulation is not significant, and the down-regulation under-procurement rate is less for the 15,000 MW wind scenario, relative to the zero-wind scenario. The increase in average up-regulation under-procurement, between zero and 15,000 MW of wind generation, is 23%, nearly identical to the increase in the average up-regulation procured. Thus, the relative under-procurement is essentially invariant. The increase in down-regulation under-procurement (12.8%), is substantially less than the increase in down-regulation procurement, so the relative under-procurement decreases with wind generation capacity additions. The increase in the root-mean-square of under-deployment, for both up-regulation and down-regulation, increase much less on a percentage basis than the average under-procurement. This implies that the more extreme magnitudes of under-procurement occur less frequently with greater wind capacity. The most severe up-regulation under-procurements actually decrease, and the down-regulation under-procurement extrema increase only slightly.

Table 6-4 Regulation Under-Procurement Metrics

Up-Regulation

Wind Scenario	Percentage of Periods	Total MWh Under-Proc.	Average Under-Proc.	RMS of Under-Proc.	Extreme Under-Proc.
0	1.29%	5,141	45.5 MW	80.1 MW	653 MW
5000	1.26%	5,320	48.2 MW	82.1 MW	634 MW
10,000 (1)	1.36%	6,201	52.0 MW	85.0 MW	638 MW
10,000 (2)	1.35%	6,004	50.8 MW	84.2 MW	643 MW
15,000	1.37%	6,712	55.9 MW	88.5 MW	632 MW

Down-Regulation

Wind Scenario	Percentage of Periods	Total MWh Under-Proc.	Average Under-Proc.	RMS of Under-Proc	Extreme Under-Proc.
0	1.18%	5,011	48.5 MW	89.2 MW	886 MW
5000	1.12%	5,148	52.5 MW	90.4 MW	911 MW
10,000 (1)	1.20%	5,439	51.7 MW	87.9 MW	946 MW
10,000 (2)	1.16%	5,301	52.2 MW	89.2 MW	940 MW
15,000	1.16%	5,562	54.7 MW	90.1 MW	927 MW

Figure 6-28 and Figure 6-29 show two example frequency distributions of up-regulation deployments for particular hours and months. The dotted lines indicate the procured regulation, and very few deployment periods exceed the procured values. The most severe under-procurement in Figure 6-28 is due to a single very large deployment outlier near 800 MW. In this particular example, the magnitude of the maximum deployment for the 15,000 MW scenario is slightly less than that for the zero-wind scenario. Because the procurement is greater for the case with 15,000 MW of wind capacity, the magnitude of under-procurement is actually less in the high-wind penetration case.

A different situation is illustrated in Figure 6-29. In this case, the up-regulation deployments are more widely scattered, and there are many deployments exceeding the procured values for both scenarios. The wide distribution is probably due to the volatility of weather, and consequently load behavior, in this spring month. The procured regulation does not cover anywhere near 98.8% of the deployments. Evidently, the variability was not present in the prior month, nor in the same month of the prior year, resulting in insufficient procurement for the highly volatile study year conditions. The number of periods exceeding the procured value is significantly greater for the 15,000 MW wind scenario. The magnitude of the under-deployments is not as extreme as in the prior example.

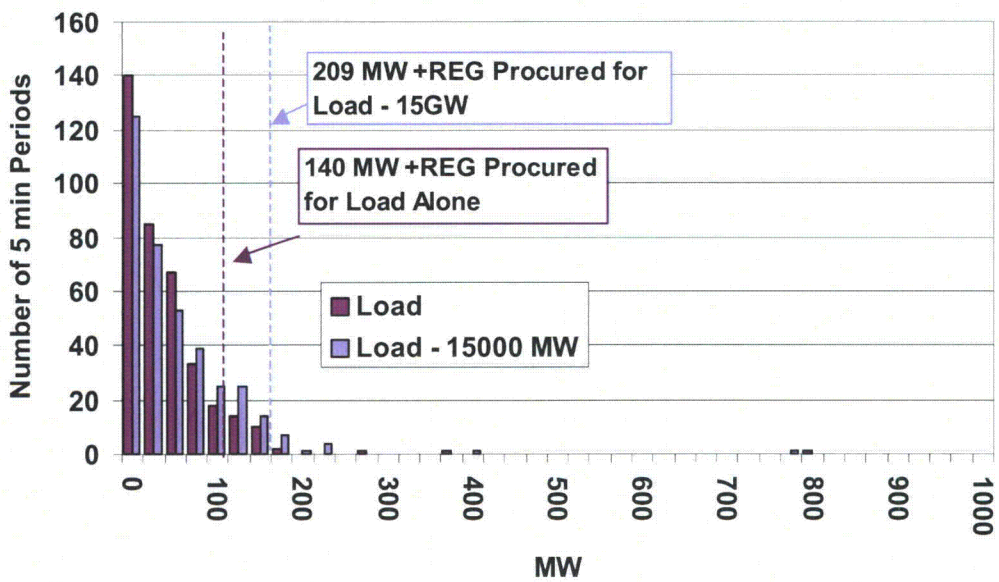

Figure 6-28 ***Frequency distribution of up-regulation deployments for 2 p.m. in January, for scenarios with no wind capacity, and with 15,000 MW of wind capacity.***

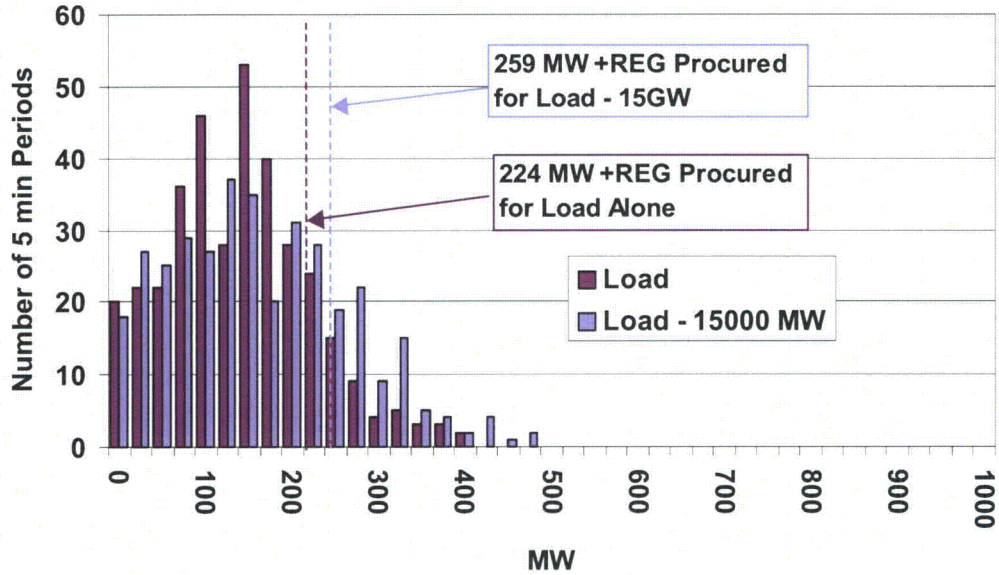

Figure 6-29 Frequency distribution of up-regulation deployments for 1 p.m. in April, for scenarios with no wind capacity, and with 15,000 MW of wind capacity.

The next group of figures indicate the temporal characteristics of the regulation under-deployments. The contour plots of Figure 6-30 to Figure 6-37 show the regulation under-procurement rates for the zero-wind and 15,000 MW wind generation capacity scenarios. Maxima in these contour plots tend to be narrow spikes, so peak values are shown numerically as indicated by the arrows. Without wind generation, the up-regulation procurement methodology falls short relatively frequently during the late morning through mid-day in the spring, and in the evening in the fall. With 15,000 MW of wind generation capacity, under-procurements are less frequent for many of the morning hours. The peak under-procurement rate, however, is greater. Without wind generation capacity in the system, the regulation procurement methodology under-predicts down-regulation needs most severely in the evenings in the early spring. This peak of under-procurement frequency, however, is greatly reduced in the 15,000 MW wind scenario.

Figure 6-34 to Figure 6-37 show the temporal characteristics of the differences in regulation under-procurement magnitudes between the scenarios with 15,000 MW wind generation capacity and zero wind generation capacity. These differential contour plots show both up- and down-regulation under-procurements expressed in terms of MW×hours and root-mean-square of deficiency. In general, the differences in regulation deficiencies are well scattered about the temporal space. An exception is the sharp peak in the MWh metric for up-regulation, pertaining to autumn evenings. The fact that this peak is created by the data for one hour-month pairing, rising from a rather benign plateau raises question if this peak is an anomaly of the study year data, or if is consistent on a year-to-year basis. ERCOT is encouraged to continuously monitor these trends as wind capacity is developed to apply as much data as possible to operating decisions.

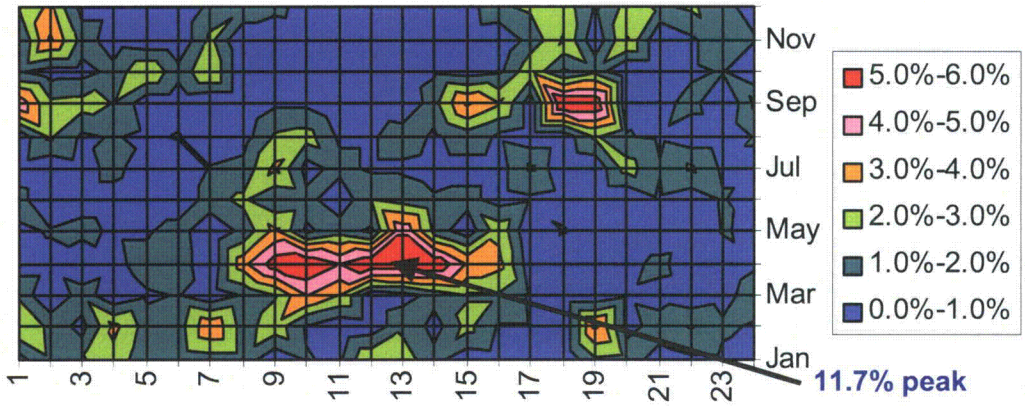

Figure 6-30 ***Percentage of 5-minute periods with up-regulation under-deployments for the zero-wind generation capacity scenario.***

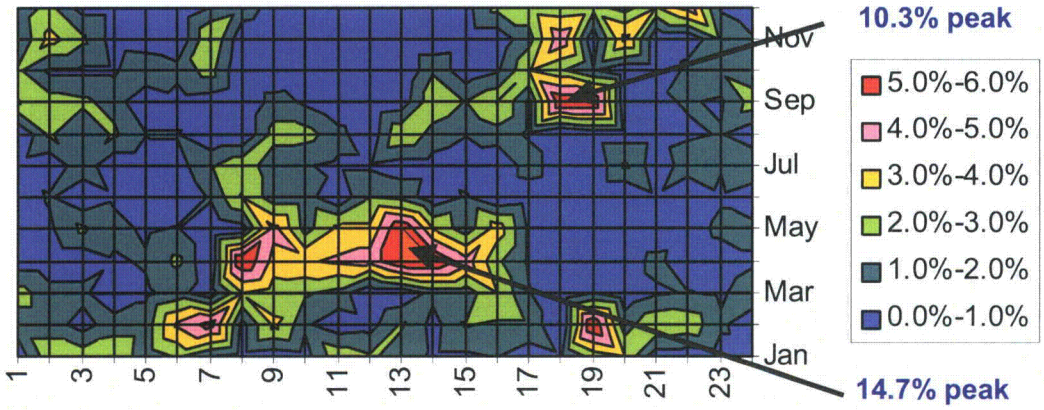

Figure 6-31 ***Percentage of 5-minute periods with up-regulation under-deployments for the 15,000 MW wind generation capacity scenario.***

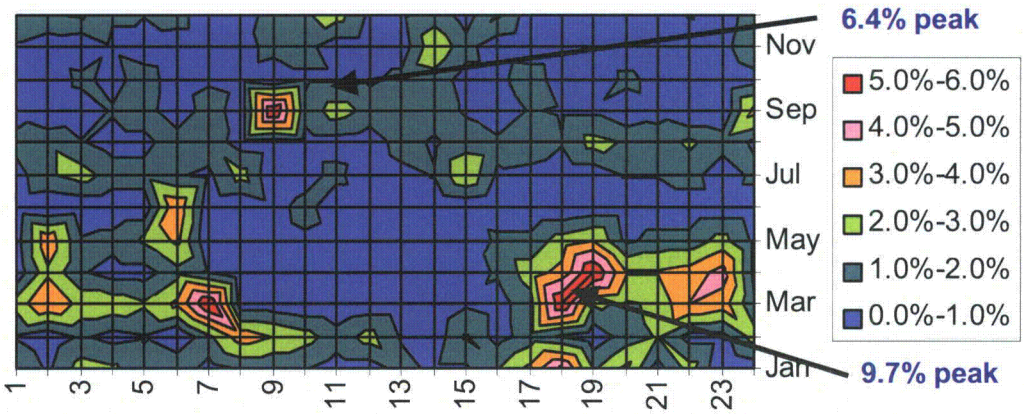

Figure 6-32 ***Percentage of 5-minute periods with down-regulation under-deployments for the zero-wind generation capacity scenario.***

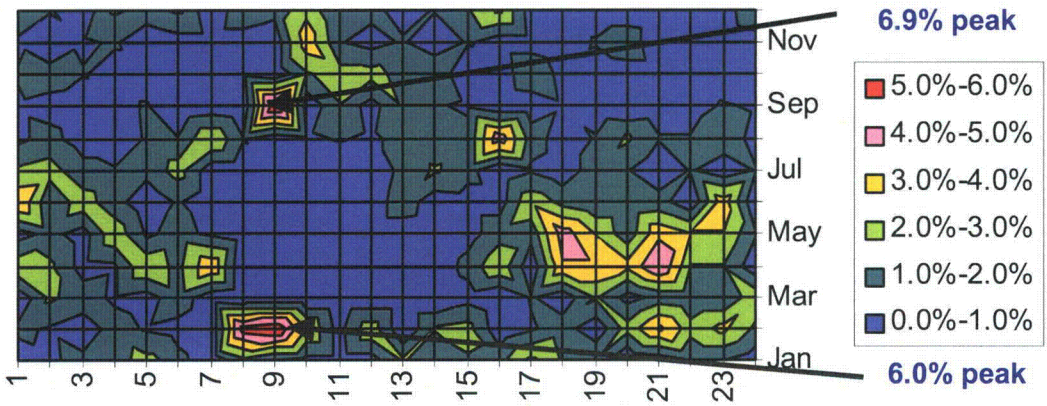

Figure 6-33 ***Percentage of 5-minute periods with down-regulation under-deployments for the 15,000 MW wind generation capacity scenario.***

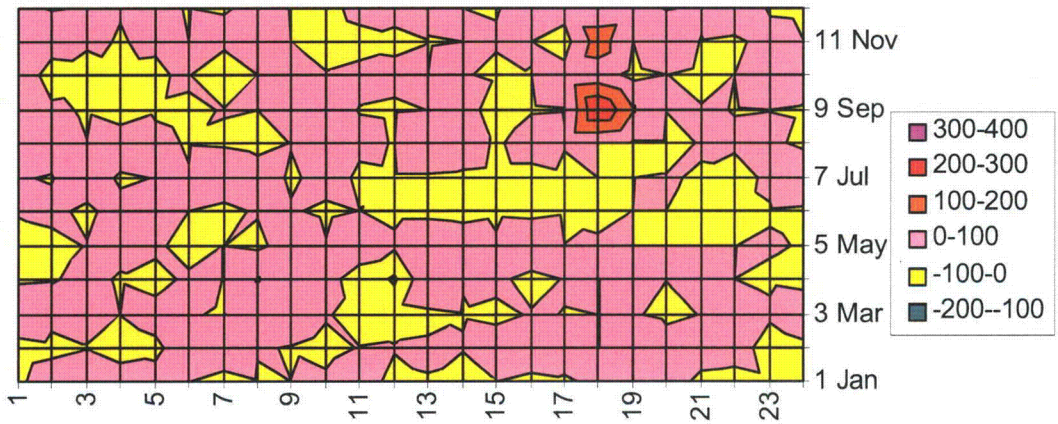

Figure 6-34 ***Differential MWh of up-regulation under-procurement; 15,000 MW wind generation capacity scenario minus the zero-wind generation scenario.***

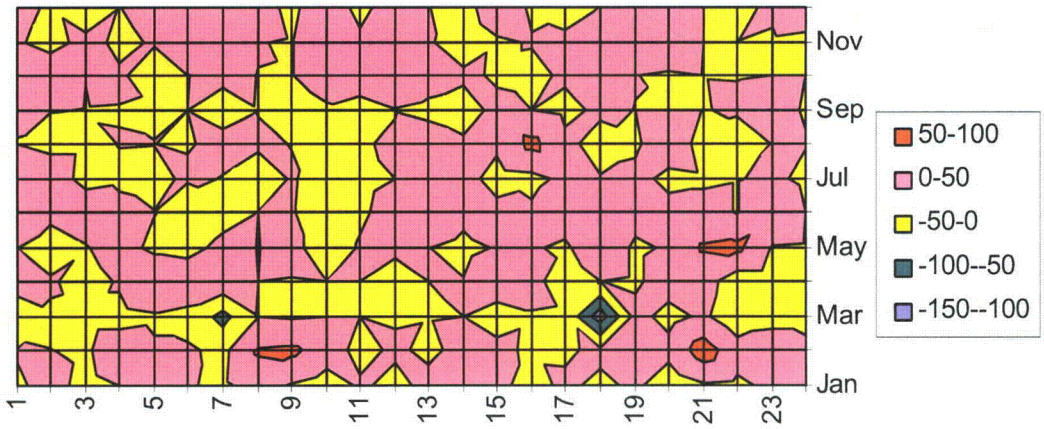

Figure 6-35 ***Differential MWh of down-regulation under-procurement; 15,000 MW wind generation capacity scenario minus the zero-wind generation scenario.***

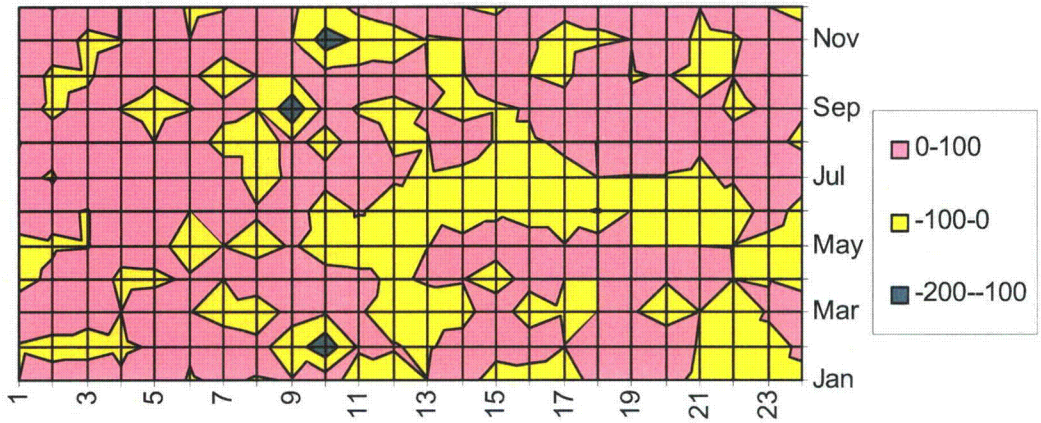

Figure 6-36 ***Differential RMS of up-regulation under-procurement; 15,000 MW wind generation capacity scenario minus the zero-wind generation scenario.***

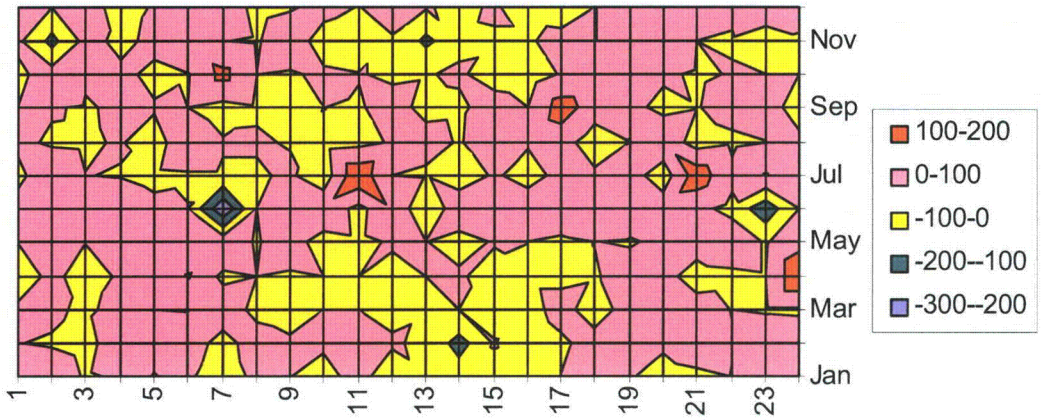

Figure 6-37 ***Differential RMS of down-regulation under-procurement; 15,000 MW wind generation capacity scenario minus the zero-wind generation scenario.***

6.3.2. Possible Methodology Improvements

Year-to-Year Wind Capacity Growth

Wind generation capacity has been added to the ERCOT system at a very fast pace over the past few years, and this pace is expected to accelerate. The present ERCOT regulation procurement methodology, applied to the net load, does not take into account year-to-year wind capacity growth when using prior-year regulation deployments to predict present-year procurement needs. The results of this study show a near-perfectly linear correlation between regulation requirements for any period of time, and the amount of installed wind capacity. Therefore, it is reasonable to apply adjustment factors to prior-year regulation deployment 98.8th percentile values to account for increases in wind capacity over the prior year. These factors depend on the time of day and month of year.

The tables in Appendix F show additive adjustments, in units of MW of regulation requirement (98.8th percentile of deployment) per GW of incremental wind capacity since the same month of the prior year. These adjustments are the smoothed differential between 98.8th percentile regulation deployments in the 15,000 MW case minus the zero-wind case, divided by fifteen. The smoothing function uses 50% of the differential for the respective month and time of day, plus 12.5% each of the differentials for the same hour in the prior and following months, and for the same month and the prior and following hours (i.e., the four "adjacent" points in the hour-of-day and month spaces). This process smoothes extreme hour-to-hour and month-to-month variations in the differential that may not be realistic.

Incorporation of Wind Forecasts

ERCOT's present methodology for regulation procurement correlates regulation requirements to time of day and month of year. This is a reasonably good assumption for system load.[6] Loads have a distinct daily cycle, and short-term variations around this diurnal cycle are not greatly influenced by weather. Although wind does have diurnal and annual patterns, wind generation output also follows multi-day cycles of weather system movement. Incorporating day-ahead wind generation forecasts can improve regulation procurement accuracy and lower costs. This results in a regulation procurement for a particular hour of day over a month that is composed of a fixed component, constant throughout the month for the particular hour, plus a positive or negative adjustment component that varies for each day depending on the forecast wind generation volatility.

One forecastable wind generation characteristics is the long-term (multi-hour) ramp rate. Subtracting the influence of long-term wind ramp rate (hourly delta divided by twelve) on the maximum regulation deployments yields the plot shown in Figure 6-38. Comparing this plot with Figure 6-22 reveals a decreased scattering of points. These results imply that the precision of regulation procurement might be increased by factoring the effects of wind generation output ramping into the regulation procurement.

[6] It is quite possible that the present methodology could be improved if regulation requirements were segregated between weekdays and weekends. This hypothesis was not investigated as the scope of this study is focused on the impacts of wind on ancillary services procurement.

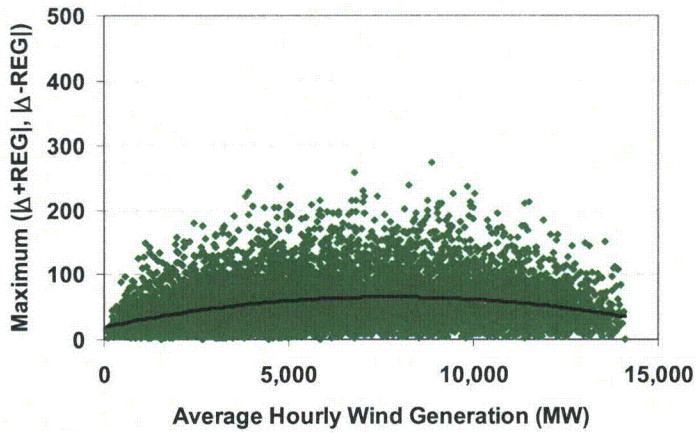

Figure 6-38 ***Incremental hourly maximum -regulation due to wind, minus the effect of wind ramp rate, versus average hourly wind generation output.***

Wind output ramping is present in both the historical data used to determine procurements, and in the real-time requirements for regulation. An algorithm that removes the influence of wind output ramping on historical regulation data, but then re-inserts the predicted influence of wind output ramping on a day-ahead basis, may be more accurate than the present methodology. This can result in an improved procurement at reduced cost.

This approach requires use of day-ahead wind forecasts to determine wind ramp rates on an hourly basis to include this influence in regulation procurements. The steps of the suggested methodology are summarized as follows:

1. Factor out wind multi-hour wind generation output ramp-rate contributions (hourly change divided by twelve) to historical deployed regulation data.
2. Determine the maximum of 98.8th percentiles for the previous month and previous year, as in the present methodology, but using these adjusted data.
3. Use the day-ahead wind forecast to determine the expected hourly wind ramp rates.
4. Adjust the regulation procurement on a day-ahead basis, applying the forecast wind ramp rates.

Another forecastable wind generation characteristic is the expected operating points on the wind turbine performance curves. Figure 6-38 shows that, with the influence of ramp rate removed, there is a visible non-linear correlation between regulation requirements and the average hourly wind generation, relative to the capacity. When the aggregate wind generation is at approximately 50% of capacity, the regulation requirements are

maximized. The apparent cause is that many wind turbines are operating on the steep part of their performance curves when the aggregate output is at the intermediate levels.

Rather than adjust ERCOT regulation procurements based on the aggregate output level, greater accuracy in regulation procurement adjustments might be obtained by a more detailed analysis. Day-ahead wind generation forecasts are based on meso-scale weather models, from which calculated wind speeds at wind plants are applied to wind generator performance curves to determine expected hourly energy output. This process can also be applied to determine the expected variability on a site basis, depending on the forecast turbulence at the site and the mean operating point on the wind turbine performance curve. An aggregate variability can be determined for the entire ERCOT wind generation portfolio using a capacity-weighted combination of these variability factors. Because the intra-hour variabilities should be generally uncorrelated between sites, root-sum-square combination of the factors would be appropriate.

This is a marked departure from ERCOT's present regulation procurement practice, for which an identical daily pattern of regulation procurement levels is repeated for each day of the month. The suggested methodology would adjust this daily pattern on a day-ahead basis, using wind forecasts. ERCOT needs to consider the implications for market operations. One possibility to minimize market changes is to determine a base regulation requirement that repeats in a constant daily cycle for each day of a month, as is the current practice. An additional regulation adjustment service could be created and procured on a day-ahead basis to include the expected effect of wind ramp rates and forecast variability.

The four-step algorithm for adjusting for wind ramp rate was tested using this study's model data, including synthesized wind generation forecasts. Results of this test do not confirm the value of the hypothesized approach, but further investigation reveals that the synthesized day-ahead wind generation forecasts used in this study have ramp rates containing much more hour-to-hour variational "noise" than the wind generation output data for the same periods. The application of the synthesized wind forecasts to predict ramp rates was not considered in the design of the synthesis process.

As ERCOT begins to use wind generation forecasting in system operations, data points of actual wind generation forecasts, power outputs, and regulation deployments will provide ERCOT the opportunity to evaluate this suggested methodology modification on an off-line basis. If ongoing analysis of the real data indicates that the methodology changes would allow regulation procurements to be decreased, while maintaining adequate procurement precision (at least 98.8% of periods covered), then this methodology change can be implemented in the ERCOT market.

6.4. Available Regulation Range

In addition to increasing the amount of regulation required, the presence of wind generation tends to diminish the amount of regulation service available from the dispatchable generation resources. This is because the wind generation displaces dispatchable generation units from the commitment schedule, and often the higher-cost units displaced are the most flexible providers of regulation service. Regulation capacity of the system becomes most constrained under conditions of low served load and high wind generation output.

Figure 6-39 shows the amounts of regulation capability, measured in MW per minute ramping capability, by generation type from MAPS analysis for the week in the study year having minimum load. This is for the zero-wind generation capacity scenario. The same week is shown for the 15,000 MW wind generation capacity scenario in Figure 6-40. Note that there are several periods when the only regulation available is provided by normally base-load coal-fired units. In one period between hours 93 and 99, there is no regulation ramping capability available using an economic unit commitment and dispatch. To provide regulation, either the unit commitment schedule and dispatch would need to be modified, or the wind generation curtailed.

The correlations of regulation down-ramping capability to system load level are shown in Figure 6-41 for the 15,000 MW wind generation capacity scenario. The hours without down-ramping available (without deviating from economic unit commitment and dispatch) coincide with the extreme low-load periods.

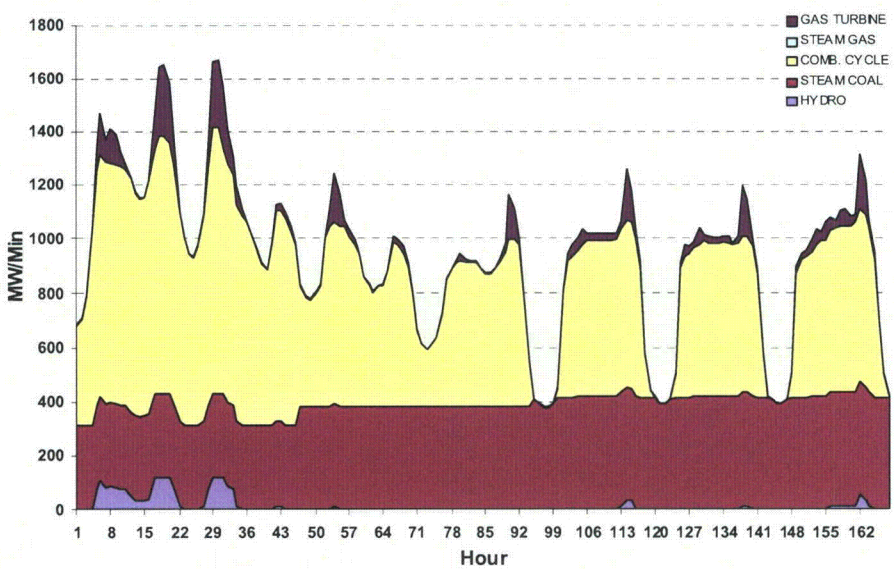

Figure 6-39 Regulation capacity provided, by generation unit type, for the minimum-load week in the zero-wind generation capacity scenario.

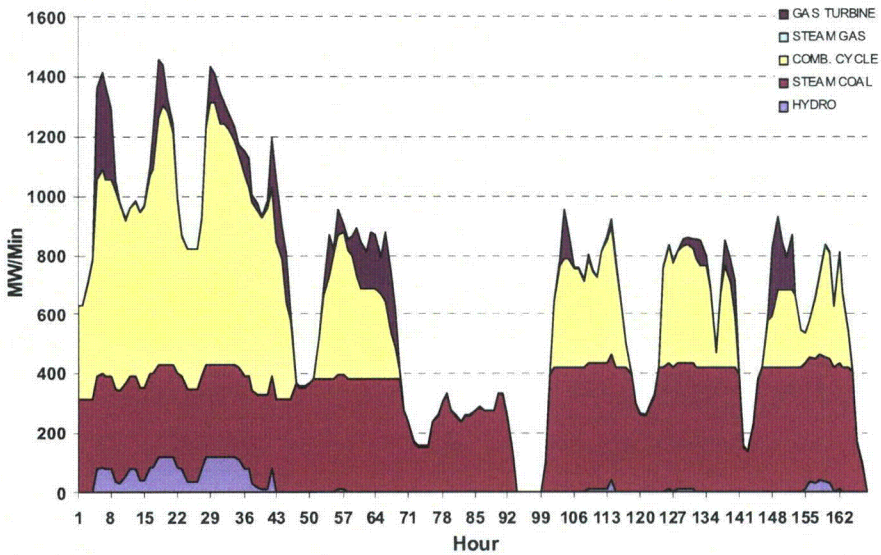

Figure 6-40 Regulation capacity provided, by generation unit type, for the minimum-load week in the 15,000 MW wind generation capacity scenario.

Currently, in the zonal market design, the ramping capability of regulation service is defined as being one-tenth of the procured regulation. This is for a dispatch period of fifteen minutes. In the nodal market, the dispatch periods are five minutes long. The ramping capability of units supplying regulation service must be such that the procured amount of regulation can be realized in five minutes or less. Therefore, in this study, the amount of regulation available, in units of MW, is assumed to be constrained by the available ramp rate in MW per minute, times five.

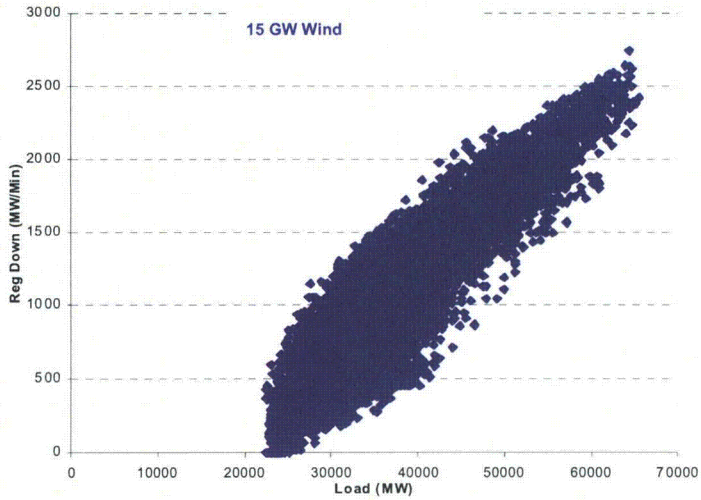

Figure 6-41 – Correlations of down-ramping capability with system load level.

Figure 6-42 shows hourly regulation procurement requirements for the study year, shown by the red (up-regulation) and blue (down-regulation) bands. Available regulation capacity, defined by the ramping capability times five, is shown by the magenta and teal bands. With load alone, in the zero-wind capacity scenario, there is ample margin between procurement requirements and available capacity. The margin is greater for up-regulation than for down-regulation. With 5,000 MW of wind generation capacity, up-regulation capacity margin is ample, but the down-regulation capacity margin is small for isolated hours. In the 10,000 MW and 15,000 MW wind generation capacity scenarios, there are hours where down-regulation capacity is insufficient for the procurement requirements. Figure 6-43 shows an expansion of the time scale for the 15,000 MW scenario. This shows that some apparent intersections of regulation procurement requirements and capacity seen in the time scale of Figure 6-42 are not actually under-capacity situations. An example is at hours 577 and 700. Up-regulation capacity remains sufficient for all the wind generation capacity scenarios investigated.

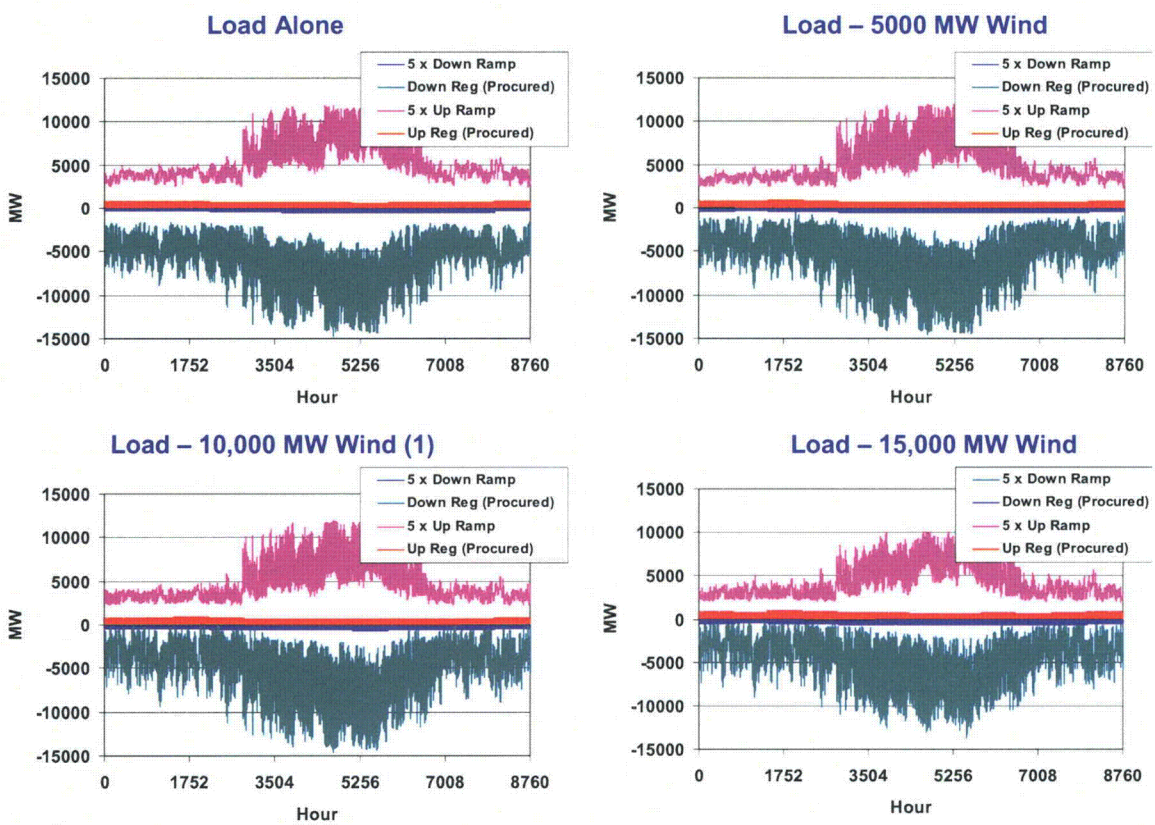

Figure 6-42 Regulation procurement requirements compared with regulation capability.

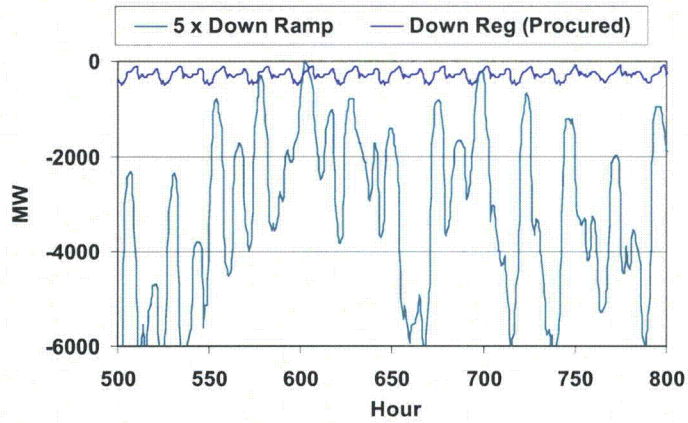

Figure 6-43 Expansion of the time scale of Figure 6-42 for down-regulation in the 15,000 MW wind generation capacity scenario.

Table 6-5 summarizes the regulation shortfalls for each wind generation capacity scenario. Even in the 15,000 MW scenario, the total number of hours where regulation capacity, based on an economic unit commitment and dispatch, is relatively small (51 hours). Of the two 10,000 MW scenarios, the second case, which has 1,500 MW of capacity in coastal South Texas substituting for an equal capacity in the Panhandle, has less frequent and less severe regulation capacity shortfalls.

Table 6-5 Regulation Capacity Shortfalls

Wind (MW)	Hours Deficient	Total MWh Deficient	Average Deficiency (MW)	Maximum Shortfall (MW)
0	0	0	0	0
5,000	0	0	0	0
10,000 (1)	11	2709	246	482
10,000 (2)	7	1097	157	316
15,000	51	10308	202	712

6.5. Costs of Regulation Service

Penetration of wind generation capacity affects both the requirements for regulation service procurement, as well as the unit price for the balance of generation (non-wind generation) to provide that service. Figure 6-44 shows the total amount of regulation service procured as a function of wind generation capacity.

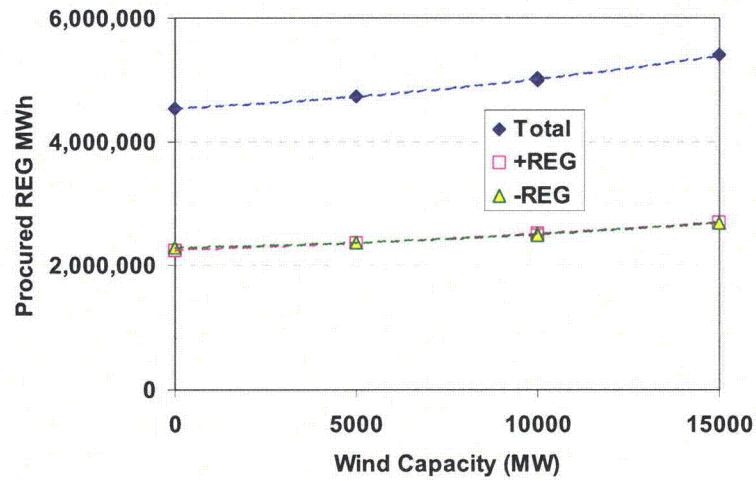

Figure 6-44 – Total annual procured regulation service as a function of wind generation capacity.

6.5.1. Per-Unit Costs of Regulation Service

The MAPS models predict the hourly opportunity costs for providing spinning-reserve services, including regulation and responsive reserve. MAPS does not, however, predict the bidding behavior of generation owners bidding into the ancillary services market. Actual hourly ERCOT ancillary services prices were obtained and analyzed, and it was found that up-regulation and down-regulation prices did have an approximate correlation with spinning reserve costs. MAPS shows many hours in a year where the opportunity costs for spinning reserve are zero. Actual regulation prices, however, do not fall to zero in these time periods. Instead, regulation prices tend to reach a "floor" of approximately $5/MWh.

In general, with increasing wind generation capacity, the unit price per MWh of spinning reserve decreases due to several factors. First, the balance of generation is provided by units with lower variable costs as wind generation capacity is increased. Second, because of the daily variability of wind generation, thermal units with long start-up times and minimum-run times tend to be scheduled for hours where their dispatch levels are reduced by wind output. This provides regulating range with virtually no opportunity costs for these high-wind hours. Third, the accuracy of wind forecasting used in day-ahead unit scheduling plays a role. If wind generation forecasts are not considered at all, or are heavily discounted, the balance of generation will tend to be over-committed.

Figure 6-45 shows the cumulative cost-duration curve for spinning reserve, as modeled in MAPS, for the wind generation capacity scenarios. For this figure, it is assumed that the day-ahead unit commitment schedule makes use of the mean value (50th percentile confidence level) wind forecast, based on current wind forecasting accuracy levels. For a few hours per year, the spinning reserve opportunity cost spikes to as high as $240/MWh,

beyond the scale indicated here. This is due to under-commitment, in turn due to under-forecast of net load.

Figure 6-46 shows the same curve where the wind forecast is perfect in accuracy. There is less over-commitment of units and the opportunity cost for providing spinning reserve is increased (overall system operating costs are decreased, however). At the opposite extreme, Figure 6-47 shows the spin cost curve where wind forecasts are ignored in the day-ahead unit commitment (i.e., wind generation output assumed to be zero). Over-commitment of the balance of generation yields to a collapse in spinning reserve prices as the amount of wind generation capacity increases.

For the purposes of evaluating the impacts of wind generation penetration on regulation procurement costs, the hourly per-unit costs of regulation are the greater of:

- Opportunity cost of spinning reserve, as determined by MAPS, or
- An estimated floor of $5/MWh

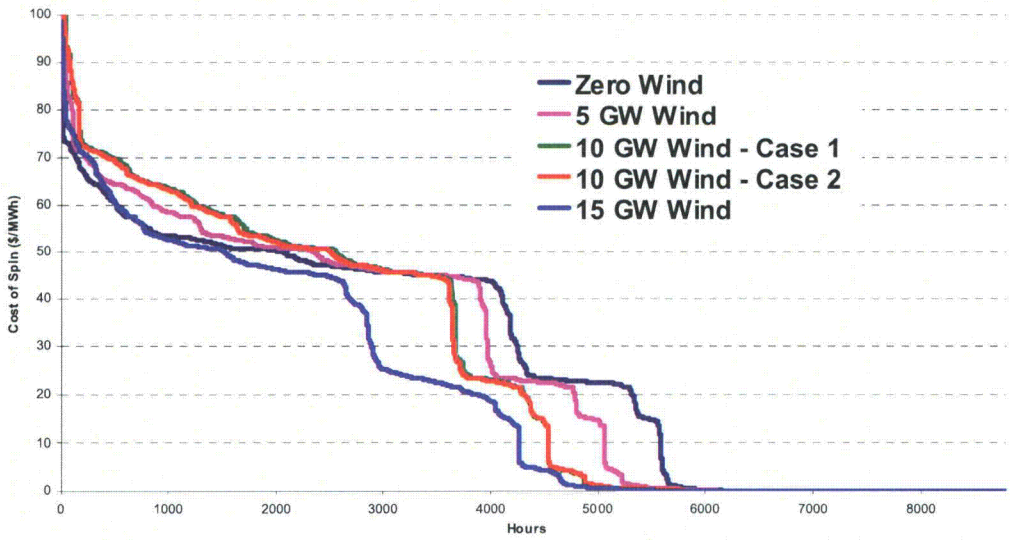

Figure 6-45 – Cost-duration curve for spinning reserve, assuming a "state-of-art" wind generation forecast (50th percentile confidence level) is used in the day-ahead unit commitment.

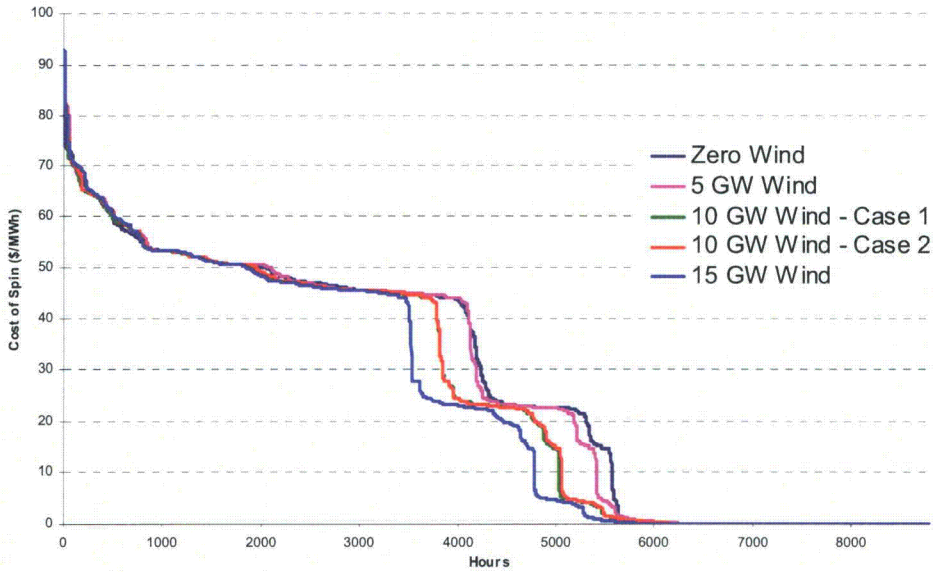

Figure 6-46 - Cost-duration curve for spinning reserve, assuming a perfect wind generation forecast is used in the day-ahead unit commitment.

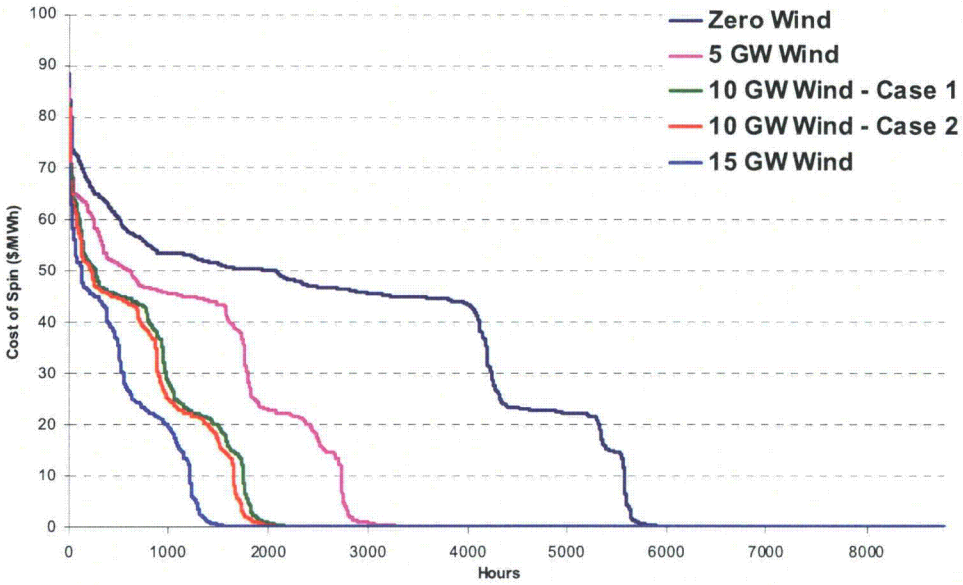

Figure 6-47 - Cost-duration curve for spinning reserve, with wind generation forecast ignored in the day-ahead unit commitment.

If any hour's economic dispatch does not provide sufficient regulating range to meet the procurement requirements, the dispatch must obviously be revised to provide the needed range. There are costs associated with this re-dispatch. The upper limit to the re-dispatch costs are the costs of curtailing wind generation equal to the amount that the regulation procurement requirements exceed the available range in the economic dispatch. The cost of this energy, priced at the hourly spot price, was added to the regulation costs as

determined above. These assumptions are deemed adequate for evaluating the relative cost impacts of the wind generation scenarios.

Hourly costs of up- and down-regulation were multiplied by the regulation procurement requirements for each hour. Figure 6-48 shows the average annual per-unit costs of up- and down-regulation for each wind scenario, for both the "state-of-art" and perfect wind generation forecasts used in unit commitment. These costs are shown relative to the costs for the load-only scenario. With the "state-of-art" wind generation forecast used in unit commitment, the average cost of regulation decreases slowly through the 10,000 MW wind generation capacity scenarios, and then collapses at the 15,000 MW level. With unit commitment based on perfect forecasting of the wind, the per-unit regulation cost decreases in a more regular fashion as wind generation capacity increases.

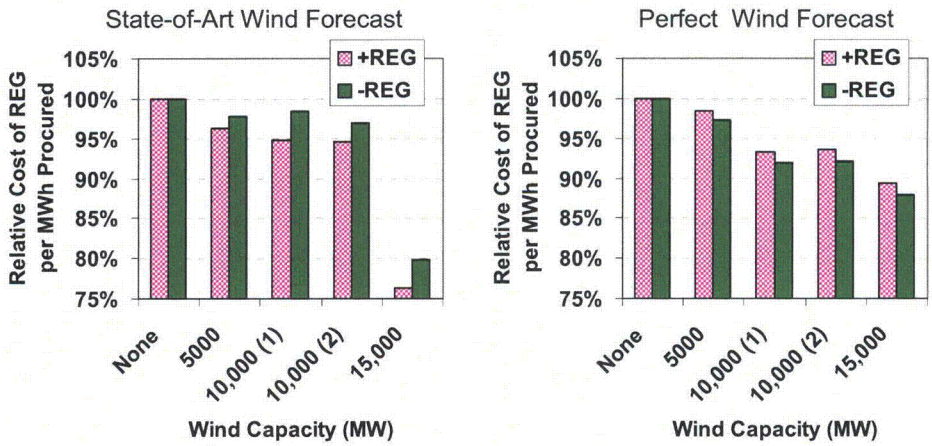

Figure 6-48 – Average per MWh costs of procured regulation.

6.5.2. Total Costs of Regulation

The tendency for regulation requirements to increase with wind generation capacity is offset by the tendency for per-unit regulation costs to decrease. As a result, the total annual costs for regulation tend to rise slightly until the 10,000 MW wind generation capacity scenarios, and then drop at the 15,000 MW level due to the collapse in per-unit costs, with the state-of-the-art wind generation forecasting applied to unit commitment. This is shown in Figure 6-49. If the wind generation forecast were perfect, the total annual regulation costs increase steadily, but very slightly, as wind generation capacity is increased as shown in Figure 6-50. The rate of regulation cost increase with wind generation capacity additions is far less than the relative increase in regulation MWh procured.